AGSC

INVESTIGATION OF AIRBORNE GAMMA-RAY IMAGES AS A RAPID MAPPING TOOL FOR SOIL AND LAND DEGRADATION - WAGGA WAGGA, NSW

BY

P. BIERWIRTH

RECORD 1996/22

AGSO

AUSTRALIAN
GEOLOGICAL SURVEY
ORGANISATION

RECORD 1996/22

INVESTIGATION OF AIRBORNE GAMMA-RAY IMAGES AS A RAPID MAPPING TOOL FOR SOIL AND LAND DEGRADATION - WAGGA WAGGA, NSW

BY

PHIL BIERWIRTH

AUSTRALIAN GEOLOGICAL SURVEY ORGANISATION
1996

DEPARTMENT OF PRIMARY INDUSTRIES AND ENERGY

Minister for Primary Industries and Energy: Hon. J. Anderson, M.P.
Minister for Resources and Energy: Senator the Hon. W.R. Parer
Secretary: Paul Barratt

AUSTRALIAN GEOLOGICAL SURVEY ORGANISATION

Executive Director: Neil Williams

ISSN: 1039-0073
ISBN: 0 642 24961 X

CONTENTS

SUMMARY

Airborne gamma-ray spectrometric (AGS) data involves the airborne measurements of gamma-rays which can be processed to derive regional chemical maps or images for three elements, potassium (K), thorium (Th) and uranium (U). These maps are largely free from the effects of vegetation or 'culture'.

General Findings

Gamma-spectrometric images represent a complex mixture of processes which include bedrock composition, mineral weathering, leaching/acidity, aeolian and alluvial deposition, and groundwater discharge effects.

In many cases, it is possible to distinguish mappable landscape units from the data but meaningful interpretation requires the integration of digital elevation and geology data. Given information on radioelement mobility, geomorphology and geology, semi-automated interpretations can be made.

After subdividing into geological and geomorphic landscapes, AGS data can provide specific information about soil nutrients, texture and chemistry. In general at Wagga Wagga, K and Th images provide information on soils. U data shows important groundwater discharge effects.

Soils/ land degradation - mapping soil types, properties and degradation using potassium and thorium images

Airborne chemical maps of K and Th interpolated from aircraft lines were verified by soil sample measurements of these elements. The U signal is extremely degraded by the acquisition system although some high U alluvial clay areas were identified.

Signatures in high relief areas are related to exposures of bedrock, geological composition, erosion and mineral weathering.

Regional sampling suggests that potassium images are directly mapping acidity (and related Al toxicity) in areas of piedmont terraces, sloping plains and inactive alluvium. These categories occupy 50 - 60 % of the map sheet area.

In alluvial areas, all three elements may be associated with clay or silt particles, thereby indicating texture and associated properties.

Results from detailed study areas:

Two areas were looked at in some detail with soil sampling, ground observations and ground spectrometer measurements. These were (1) a 7 x 12 km section of metasediment hills at Ladysmith including a part of the Kyeamba valley and (2) flat alluvium on the Bullenbong plain in the north-west.

(1) Ladysmith.

In intermediate and lower slopes of metasediment areas, the K image maps leaching, the degree of development of the bleached A2 horizon and solum depth. Acidity relationship with K was not observed due to a narrow range in pH and likely pH measurement errors.

Evidence suggests that loss of Th probably occurs as a result of adsorption onto and transport with colloids.

Variations across the landscape of concentrations of radioelements in the A horizon are preserved at least through the E and B Horizons.

Airborne surveys are repeatable for K and Th but not U.

(2) Bullenbong Plain

In flat country, K and Th can be used to map alluvial deposits (K - recent deposits, Th - recent and older deposits). Leaching over time shown by the K image is not seen in the Th image and hence thorium data can be used to map older alluvial channels.

Thorium image data can be used to map aeolian deposits depending on the radiometric variation of the host landscape.

Cracking clays and gilgai show low thorium concentration (gamma-measured). This may be due to deposition of montmorillonite rich clays with lower Th during a more arid period. More recent channels with higher amounts of illite and kaolinite clays have a higher thorium response. Ground spectrometer 'uranium' and thorium measurements together with XRF measurements of thorium isotopes indicate that at least part of the lower thorium response in cracking clay areas is due to the release of radon gas (^{220}Rn in the thorium-232 decay chain).

Soil salinity

At Kyeamba Creek, mapped salt affected land, although not discretely distinguishable, is mostly contained within regions of low K . These areas are mainly leached areas of footslope colluvium, generally not within floodplains.

Groundwater discharge effects

Sizeable 'Uranium' anomalies (> 9 sq.km) in low lying areas, not related to bedrock, were found on the Wagga Wagga sheet area. These:
- relate to above surface concentrations of radon gas
- were measured because of windless conditions at the time of survey
- radon anomalies emanate from near surface saline and radium bearing groundwaters in the Wagga Wagga town area and Kyeamba Creek, and freshwater springs in 'The Rock' area.

Water samples from the Kyeamba Creek area indicate radon levels near and above safe levels for drinking. Implications are that:
- there is potential for ground radon surveys for mapping depth to water table.
- potentially harmful radon build up may occur in Wagga Wagga homes where groundwater tables are high.

Conclusion

AGS data is a valuable tool for mapping soil types, soil properties and aspects of degradation. While not the complete answer, this data in combination with DEM's and traditional methods can improve both the speed and accuracy of soil surveying. In some landscapes, gamma chemical images can rapidly detect landscape properties - such as leaching, ancient alluvial patterns,

windblown materials, basin-fill colluvium, radon discharge and sediment provenance - that are not achievable by other remote sensing methods.

Models for mapping continuous soil properties or soil-type units will often be specific to geomorphic or geological units. Computer generated interpretations of AGS data should therefore include the analysis of geology and digital terrain data.

1. INTRODUCTION

1.1 Aims

This study was conducted as part of a collaborative project, funded by the Murray Darling Basin Commission, involving AGSO, CSIRO Division of Soils (Canberra), Australian National University (Centre for Resource and Environmental Studies) and NSW Department of Land and Water Conservation.

For land management, the understanding of soil and landscape properties is crucial. Traditional methods of mapping soils, both in terms of definable units and soil properties, commonly involves interpreting and modelling landform. The use of aerial photography, topographic modelling, geological maps and field sampling still provide the basis for all soil survey programmes. Previous studies (Martz and de Jong,1990; Wilford,1992) have indicated the potential of gamma-spectrometric data for the rapid mapping of soil types and deriving additional properties not readily observed by other methods. Given that large areas of Australia have not been adequately surveyed, the aim of this study was to investigate the usefulness of AGS surveying for mapping soil properties and how it might be used in conjunction with existing soil mapping methods.

1.2 Source of Gamma-rays

Airborne gamma-spectrometry (AGS) provides spatial images of the geochemistry of the upper rock/soil layer with only minor effects from vegetation. The abundance of K, Th and U in near-surface materials are measured by detecting the gamma-rays produced during the natural radioactive decay of isotopes of these elements. Since gamma-rays are strongly attenuated in rocks, soil and air, most of the radiation emanates from shallow ground depth - approximately 90% of measured gamma-rays are received from the top 30-45 cm for a dry overburden of density 1.5 g/cm^3 (Grasty, 1976) (see Figure 1). The measurement of particular gamma-ray wavelengths makes it possible to determine the quantities of various isotopes. Potassium abundance is measured directly using the decay of ^{40}K at 1.46 MeV (see Table 1). Uranium and thorium abundances are inferred from the abundance of gamma-emitting daughter products (^{214}Bi and ^{208}Tl respectively) (Durrance, 1986). This assumes equilibrium in the uranium and thorium decay series which are shown in Table 2. In some cases, the quantity of isotopes measured (see Table 1) may be a function of the mobility of intermediate decay elements rather than the parents ^{238}U and ^{232}Th. This is discussed in greater detail below.

Table 1. Data channels/images available from the AGSO acquisition system.

Channel/Element Analysed	Isotope sensed	Gamma-ray energy (MeV)	Wavelength (nanometres)	Energy Window (MeV)
potassium	^{40}K	1.46	8.50 x 10-4	1.37 - 1.57
uranium	^{214}Bi	1.76	7.05 x 10-4	1.66 - 1.86
thorium	^{208}Th	2.62	4.74 x 10-4	2.41 - 2.81
total count				0.40 - 3.00
digital elevation				

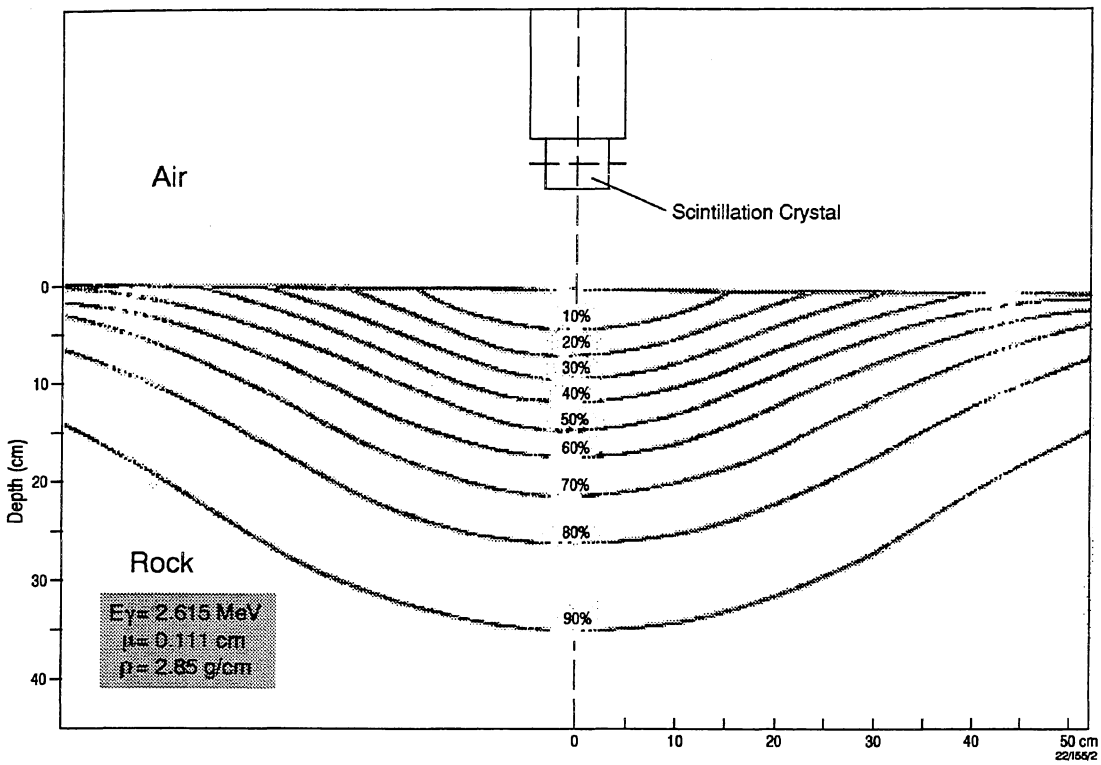

Figure 1. Volume of rock measured by a gamma-ray spectrometer (from Killen, 1977)

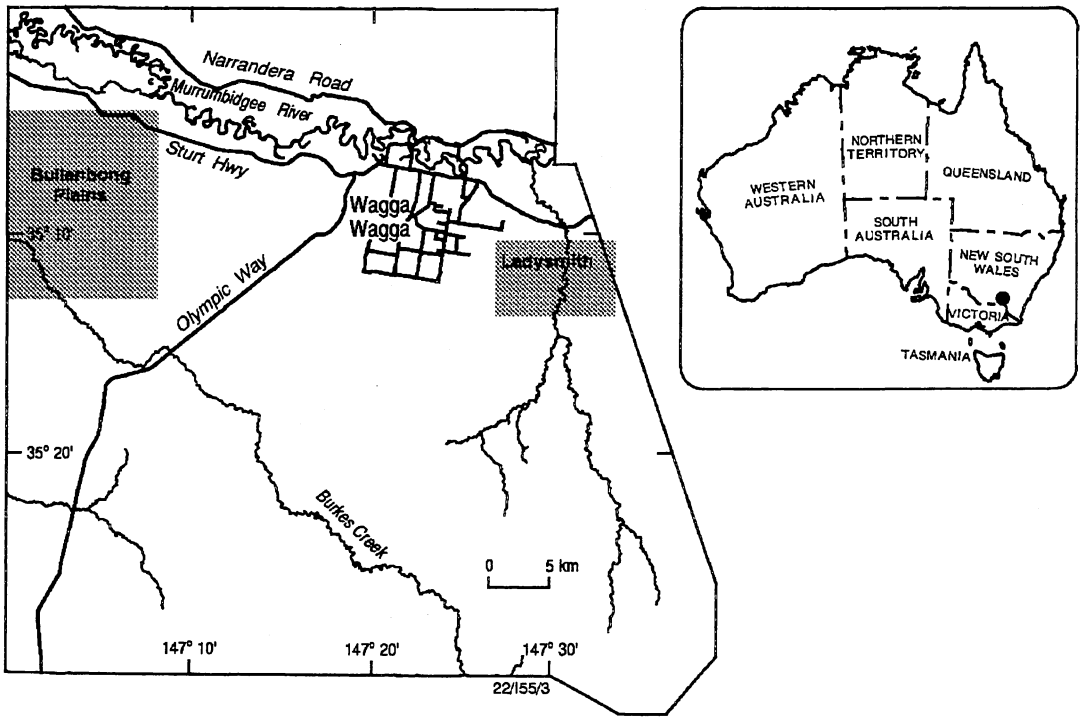

Figure 2. Location of the Wagga Wagga 100,000 sheet area, Kyeamba valley and detailed study areas.

Table 2. Uranium-238 and Thorium-232 decay series.

Uranium-238 Series Isotope	Half-life	Thorium-232 Series Isotope	Half-life
uranium-238	4.51×10^{9} years	thorium-232	1.41×10^{10} years
thorium-234	24.10 days	radium-228	6.7 years
protactinium-234	6.75 hrs	actinium-228	6.13 hrs
uranium-234	2.47×10^{5} years	thorium-228	1.9^{10} years
thorium-230	7.5×10^{4} years	radium-224	3.64 days
radium-226	1602 years	radon-220	55.3 sec
radon-222	3.82 days	polonium-216	0.145 sec
polonium-218	3.05 min	lead-212	10.64 hrs
lead-214	26.8 min	bismuth-212	60.60 min
bismuth-214	19.9 min	polonium-212	3.04×10^{-7} sec
polonium-214	1.64×10^{-4} sec	thallium-208	3.10 min
lead-210	22 years	lead-208	Stable
bismuth-210	5.013 days		
polonium-210	138.40 days		
lead-206	Stable		

1.3 Mineral sources of radioelements.

Potassium (K) is an abundant element comprising 2.5% of the Earth's crust. Common minerals containing significant K are feldspars and micas - orthoclase, leucite, nepheline, biotite, muscovite, sericite and phlogopite (Mares, 1984), and their weathering products such as illite clays.

Uranium (U) is present in significant quantities in accessory minerals zircon, sphene, apatite, xenotime and monazite.

Thorium (Th) is mostly found in epidote, zircon, sphene, apatite, rutile, xenotime and monazite.

Table 3. Average K, U and Th values for various rocktypes (after Galbraith and Saunders, 1983)

Igneous	K%	U (ppm)	Th (ppm)
Ultrabasic	0.01	0.007	0.02
Basic	1.0	0.8	3.4
Intermediate	2.4	3.0	9.8
Acidic	3.5	4.1	21.9
Sedimentary			
Carbonate	0.3	1.6	1.6
Sandstone	1.2	1.9	5.7
Shale	2.7	3.7	11.2
Metamorphic			
Amphibolite	0.6	0.9	2.0
Gneiss	3.4	2.3	10.6
Schist	2.5	4.1	13.5

Table 3 shows average radioelement concentrations in various general rock types. Basic igneous rocks such as basalts have low concentrations for all three elements whereas acid igneous rocks (e.g. granites) often have high concentrations of gamma emitting elements due to the presence of K-feldspar, micas and accessory minerals. In sedimentary rocks, K, U and Th are often present in the clay or illite component causing shale to have a higher response.

1.4 Element weathering and mobility

As well as the composition of parent material, the spatial distribution within the landscape of K, U and Th and the decay products of U and Th are a function of physical and chemical weathering processes. This is particularly true in Australian landscapes where weathering and erosion have been operating for some time. The distribution patterns therefore will relate to primary mineral content and the weathering patterns of these minerals influenced by the geomorphic status and climate of a region.

Physical transport of minerals by wind, slope wash and alluvial processes accounts for much of the distribution of radioelements. In a study of Canadian Prairie soils by Martz and de Jong (1990), the major distribution mechanism of radioelements was found to be adsorption onto clays and surface dispersion downslope, although some evidence was found for leaching of U series elements in the upper soil layer.

Upon chemical breakdown of mineral components, most elements are known to be mobile (being either soluble or attached to colloids) depending on the chemical conditions which in turn may be a function of the mineralogy, age of the landscape and climatic factors. For example, loss of potassium is consistently observed during most stages of rock weathering (Scheepers and Rozendaal, 1993; Dickson and Scott, 1992) and K is recognised as being relatively mobile in landscapes (Hudson, 1995). As a result of hydrolysis, K^+ is released from K-feldspar and micas during the formation of illite, adsorbed onto other clays or removed by fluid migration (Wedepohl,1969). Acid solutions aid the release of K^+ by substituting H^+ in the early stages of weathering which may initially also increase pH (Wollast,1967). AGS detected spatial patterns of K distribution therefore depend on the mineralogy, age (ie weathering state) and geomorphic setting of soils.

Since airborne U and Th data are derived from gamma emissions due to decay products ^{214}Bi and ^{208}Tl respectively, it is important to understand mobility aspects of all the parents of these elements that have reasonably long half-lives. For example, AGS uranium anomalies may be due to groundwater deposition of ^{226}Ra (Giblin and Dickson, 1984). In the uranium decay chain (see Table 2), isotopes of uranium and radium are soluble under various chemical conditions (Langmuir, 1978; Dyck, 1978). U isotopes are usually complexed - the form depending on pH and oxidation state. In oxidised waters at low pH UO_2 dissolves while at high pH U mobility is related to complexing with carbonates and phosphates. In anoxic conditions, U generally is immobile and precipitates, although at pH below 3-4 uranous (U^{4+}) fluoride complexes may be formed (Langmuir, 1978). Radium is present in both the uranium and thorium decay series (Table 2) and its mobility is reported to be associated with acidity and salinity (Dyck,1978; Dickson et al, 1987; Dickson and Herczeg,1991). Radium is often dissolved in acid spring waters in association with ferric-hydroxides (Dickson et al, 1987). It is also found in association with saline waters and concentrates in salt lakes (Dickson and Herczeg,1991) possibly due to complexing with the chloride ion in solution (Dyck, 1978). In areas of high oxidation potential, radium precipitates either by adsorption or with Ca or Ba sulphates (Beck and Brown,1987).

Thorium isotopes are relatively immobile (Langmuir and Herman, 1980). Complexing with organic compounds increases solubility so that in areas of high organic matter or humic acids removal of thorium may occur in near neutral pH conditions. In support of these experimental studies, accumulations of thorium have been observed in soil horizons directly below layers with a high organic matter content (Mortvedt, 1994).

In general, most of the parent and decay isotopes of K, Th and U are known to adsorb onto fine organic and mineral colloids depending on the chemical conditions (Wedepohl, 1969). Movement of these colloids by physical processes is therefore important in the mobility of most elements.

Radon isotopes ^{222}Rn and ^{220}Rn are present in the uranium and thorium decay chains respectively. These are gases that may be released from soils and detected by airborne signals (Grasty, 1994). The degree of emanation depends on concentration (defined by geological factors) or as a result of soil structure factors such as porosity and degree of cracking. Groundwater is sometimes observed to have high radon concentrations which can be harmful to humans (Graves,1987). ^{222}Rn is directly produced from the decay of ^{226}Ra which may be dissolved in the water. Loss of radon can also result in reduced signal for both the airborne U and Th data (this report).

1.5 Gamma-ray data acquisition and processing.

The Australian Geological Survey Organisation operates an aircraft which simultaneously acquires gamma-ray and magnetic data on a regional basis. Since 1990, more detailed surveys have been flown to support the national geoscience mapping program. More recently, the gamma-ray data has been acquired in 256 channels allowing full spectrum analysis, although the survey for this study used the four windows shown in Table 1. The detector system is a 32 litre pack of sodium iodide (NaI) crystals. To capture enough signal, an aircraft must fly at low altitude generally at a maximum of only 120 metres. When subjected to gamma-rays, the crystals emit visible light or 'scintillations' that are converted to a measurable electric pulse (Grasty,1976). The AGSO system also acquires magnetic field intensity and elevation information. The former is an important data set, showing sub-surface geology, but not included in this study. Surface elevations are derived by comparing radar altimeter readings measuring height above ground with GPS altitude.

The first Wagga Wagga data were acquired over a nine day period at the beginning of May, 1992 - see Figure 2 for location. The survey was sporadic due to rainy conditions. A reading in each of the four channels (see Table 1) was collected every 70 metres along flight lines spaced approximately 400 metres apart. Significant overlap between sample points occurs due to the large 'footprint' - 50% of received gamma-rays emanate from an area of 180 metres in diameter. The line data are then interpolated to form a grid of values or image. The Wagga data was gridded to form 50 metre pixels. In reality, due to the unfocused nature of the acquisition system, the true pixel size is probably more than 100 metres except where a source has strong emittance. A second small airborne survey was flown in early November, 1993 at 100 metres line spacing and gridded to a 50 metre pixel.

Prior to the creation of gamma-ray images, three important corrections are applied to the data:
1) Background correction. Cosmic radiation and gamma-rays due to atmospheric radon contribute to the counts recorded by the sensor. Background levels are estimated from measurements at high altitude or above a large body of water and then removed from the data (Minty, 1988). An assumption, sometimes in error, is that radon gas has uniform distribution in the atmosphere. This means that spatial atmospheric effects may occasionally be seen in the 'uranium' channel.

2) Terrain clearance height correction. Since gamma-rays are rapidly attenuated in air, the effects of variations of aircraft altitude need to be corrected for. This is done by standardising to a specified altitude using an equation that defines the exponential decay of radiation through air. One problem with the correction is that geometry effects are not adequately modelled, resulting in misleading spectral signatures and locational errors. This will be discussed later.
3) Spectral stripping. Due to the nature of the detector, a certain fraction of 'thorium' window photons are incompletely absorbed in the crystal and appear as counts in the lower energy 'uranium' and potassium windows (Grasty,1976). Similarly, 'uranium' window bismuth-214 photons appear as counts in the potassium window. This is known as Compton scattering which must be corrected for. The ratios of energy transfer are the coefficients which can be determined from calibration pads and are used to 'strip' the data.

After 'stripping', the data is reduced to counts due to K, U and Th. To convert to elemental abundances, sensitivity factors are required for each element. These are generally found for aircraft systems by calibration flights over a carefully selected ground test strip (Minty, 1988) and sometimes (as for hand-held instruments) concrete pads with pre-determined radioelement concentrations are used.

2. STUDY AREA / GEOLOGY.

The airborne survey was flown to encompass the Wagga Wagga 1:100,000 map sheet and the Kyeamba Ck catchment to the east (see Figure 2). The data were acquired to aid geological mapping and also to support soil and land degradation studies of the sheet area. The geological map (Figure 3) was compiled by the interpretations of gamma ray and magnetic data, aerial photographs and field work (Raymond, 1992). The geology is a Paleozoic sequence of Silurian granites intruding Ordovician interlayered siltstones and sandstones of marine origin. These units are unconformably overlain by terrestrial Devonian sandstones. Large areas of alluvium and colluvium cover the west of the map sheet area. Geology units have been used as a base for further subdivision into soil-landscape units (Chen and McKane, 1996).

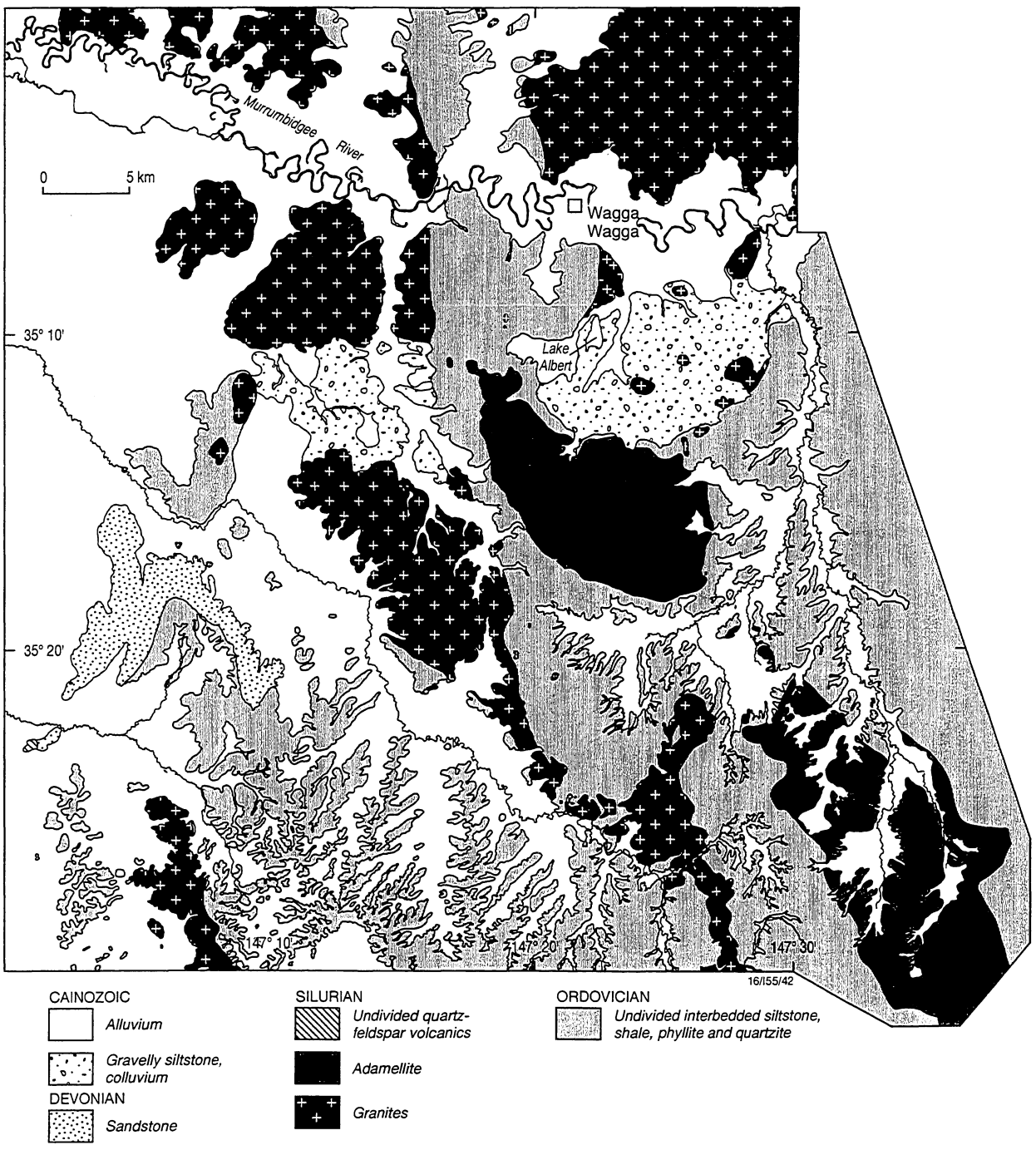

Figure 3. Geology of the Wagga Wagga 1:100,000 map sheet and Kyeamba valley (after Raymond, 1992)

3. ASSESSMENT OF RADIOMETRICS

3.1 Regional Interpretation

The four images available from the radiometrics are shown in Figure 4. It is clear that combinations with other types of data are required for interpretation. Figure 5 shows the potassium concentration coded in colour and combined with a SPOT satellite derived digital elevation model (DEM). The DEM has been illuminated from the east to produce the shading effect and the result was substituted into the intensity of the colour-indexed potassium image using the HSI procedure (Gillespie, 1986). Geological units are also overlain on the image.

3.1.1 Bedrock composition

Initial interpretation involves understanding the influence of bedrock compositions on gamma-ray signatures. High concentrations of potassium and uranium (Figures 4 and 5) relate to areas of granite and adamellite outcrop and subcrop due to the presence of K-feldspar and mica (see Tables 4 and 5). The same areas may be either high or low in thorium (see Figure 4 and Table 5). Shallow lithosols on Ordovician metasediment ridgetops give high concentrations of both potassium and thorium which are associated with sedimentary clay minerals. Sandstones, being mostly quartz, are low in all three elements.

Table 4. Mineralogy analysis by X-Ray diffraction of samples from the Wagga Wagga region. Relative mineral values are instrument intensities in counts per second.

Area	Quartz	K-feldspar	Plagioclase Feldspar	Mica	Clay fraction
Granite Soil	1590	380	160	230	mica (illite)
Granite derived alluvium	2480	550	50	122	
Metasediments Soil	2750	10	54	230	mica (illite)
Sandstone colluvium	5270	50	0	0	
Alluvial soils- Murrumbidgee R	2880	130	0	100	mica (illite)
Alluvial soils - Kyeamba Ck.	2040	30	60	230	mica (illite)

Table 5. Radionuclide concentrations derived from AGS for outcrop/shallow soils over major lithologies on the Wagga Wagga 1:100,000 sheet.

LITHOLOGY	K %	U ppm	Th ppm
Mount Flakney Adamellite	4.5	5.1	7.9
Wantabdgery Granite	3.4	4.4	26.5
Ordovician Metasediments	2.8	3.0	19.4
Devonian Sandstone	0.7	1.7	7.1
Alluvium - Murrumbidgee R.	2.2	2.9	14.8
Alluvium - Kyeamba Ck.	1.7	2.4	14.8

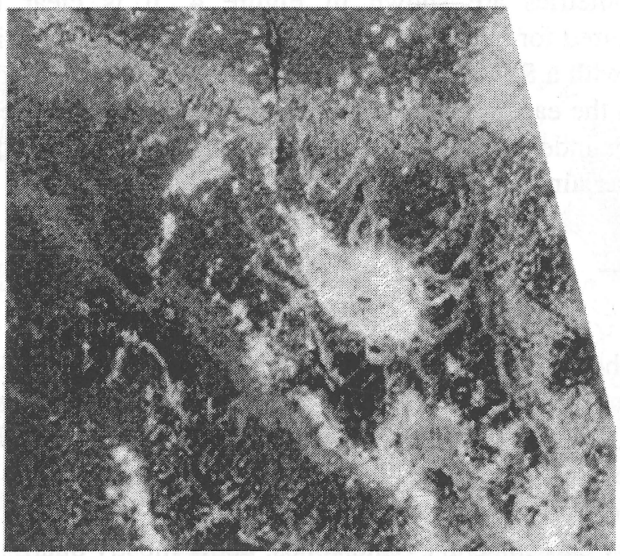

Figure 4(a). AGS potassium concentration for the Wagga Wagga 1:100,000 sheet. Bright = high.

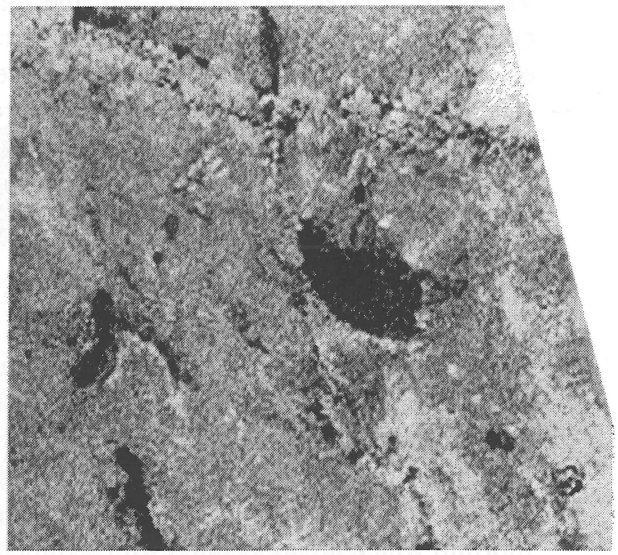

Figure 4(b). AGS thorium concentration.

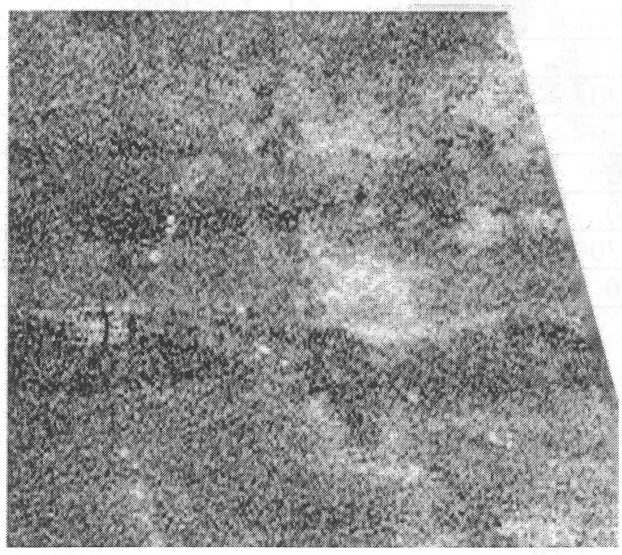

Figure 4(c). AGS uranium concentration

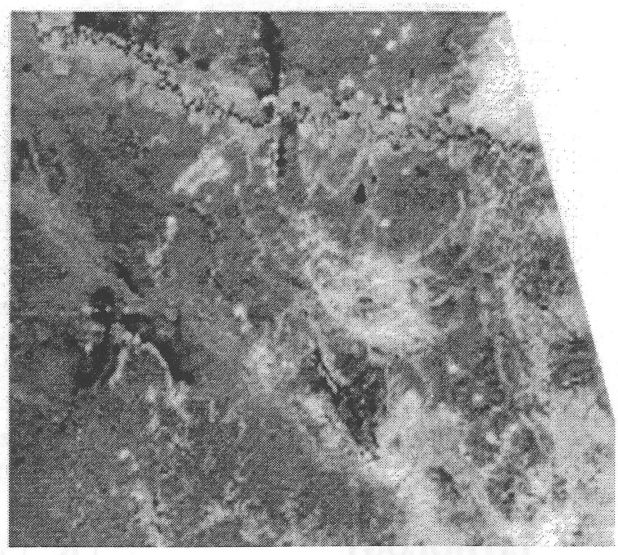

Figure 4(d). AGS total count

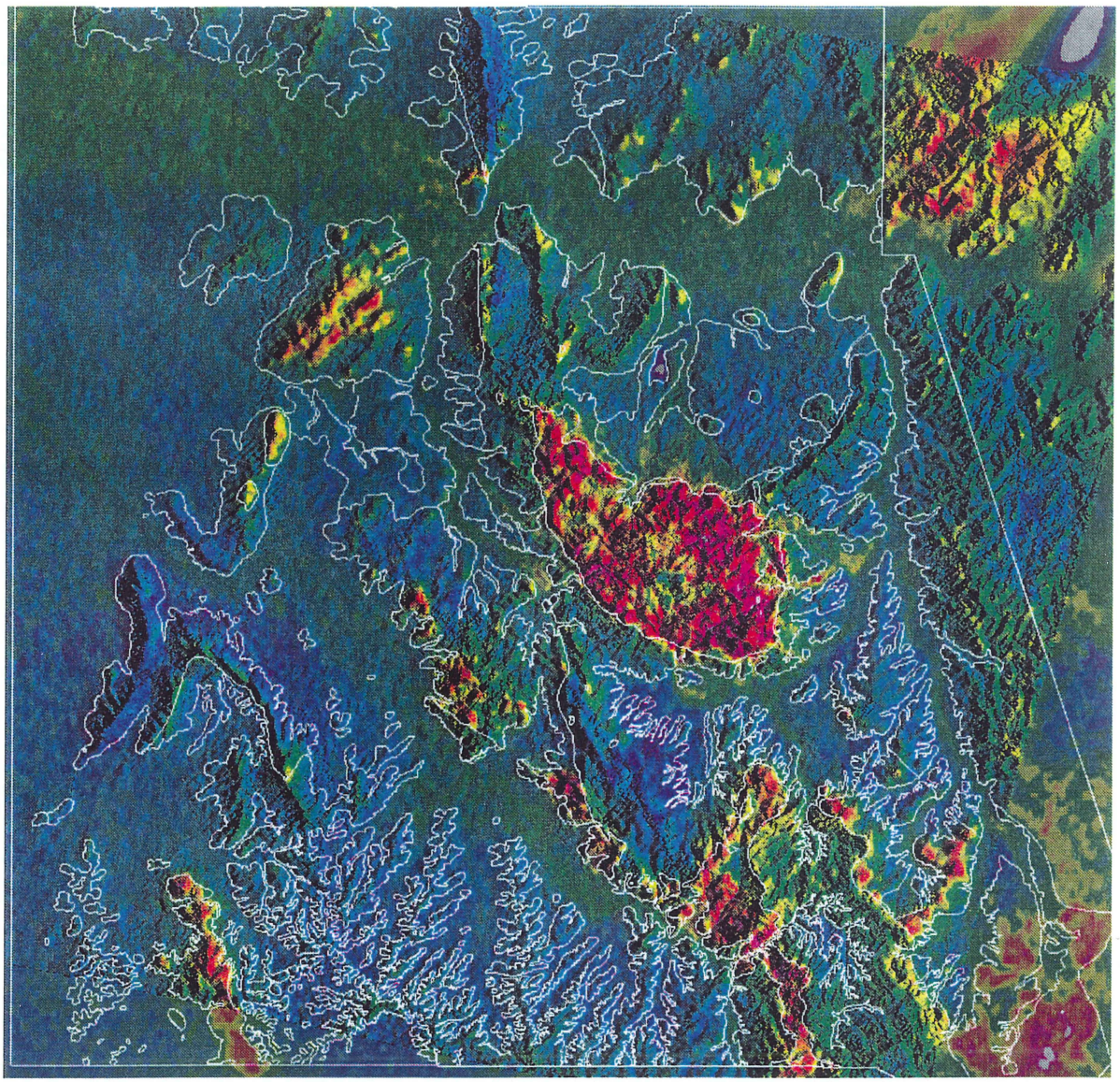

Figure 5. Airborne derived potassium concentration draped over a SPOT DEM shaded from the east. Geology boundaries are overlain. The scene is 60 km across. Purple = 4.5%K through red, yellow, green, light blue, dark blue = 0.5%K.

3.1.2 Geomorphic controls

As discussed above, shallow bedrock areas are often bright in gamma-ray images. These are generally areas of active erosion where fresh material is continually being exposed. As weathering proceeds, minerals breakdown and soils develop, there is often a loss of radioelements which are transported downslope and/or down profile attached to finer particles (Dickson and Scott, 1992). In these geomorphically active areas gamma responses are a function of bedrock composition, the degree of weathering and soil thickness.

Away from actively eroding areas, there are large areas of residual to semi-residual slope colluvium and alluvium in the Wagga region. In geomorphically inactive areas such as gentle slopes, geochemical weathering and fluid mobility of elements becomes important in understanding radiometric patterns. Recent alluvial deposits are elevated in both K and Th associated with particles that have been removed from upland areas. Both K and Th are known to adsorb onto clay particles and some K may be present within the clays (Wedepohl,1969). This means that alluvial areas can be identified by radiometric signatures which may be used to predict clay content and grain size. Residual and alluvial areas are discussed later in the detailed study areas.

3.1.3 Analysis of regional samples

uring the compilation of the soil-landscape map (Chen and McKane, 1996), a number of soil mples were collected from across the Wagga Wagga 1:100,000 sheet. Subsequently a portion of these were analysed for K, Th and U contents (K by Atomic Absorption analysis and U,Th by X- to support the airborne gamma-ray interpretations. The general landscape category en and McKane (1996) and the properties analysed are shown in Table 6.

ble 6. Number of regional soil samples in simplified landscape categories and soil properties alysed.

Landscape Category	A Horizon	E Horizon	B Horizon	Total
Piedmont, Terraces and sloping plains	13	4	3	20
Hilly areas of granites	15	6	0	21
Sandstone areas	7	1	0	8
Hilly areas of metasediments	13	3	5	21
Alluvial Plains, Swamp	14	6	5	25
Soil Properties measured	depth, particle size, EC, pH, CEC, exchangeable cations, Total K, U, Th, airborne pixel counts (K, U, Th, total count)			

The nearest pixels (to sample locations) from the gridded airborne images were extracted and also compared with soil properties. Figure 6a and b show the relationship between image values and A-horizon sample results for potassium and thorium. Both graphs show a correlation between airborne readings and actual contents in the ground. The correlation is surprisingly good (R = 0.84) considering that point samples are being compared with 100 metre 'footprint' values, some of

which are interpolated between aircraft lines spaced 400 metres apart. U data is not presented due to the poor correlation which was expected due to significant noise present in the U image.

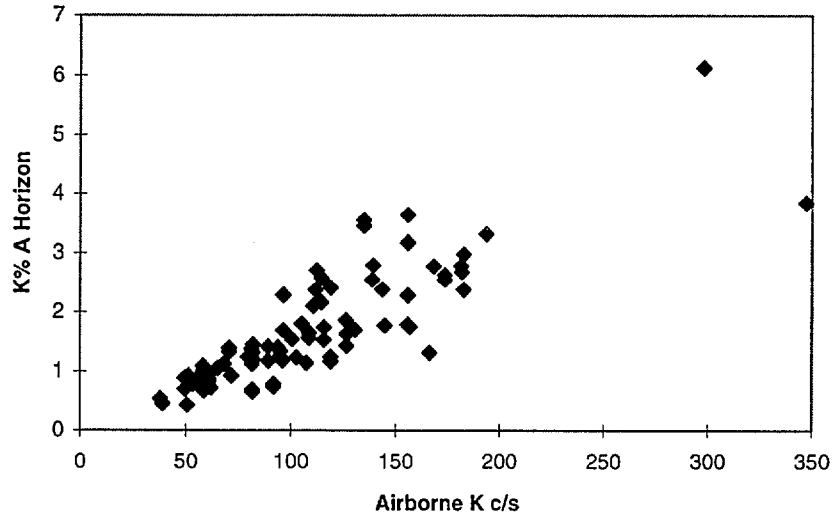

Figure 6(a). Relationship for potassium between point A Horizon samples and nearest image pixel values from the 400 metre line spacing survey.

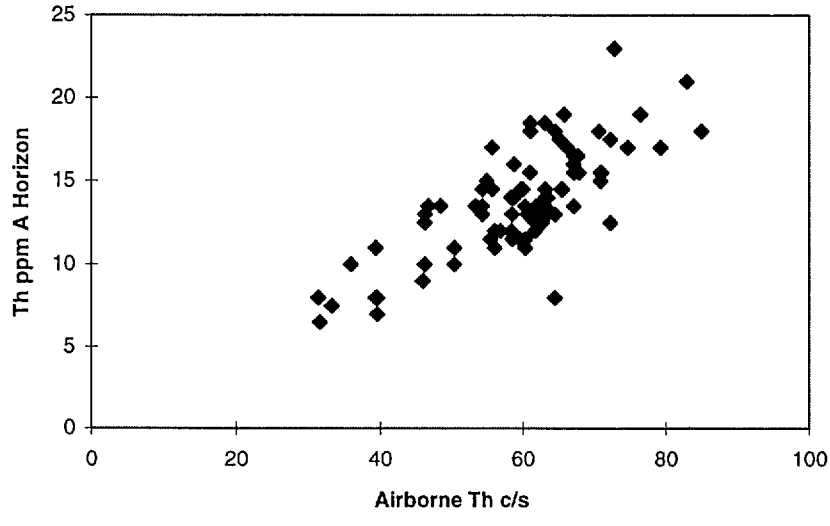

Figure 6(b). Relationship for thorium between point A Horizon samples and nearest image pixel values from the 400 metre line spacing survey.

Some relationships exist between radionuclides and soil properties for all samples. A logarithmic relationship is observed between thorium concentration and clay content (see Figure 7) suggesting that thorium adsorption onto clays is an important mechanism for thorium distribution. Interestingly no such relationship exists for potassium and uranium.

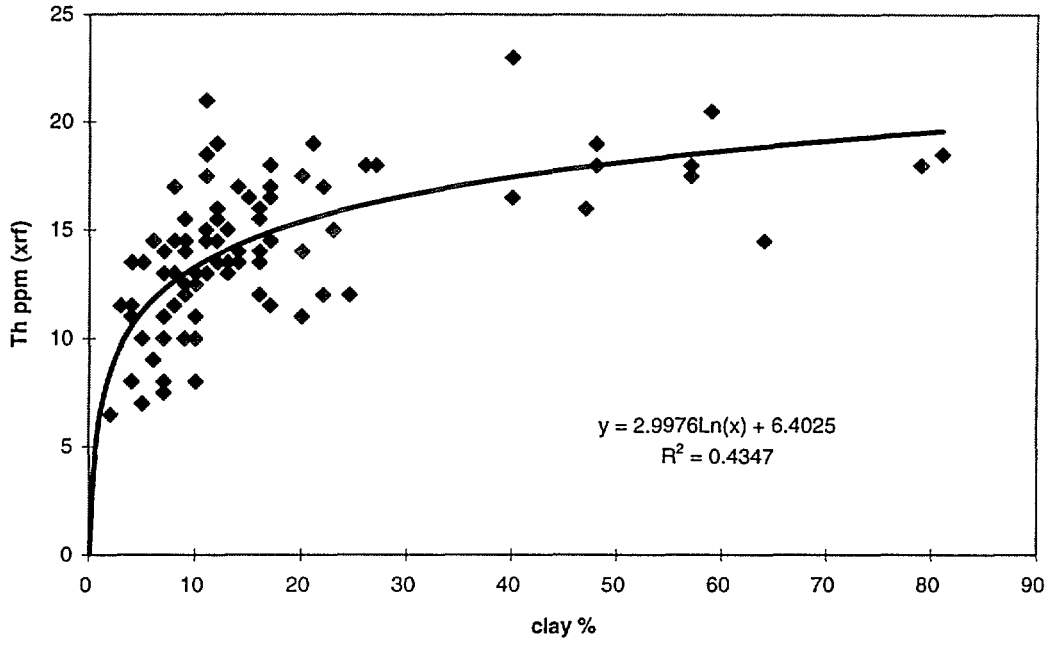

Figure 7. Thorium concentration, measured by x-ray fluorescence, versus clay in regional samples determined by particle size distribution analysis.

3.1.3.1 Geomorphic subdivision

The samples were then divided into the landscape categories shown in Table 6 to understand radioelement distribution as a function of landscape.

Figure 8 is a plot of K versus coarse sand content in samples from the terraces and sloping plains, granite and metasediments. This indicates that K content may be a function of the presence of lithic fragments in the metasediments and feldspars or fragments in the granite areas. The relationship is strongest in the piedmont terrace and sloping plain category and these areas being geomorphically stable, the grainsize itself may be a function of weathering maturity. In sandstone and alluvial areas, grainsize relationships for potassium were not so clear. In alluvial areas, samples in the A horizon appeared to show a relationship between K content and silt sized particles (R = 0.67, 14 samples) whereas below the A horizon, K related to clay content (R = 0.80, 11 samples). This would be explained by the more recent deposition of silts due to increased erosion caused by land clearing in European settlement times.

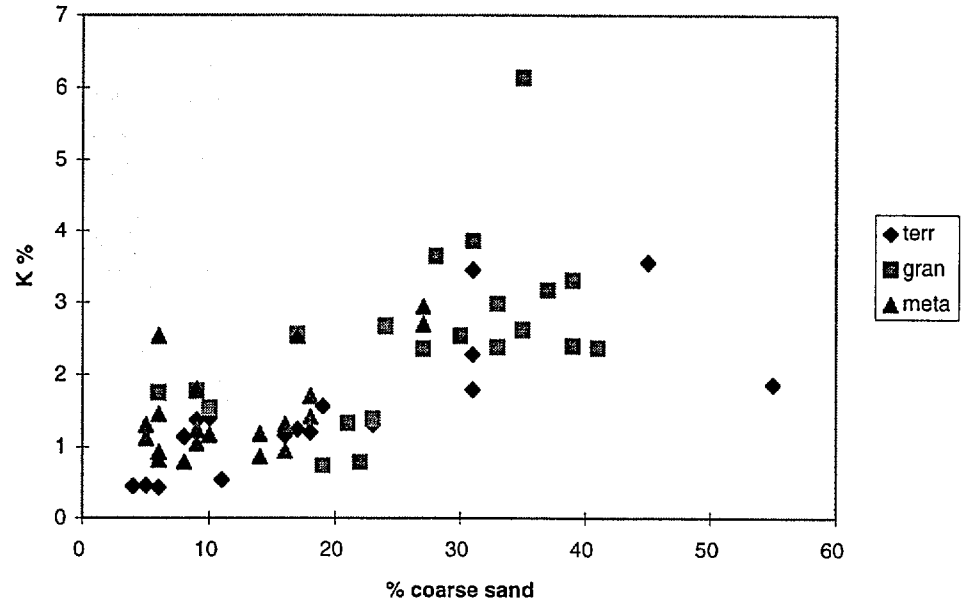

Figure 8. Relationship between K and % coarse sand in samples from A and E Horizons of piedmont terraces, granite and metasediment areas.

Regionally, the 'piedmont terraces and sloping plains' category is representative of stable areas. Figure 9 shows a significant relationship for this category between pH and K measured from samples (R = 0.87) and by airborne gamma methods (R = 0.66).

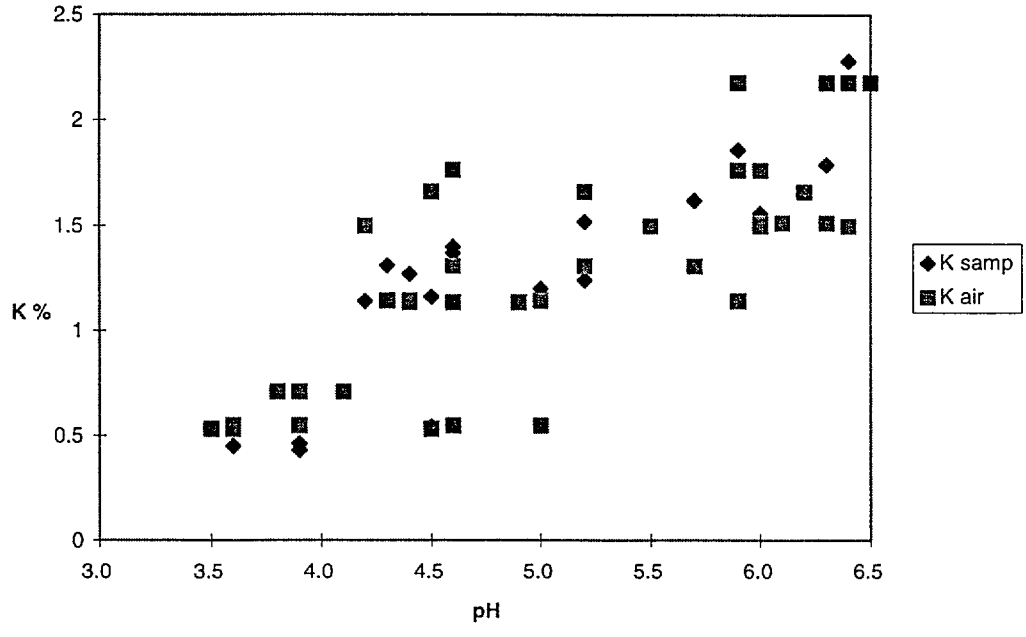

Figure 9. Sample results for K and pH in the A Horizon for 'piedmont terraces and sloping plains' .

This is a highly significant result in that sample K measurements suggest that K mapping in these areas is a surrogate for pH mapping. Potassium distribution is most likely to be a function of the degree of leaching and hence relates to pH. This is discussed in greater detail in the later section on

detailed study areas. Airborne readings indicate that pH can be mapped directly with the airborne gamma-ray detection system albeit in an averaged sense. Other relationships observed probably relate to the pH association - negative K relationships with Phosphorous sorption (R = -0.56), Exch. Na (-0.45), Exch Al (-0.51) and weakly Organic Carbon (-0.35). Figure 10 shows that soils in this area below about 1% K may be acid enough to produce near toxic levels of available Aluminium.

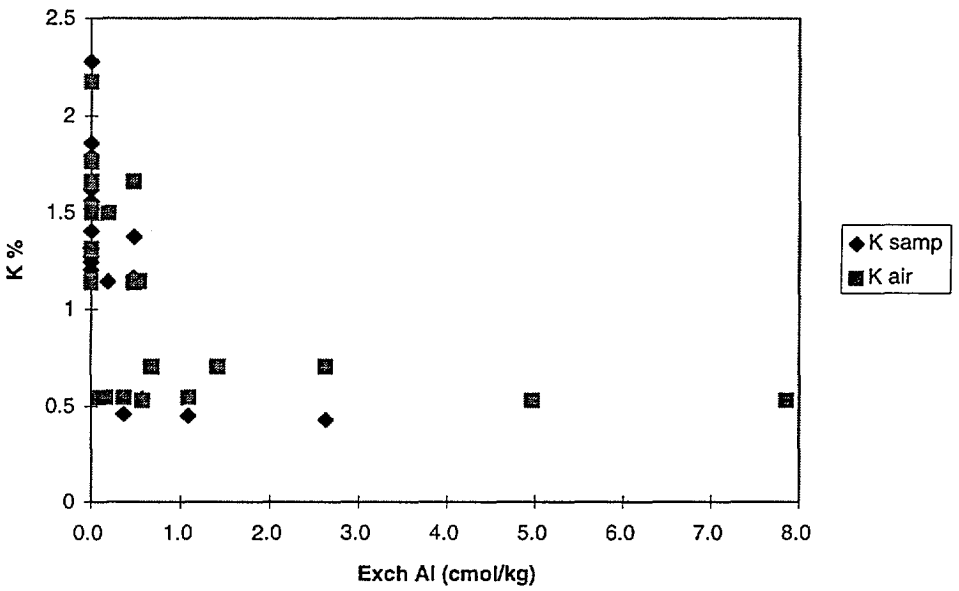

Figure 10. Airborne and soil measurements (A Horizon) of K versus soil Exchangeable Al

Thorium results for the categories were similar. Again the positive relationship with clays was evident in all areas, particularly so for 'piedmont terraces and sloping plains' (R = 0.8, n = 20), and generally there was always a positive correlation coefficient with exchangeable cations.

For uranium, a negative relationship (R= -0.42) is indicated with pH which may be a function of substitution with the Ca ion in carbonate complexes. This is also discussed further in the following section.

3.2 Detailed study sites analysis

In order to study the effects of local geology and landforms on gamma-ray response, two areas were chosen for detailed sampling and analysis. Locations of these areas are shown on Figure 2. The Ladysmith study site corresponds with the area of the experimental 100 m spaced second airborne survey.

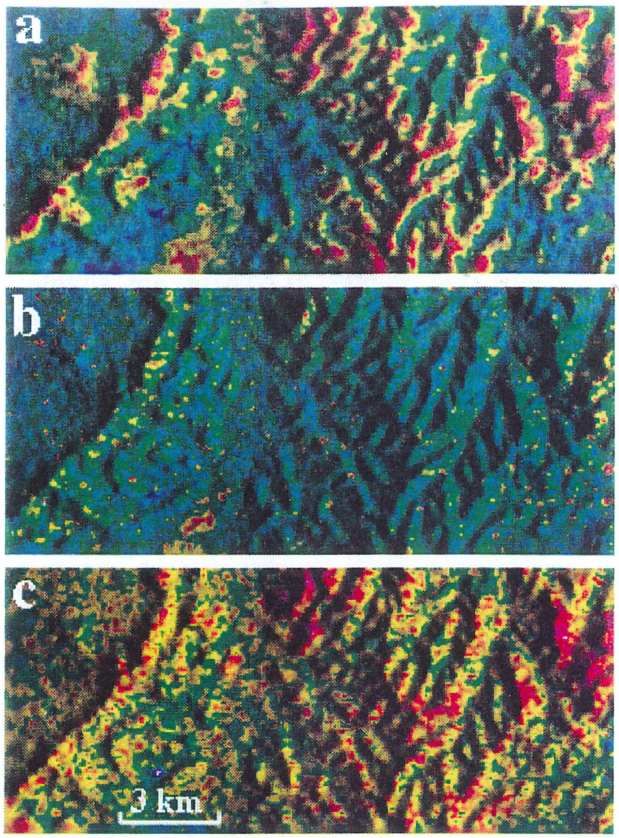

Figure 11. Ladysmith AGS data. (a) Potassium draped on shaded DEM. All data is derived from the AGSO 100m spaced airborne survey. Red = 3%K, Blue= 0.9%. (b) Uranium, R = 6ppm, B = 1.2ppm (c) Thorium, R = 20ppm, B = 10ppm.

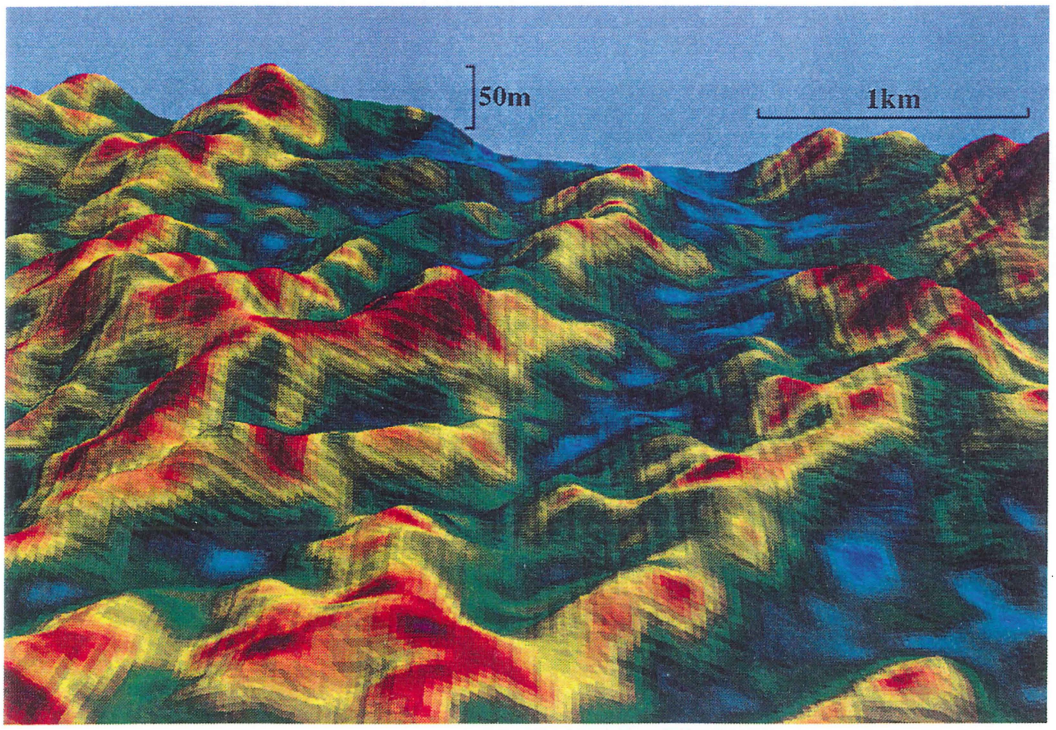

Figure 12. 3D perspective of part of the Ladysmith 100m line-spaced airborne survey. K concentration (Red = 3%, Blue = 0.9%) draped over the DEM. 3km across scene.

3.2.1 Ladysmith area (Ordovician Metasediment Hills)

3.2.1.1. Study area and sampling

The Ladysmith study area is approx. 7 x 15 km of rolling hills and comprises mostly one lithology - Ordovician Metasediments (see Figure 2). These are slightly metamorphosed shales and sandstones of marine origin. Minerals present are dominantly quartz, muscovite and illite. The latter two contain most of the K, U and Th and the breakdown of these minerals controls the dispersion of radioelements. Figure 11(a),(b) and (c) show part of the study area with remotely-sensed potassium, uranium and thorium draped over a digital elevation model (DEM). Figure 12 is a 3D perspective showing potassium for part of the area. At the tops of ridges soils are shallow and high levels of potassium and thorium relate to erosional dispersal of clays as the bedrock breaks up. Away from ridges, loss of these elements is suggested. The question is - what is the process and how does it relate to soil properties?

The area was analysed, both for soil properties and terrain attributes, as part of the Wagga Wagga study. A system of soil cores distributed across the landscape (76 sites), each divided into horizons, and a 20 metre DEM were used to generate soil and terrain variables. These sites were selected to represent a range of hillslope/catenary positions (Gessler and Ashton, 1996). Gamma-ray emitting elements in a subset of the soil samples (23 sites, 52 samples) were analysed using X-ray diffraction (XRF, U and Th) and Atomic Absorption (K) techniques. Ground gamma spectrometer measurements were also collected at the sample sites.

3.2.1.2 Gamma emitting elements v terrain attributes

As observed in Figures 11 and 12, there is a relationship between gamma-emitting elements (particularly K) and topography. An immediate question is whether the airborne readings are in some way influenced by height corrections performed on the data as described in section 1.5. The correlation between airborne and ground spectrometer readings (Figure 13) indicates that the topographic relationship is not totally related to processing of the airborne data. There may be some effect at the tops of ridges (highest K values in Figure 13) where altimeter spot height measurements are not valid for the total footprint. A perfect correlation is not expected given the difference in airborne and ground 'footprints' (approx. 100 m versus 5 m).

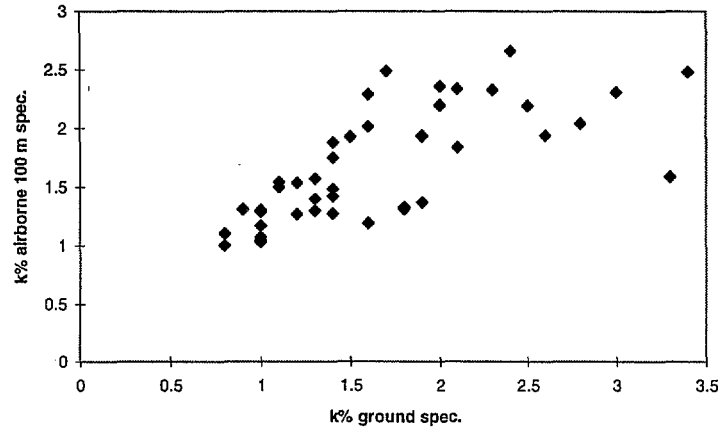

Figure 13. Comparison of ground spectrometer and airborne 100m line spacing measurements of potassium measurements.

The association of K concentration and topography shown in Figure 12 is further evidenced by Figure 14 below which is a plot of elevation of sample sites and airborne measured K for the nearest pixel.

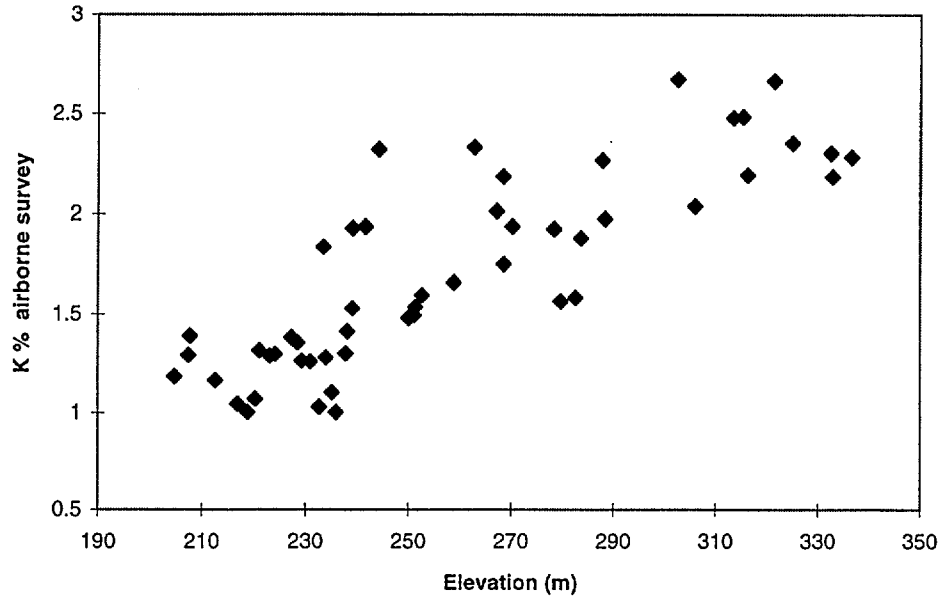

Figure 14. Airborne potassium values taken from the gridded 100m line-spaced survey versus elevation.

Other terrain variables which show relationships with K are the upslope mean values for profile, plan and tangent curvature. Figure 15 shows the effect of plan curvature on K values and a similar relationship exists with profile and tangent curvature. Plan curvature measures the concavity/convexity across the slope (Gessler et al. 1995). Positive values indicate concavity and indicate converging flow, ie areas of increased water flow through the soils. In these areas, potassium is reduced indicating leaching by the increased water flow.

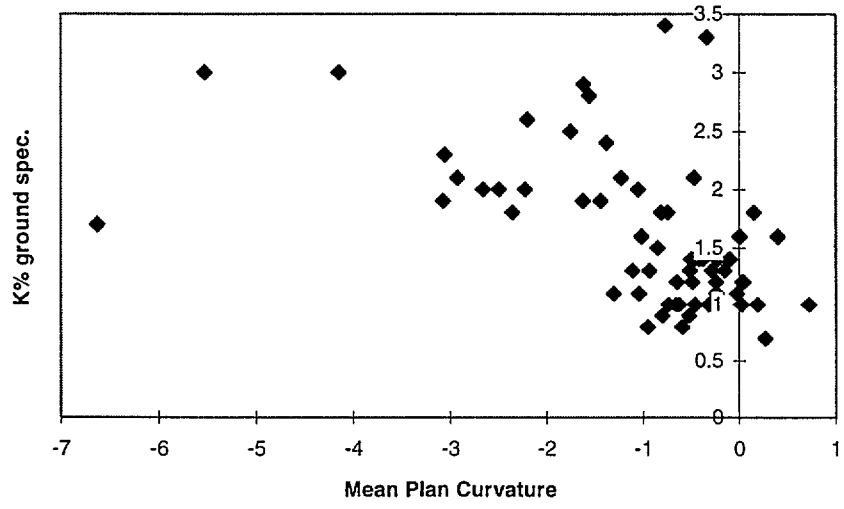

Figure 15. Potassium measured by ground spectrometer versus plan curvature.

3.2.1.3. Gamma emitting elements v soil properties

Gamma emitting elements in this area have actually been measured four times - twice by airborne gamma methods, by ground spectrometer and also by laboratory analysis of soil samples., Measurements of gamma emitting elements, within actual soil samples, were considered the most reliable for determining relationships with soil and terrain variables since gamma-ray measurement involves averaging over a 'footprint' area.

In general there were few direct correlations between gamma elements and soil properties. Unfortunately, grainsize analysis was not done on the samples due to limited resources (Gessler and Ashton, 1996). Table 7 shows the general trends down-hole of soil properties. While exchangeable cations show a strong depletion in the E(A2) horizon, the radioelements (K,U,Th) and pH increase gradually down-hole.

Table 7. Average values of soil properties and gamma-emitting elements in the different horizons.

Soil factor	*A horizon*			*E Horizon*			*B Horizon*		
	Mean	St.Dev	N	Mean	St Dev	N	Mean	St Dev	N
Depth (cm)	6.18	6.78	76	22.6	41.55	40	79.91	45.95	109
pH (1+5 $H_2$0)	5.4	0.48	76	5.58	0.35	40	6.72	0.9	109
EC (uS/cm)	107.61	81.46	76	53.3	0.74	40	58.84	167.33	109
Total C (%)	2.26	1.74	76	0.4	0.37	40	0.22	0.16	109
Exc. Ca (cmol/kg)	2.71	2.64	76	1.03	0.04	40	4	2.03	109
Exc. Mg "	0.87	0.91	76	0.46	0.25	40	4.16	2.34	109
Exc Na "	0.05	0.06	76	0.04	1.6	40	0.31	0.51	109
Exc.K "	0.77	0.41	76	0.28	2.12	40	0.5	0.3	109
CEC "	7.04	3.4	76	3.53	0.54	40	10.34	3.72	109
ESP (%)	0.81	0.8	76	1.36	0.65	40	8.98	3.96	109
U (ppm,XRF)	4.09	0.72	23	4.2	2.22	15	4.89	1.32	14
Th (ppm,XRF)	16.76	1.64	23	18.47	0.62	15	21.43	6.57	14
K (%,AA)	1.65	0.53	23	1.83	0.78	15	1.88	0.43	14

As mentioned before airborne gamma-ray data at the Ladysmith study area shows a loss of potassium in downslope soils. This is verified by ground measurements and correlations with sample K content and K relationships with terrain variables. Regional samples have shown that in residual soils leaching and pH affect the K distribution (see Figure 9) and given that downslope soils at Ladysmith are colluvial and residual similar processes may operate here. Also as discussed earlier profile, plan and tangent curvature relationships with K at Ladysmith (see Figure 15) support the proposition that through-soil water movement influences K content. Possible explanations for K loss downslope are:

1) weathering and breakdown of minerals release the elements for removal by percolating waters and colloids

2) K, Th and perhaps also U are contained within or are adsorbed onto clay particles, derived from weathering of bedrock, which are transported downslope by alluviation and removed from the lower landscape.

3) a combination of both 1 and 2.

In the A1 and E horizons, weak relationships were observed between CEC, which is often related to clay content, and sample K and Th contents (R ~ 0.5). This indicates that at least some of the distribution patterns of these elements may be due to surface transport of clays. However, in a geomorphic context clays would be expected to accumulate lower in the landscape which doesn't fit with the observed distributions of K and Th on the surface.

To test for leaching as a K removal process, relative levels of exchangeable Calcium were examined in the E and upper B horizons - a high Ca (B)/Ca(E) ratio indicates more leaching. A strong correlation was observed between sample K and the ratio (Figure 16a). This suggests that areas with lower K in the E horizon have strongest leaching. A weaker relationship exists with Ex Mg and the same correlations occur with Thorium.

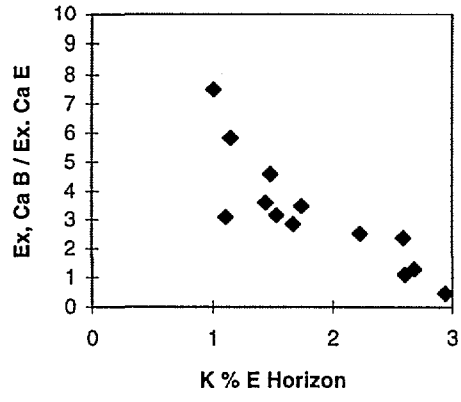

Figure 16(a). K in the E horizon v Calcium leaching

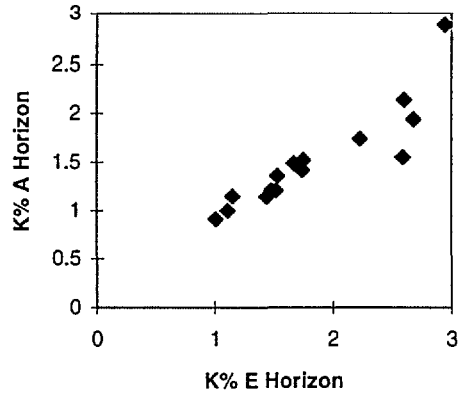

Figure 16(b). K in E versus A horizons.

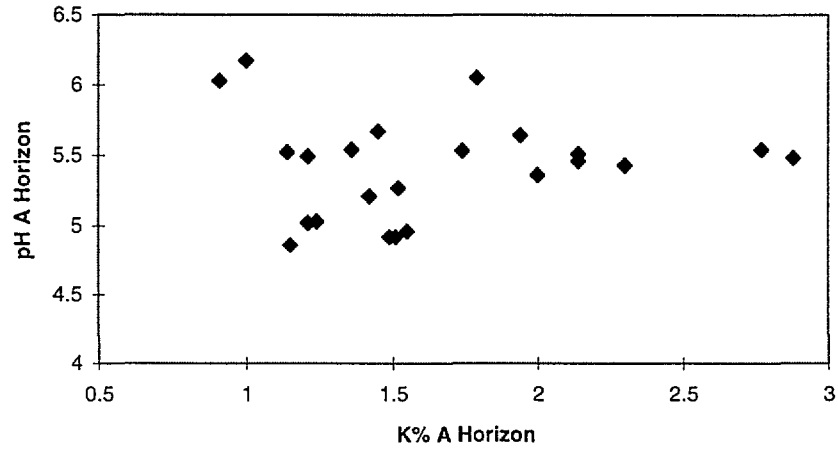

Figure 16(c). K versus pH measured in A Horizon samples.

Figure 16b shows that K concentrations between the E and A horizons are strongly correlated and a similar relationship exists with K in the B horizon (N = 14, R = 0.81). This shows that gamma-ray measurements at the surface will give an indication of the extent of leaching and development of the E horizon. Where leaching is strongest, the whole profile is depleted in K whereas exchangeable Ca is depleted in the E horizon. This is likely because we are comparing total K,

which slowly becomes available for leaching, with available Ca which leaches readily. The fact that K and Th are depleted in zones of increased leaching indicates downward and lateral water movement is a dominant factor in the removal of these elements.

Removal of cations due to leaching in the E horizon relates to acidity (Buckman and Brady, 1960). The relationship between K and pH shown in regional samples of residual terrains was not observed at Ladysmith overall (Figure 16c) or in footslope colluvium. Although leaching relationships are observed, this does not strongly relate to acidity. This may be because the terrain at Ladysmith is younger and more active in terms of erosion than the older landscapes.

Other correlations at Ladysmith

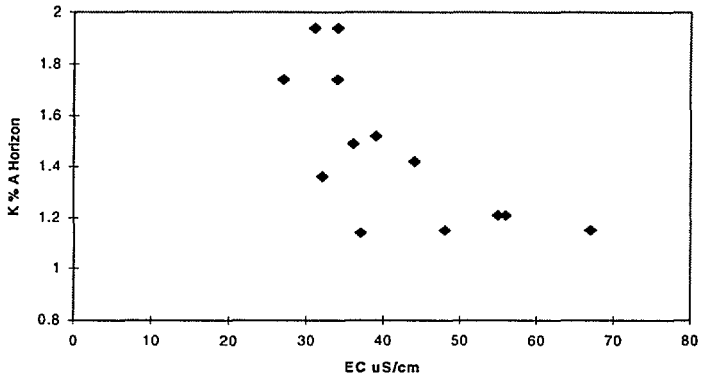

Figure 17. K % in A horizon v EC in samples 100-200 cm deep

Figure 17 shows an apparent relationship between A horizon sample K with the salinity of samples (from the same hole) at depth. One possible explanation is that areas with increased leaching (and hence less K) lower in the landscape may contain more clay and EC may only relate to clay content.

Figure 18 shows that in this area solum depth increases as potassium decreases. At least in some areas, gamma-ray detection methods may provide a means of measuring solum depth over the landscape.

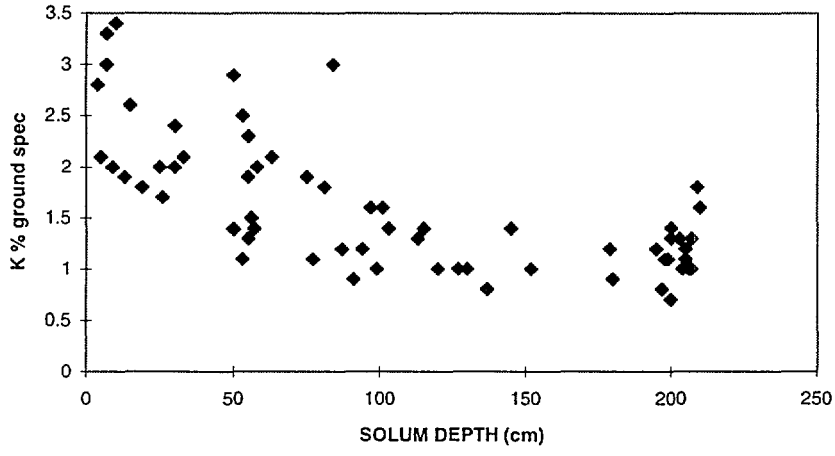

Figure 18. Solum depth versus ground spectrometer K.

3.2.1.4 airborne versus ground measurements

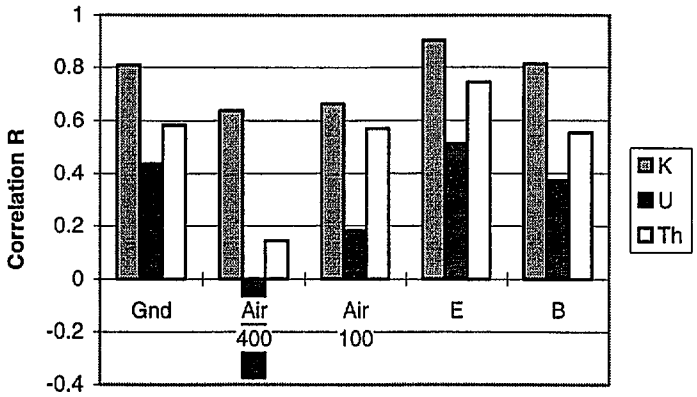

Figure 19. Correlations of radioelement concentrations in the A Horizon with ground spectrometer readings (gnd), 400 m line spaced airborne readings, 100m spacing and XRF/AA concentrations in the E and B Horizons.

Sample, surface and airborne results show the highest correlation coefficients with potassium. Figure 19 shows a range of correlation coefficients for K,U and Th in the A Horizon relative to measured concentrations in the E and B horizons as well as ground and airborne spectrometers. K and Th in the A Horizon positively correlate with the same element concentrations further down the profile and all spectrometer results. The strength of correlation for both K and Th is progressively less for ground, 100 metre spaced and 400 m spaced airborne spectrometers. Thorium and Uranium relationships are weaker probably due to the inaccuracy of the XRF technique (detection limit 0.5ppm). Airborne U values are too noisy due to low gamma-ray emissions.

Airborne image data for K and Th have low noise and these elements show the same patterns of mobility. K shows better relationships with soil properties, and spatial distributions of K in the A horizon are reflected in the lower horizons (see Figure 19 and Figure 16b).

3.2.2 Bullenbong Plain (Flat lands - alluvium)

3.2.2.1. Study area

In areas of low relief, such as the Bullenbong Plain, traditional soil-landscape mapping has problems with accuracy and efficiency since there are no topographic relationships for correlation. In such areas, soils may vary as a result of complex alluvial/sedimentary processes. The main aim of studying this area in detail was to determine if gamma-ray data can be a useful mapping aid in the vast expanses of very low relief land in Australia. The area of detailed investigation is located 25 km west of Wagga Wagga (see Figure 2). The area of 180km^2 is flat to gently undulating. It has been mapped in the Wagga Wagga soil landscape report (Chen and McKane,1996) being comprised of 6 soil landscapes (see Figure 21). Aerial photos, topographic or geological maps offer few, if any, clues to the soil surveyor of what soils are present. Lacking rock outcrop and current geomorphic activity, it is part of an old landscape which grades into the Riverine Plain of the Murray Basin to the north and west of the trial area. For the original mapping, the lack of information in aerial photos meant that a large number of sampling and notebook sites were required to delineate the unit boundaries. Conversely in areas of significant relief, air photos and DEM's can be used efficiently to establish the unit boundaries.

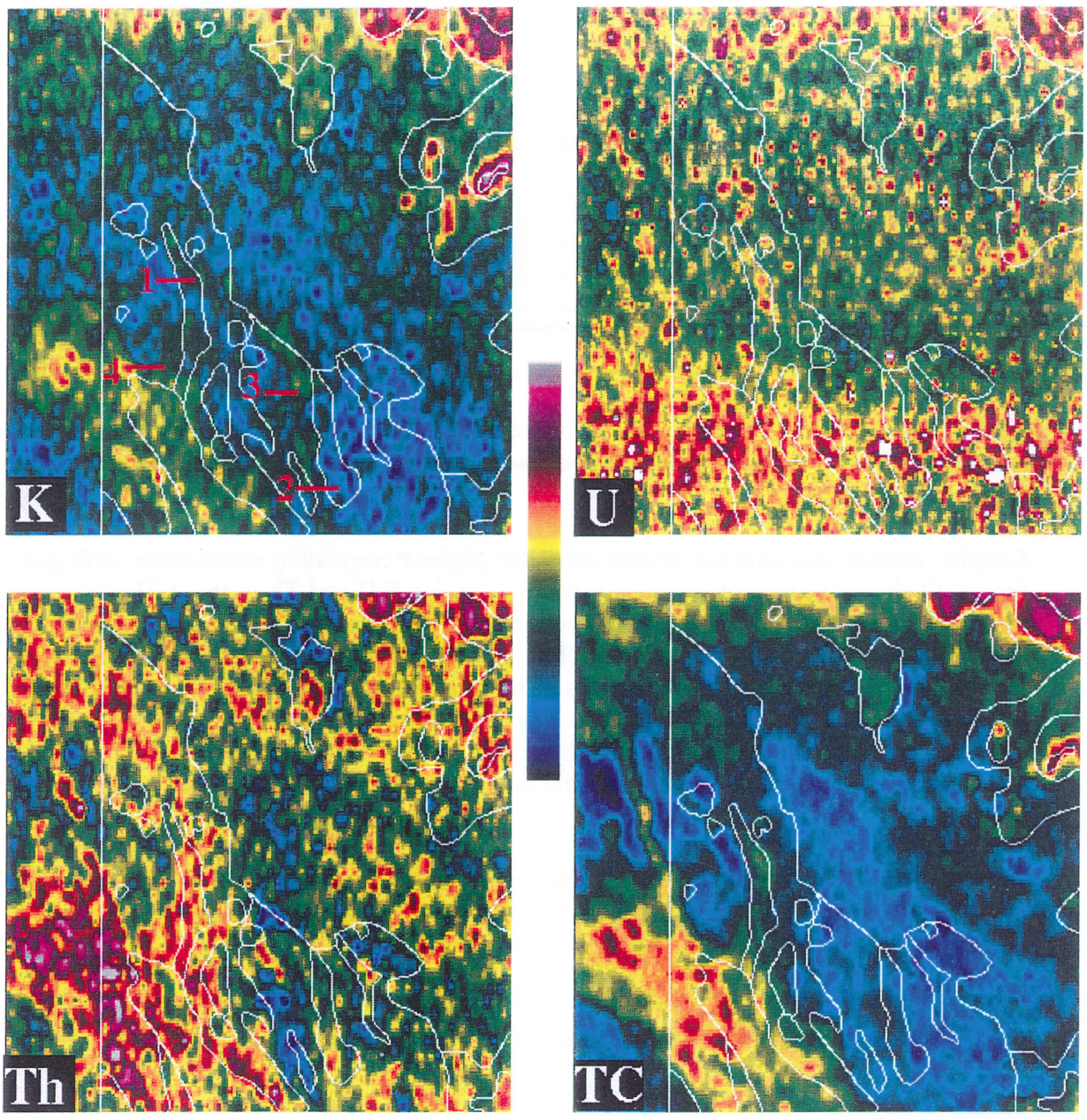

Figure 20. Bullenbong Plain AGS data. Element concentrations and total count (TC) are relative (see colour scale - blue = low). White lines are soil-landscape units (see Figure 21) Red lines (1-4) on the K image are ground follow-up traverses. Australian map grid coordinates (Zone 55) are: top-left = 497115E,6118852N, bottom-right = 512515E,6103002N.

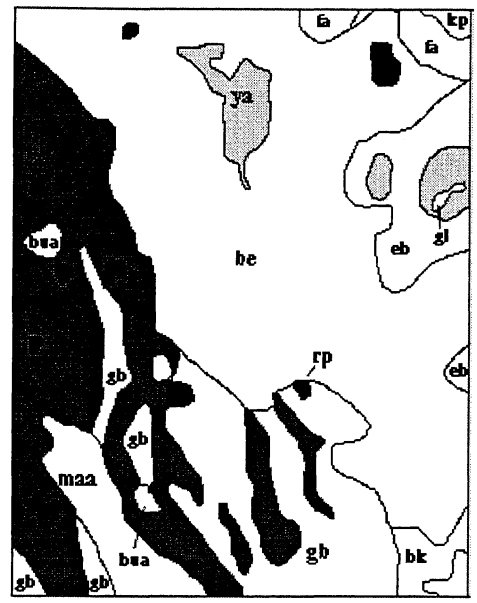

Figure 21. Soil-landscape units mapped on the Bullenbong Plain (after Chen and McKane, 1996)
Active alluvial areas
kp,fa - Murrumbidgee River floodplain soils, minimal prairie soils, brown earths.
maa - Burke's Creek alluvial sediments, red earths, red and yellow podzolic soils (sandy topsoil).
Alluvial plains
gb - red brown earths, yellow, red and grey-brown podzolic soils.
be - thick alluvial clays (with windblown clay addition), non-calcic brown soils, red and brown earths.
bu, bua - lower Burke's Creek alluvials, grey and brown clays, brown chromosols, grey-brown podzolics, local gilgai.
Swamp
rp - grey and brown clays.
Granite landscapes
gl (low hills), eb, ya (undulating rises) - red earths, non-calcic brown earths.
Metasediment landscapes
bk - footslopes, red podzolics, non-calcic brown soils, red earths.

The gamma-radiometric images for the area are shown in Figure 20 with landscape unit boundaries overlain. The total count image represents a combination of the effects of the three elements and shows patterns of alluvial channels. K, U and Th images are remarkably uncorrelated apart from the active alluvial floodplains in the north (Murrumbidgee River) and south-west (Burke's Creek) of the area. High thorium and total count in the middle left of area shows what appears to be an older alluvial system joining the two modern floodplains. However the same feature is not discernible in the K image - this may be a result of K leaching which has been observed in both regional and Ladysmith samples.

3.2.2.2. Ground truthing of image data

To investigate the image variations, four traverses were conducted (see Figures 20a,22,23 and 24) which included ground spectrometer readings, bulk soil sampling to 30 cm depth and field observations. Figure 22 shows the comparison between airborne and ground results for the first traverse. Between sites 4 and 5, a heavy rainstorm hit the area resulting in temporary surface

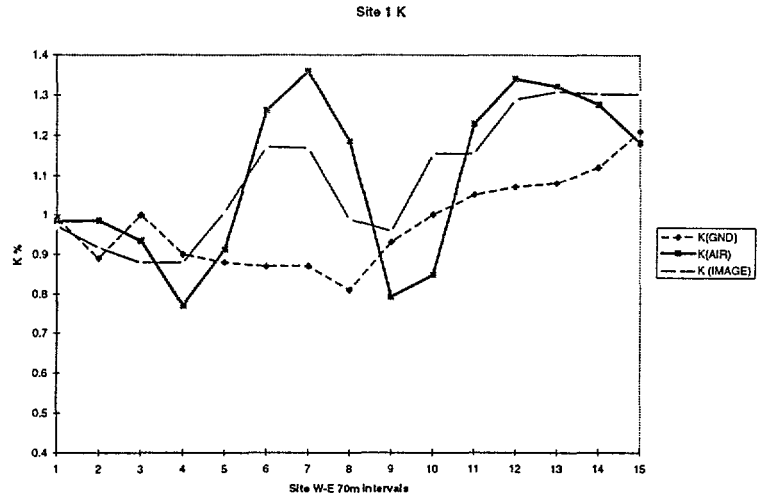

Figure 22(a). Potassium along profile (Traverse 1) measured by ground and airborne gamma methods. 'Air' values are airborne profile values. Nearest 'image' values were extracted from the interpolated grid. Sites 1 to 15 are west to east.

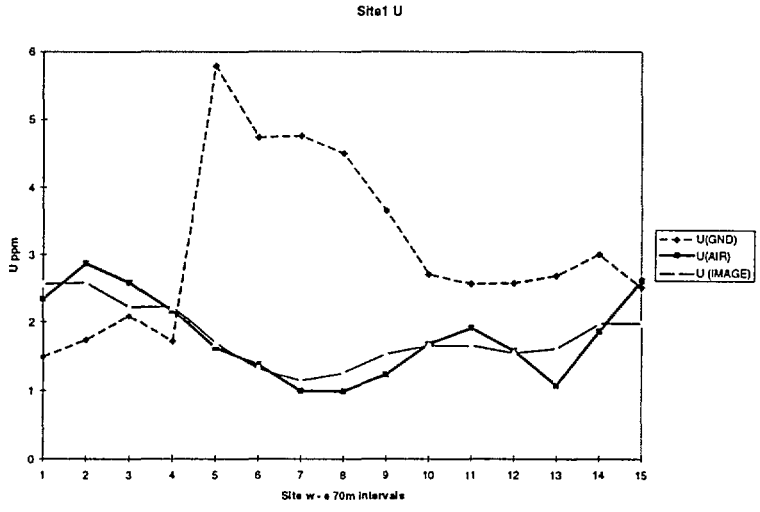

Figure 22(b). Uranium series concentration along Traverse 1

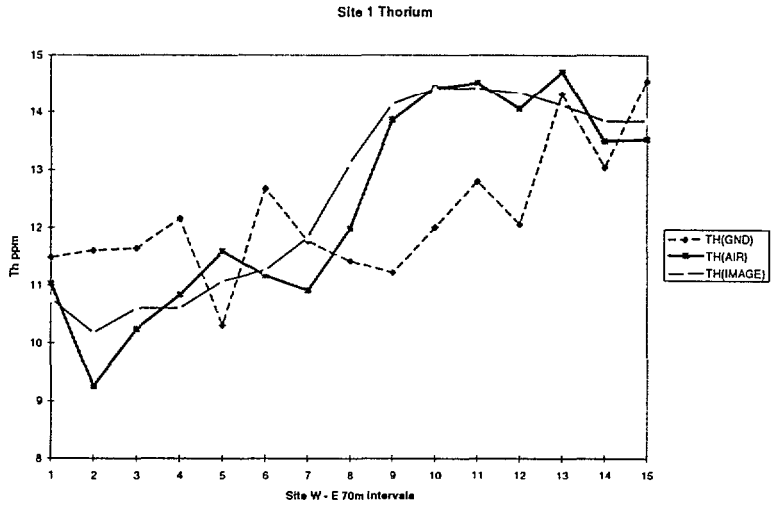

Figure 22(c) Thorium series values along Traverse 1

saturation. The U graph (Figure 22b) shows the effect of precipitation of radon daughter products (see Table 2) washed out of the atmosphere. This is a commonly observed phenomenon after rain (Charbonneau and Darnley, 1970) and the resulting radioactivity gradually decreases as the deposited elements decay. Poor correlations and unusual ground readings (in Th and K data) at site 5 and after may be due to the attenuation of gamma-rays by surface water or temperature fluctuations of the crystal. Ground and airborne K data are so different that it is suspected that local variations of K, away from the traverse, are the cause. Table 8 gives general soil observations along the traverse. Lower values of both K and Th generally appear to relate to the presence of gilgai and grey cracking clays. Soil samples of the top 30cm, collected at sites 12 and 15, shows a decrease in clay content (from 62 to 43%) and associated exchangeable cations together with an increase in fine sand particles at the end of the traverse. This supports the image interpretation that the high thorium area traversed at site 15 of traverse 1 shows an earlier alluvial system.

Table 8. General soil description along traverse 1

Traverse site	**General soil description (top 30 cm)**
1-2	Gilgai
3	Grey to pink/yellow cracking clay
4	Gilgai
5-8	Grey to pink/yellow cracking clay
9-12	greyish yellow brown cracking clay
13-15	dull yellow brown non-cracking clay

Observations of soils and spectrometer measurements along other traverses were somewhat inconclusive. Soil sample results from all traverses were combined to test for any associations between soil properties and gamma elements. Airborne readings from the nearest pixel were also used in this analysis. The four highest K and Th ground spectrometer readings were all from traverse 4 which was located near the present course of Burke's Ck. This is due to recent floodplain deposition of K and Th bearing clays and silts (this is evident on K and Th images - see Figure 20). Figure 23 shows silt percentage versus gamma measured K concentrations. This pattern is similar for the thorium data. Thus, for areas of recent alluvial deposition, K and Th images give grainsize information of the upper soil layer. Correlations between these elements and other soil properties in the remaining areas are less clear.

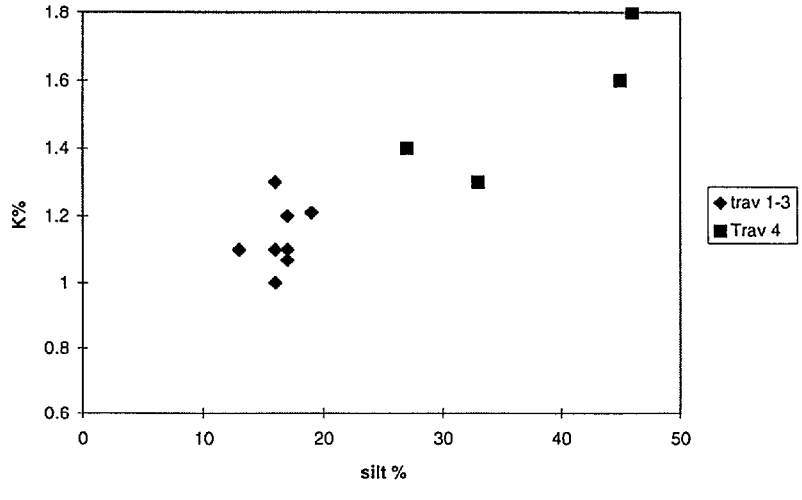

Figure 23. Silt content in the top 30cm versus ground spectrometer measured K on the Bullenbong Plain.

The four samples associated with modern floodplain deposition were removed from the analysis as outliers. The dominant variation in airborne K patterns away from recent deposition areas is suspected to be due to leaching. This is not supported by pH relationships (samples from recent alluvial areas are more acid - pH = 4.7), although samples with low K readings have high exchangeable Al values, possibly indicating that leaching is occurring. In this area, the Thorium image appears to show the most promise in terms of mapping soil variations. Both ground and airborne measurements of Th correlate with 'clay dispersion' which measures the ease in which clay disperses in water (see Figure 24).

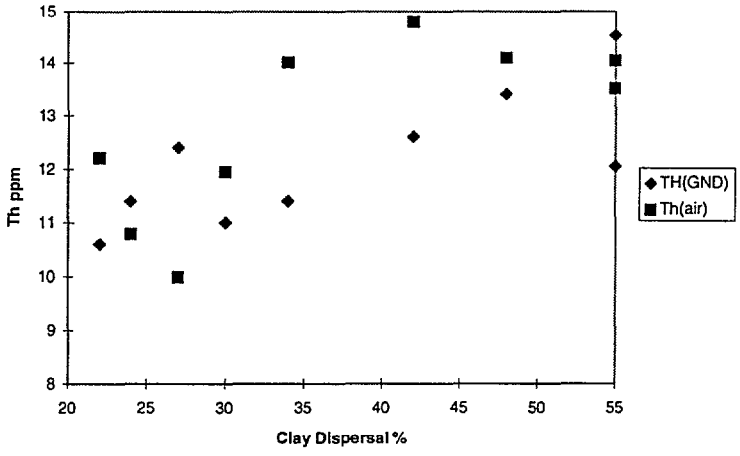

Figure 24. Soil clay dispersal versus airborne and ground measurements of Thorium

The fact that a relationship exists between Th and dispersion properties, and that clay content and Th are not correlated, indicates that Th values are related to clay type. This agrees with observations in the field that low thorium areas in the image data relate to swelling and cracking clays, ie montmorillonite group clays. Conversely, higher thorium areas relate to greater proportions of non-swelling clays such as kaolinite and illite. A negative relationship also occurs between Th and exchangeable K [N = 9, R = -0.6 (gnd), -0.76 (air)] and organic carbon [N = 9, R = -0.46 (gnd), -0.51 (air)] which may indicate the effects of the different soils on vegetation productivity. Although there appeared to be a relationship between exch Na and clay dispersal (N=13, R = 0.59), a Th versus exch Na was not evident.

Uranium ground readings show relationships with both clay content and clay dispersal properties, indicating that both clay abundance and type influence the U readings. Curiously the airborne U image data shows a positive relationship with clay content, including the recent alluvium samples, but no correlation with the amount of clay dispersal. This is somewhat surprising since less information is expected from the airborne U data which is often noisy.

3.2.2.3 Interpretation of geomorphic units

In terms of sediment provenance, the airborne gamma-ray data for the Bullenbong plain is useful for understanding geomorphic history and determining soil types at the surface. High values of K (> 1.4%) and Th (>15 ppm) in the respective images (Figure 20) show areas of recent deposition. Samples of the top 40 cm in these areas showed high levels of silt. Away from the current floodplains, soils are much older and there is little correlation between Th and K data. This is because K is strongly influenced by leaching effects over time and Th shows different phases of deposition and source materials. Intermediate thorium values (12.5 - 15 ppm) relate to an older

phase of alluvial deposition with low silt and the clays are mainly non-smectites, ie illite and kaolinite. In some areas, Th values in this range also relate to the deposition of wind-blown clays or 'parna' (see middle right of image). Low thorium areas (< 12.5 ppm) represent the earliest phase of alluvials where the dominant clay is montmorillonite and seasonal cracking is common. Montmorillonite forms in conditions where leaching is absent (Buckman and Brady, 1960) but in general smectites may form in a variety of environments (Velde, 1995). This earliest phase of deposition may relate to a period of aridity and subsequent phases possibly relate to wetter climatic conditions. Alternatively, smectite areas may be a result of lake deposition. The most recent deposition of silt is probably a result of increased erosion due to land clearing in the last 100 years.

The difference in thorium gamma response between cracking and non-cracking clay soils is not conclusively a function of different source materials for the different phases of alluvial deposition. There is some evidence to suggest that radon gas release from cracks in the soil may reduce the amounts of detectable daughter products in both the ^{232}Th and ^{238}U chains (see Table 2). Ground readings for both U and Th were consistently lower on cracking clays than non-cracking areas. The only real test was to compare gamma measurements of daughter products against the parent element. Figure 25 shows XRF results for all thorium isotopes in surface sections of regional samples versus the nearest image values from image data. Only five of the regional samples were designated 'cracking clay' and theoretically, if ^{220}Ra is being lost from the system, XRF values should be larger than ground readings. The fact that four of the five 'cracking clay' samples are further from the 1:1 line toward the XRF value in Figure 25, suggests that radon loss is a significant factor in airborne Th signal differences for the clay types - it may be the only factor.

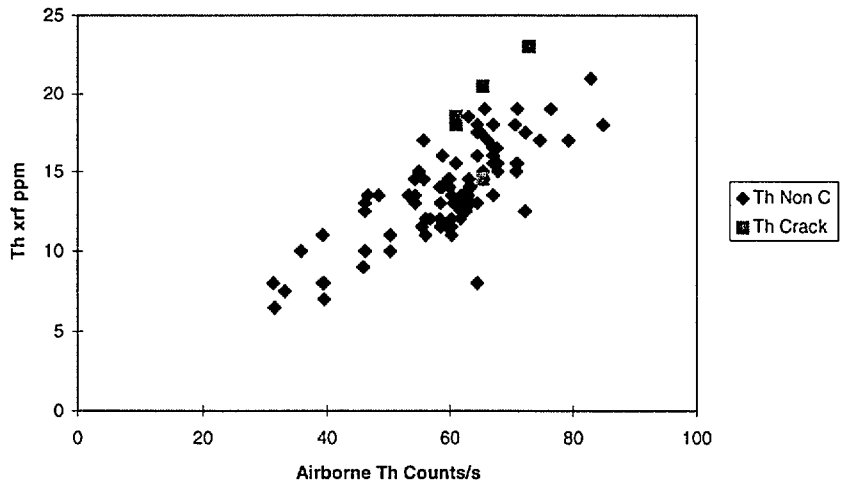

Figure 25. Thorium in regional samples (measured by XRF techniques) compared with airborne measured ^{208}Tl possibly showing the loss of ^{220}Ra from cracks.

3.3 Comparison with soil-landscape mapping

Given that the Wagga Wagga sheet was mapped into soil-landscape units (Chen and McKane,1996), it would be useful to compare the units in terms of gamma-ray signatures. This could both aid in the interpretation of the gamma-ray data and determine whether landscape units can be directly derived from the data.

3.3.1 Whole area

Figure 26 shows a K versus Th plot of means for all landscape units broken up into alluvial plains, piedmont terraces/ sloping plains and hilly areas of respective bedrock types.

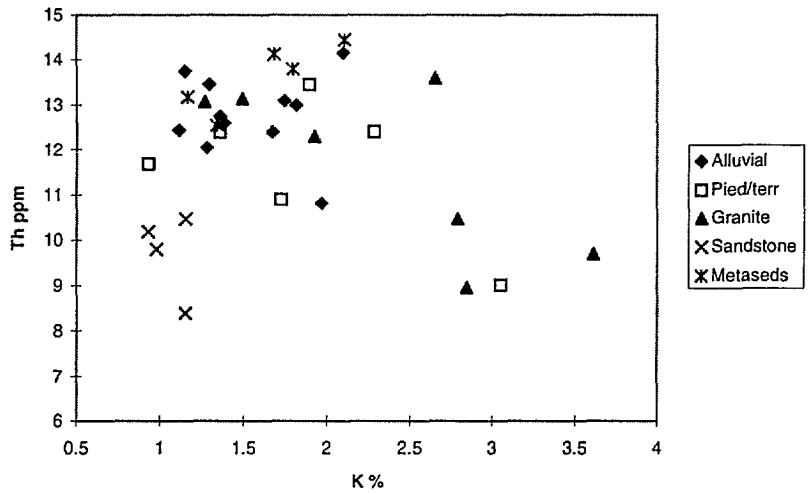

Figure 26 Mean K and Th values for mapped soil-landscape units for hilly bedrock areas and other categories.

Standard deviations are not displayed but there is significant overlap between units. Sandstone derived units and some granite units are distinctly separated but remaining units are closely clustered. Uranium data not included in this graph is the least discriminating and, in fact, is probably not useful due to noise and airborne radon signatures (as discussed later). Computer derived classification, therefore, of the gamma-ray data on it's own is likely to produce a result which relates poorly to landscape unit mapping. Part of the reason for the lack of separation of landscape-units is there can be similar gamma-element signatures between source bedrock areas of different types and alluvial areas containing source materials. Also similar signature defining processes (such as leaching in mid-slope areas) may operate in different landscapes. The airborne gamma-ray data is better interpreted by first subdividing a region into areas of unique geology and landform. This means that gamma data becomes useful when combined with geology and digital terrain attributes.

3.3.2 Ladysmith study area

The Ladysmith study area, subject of the more detailed 100m spaced airborne survey, is mostly comprised of hilly areas of Ordovician metasediment geology. Figure 27 shows metasediment landscape-units in terms of airborne K and Th signatures. Units Li, Ld and Pu grade from shallow soils on steep hills to deeper soils on undulating rises. Bk and Bka are deep soils on footslopes. As described in section 3.2.1, K and Th concentrations separate landscape units quite well. The overlap may in part be due to the scale and detail of landscape-unit mapping relative to the airborne data.

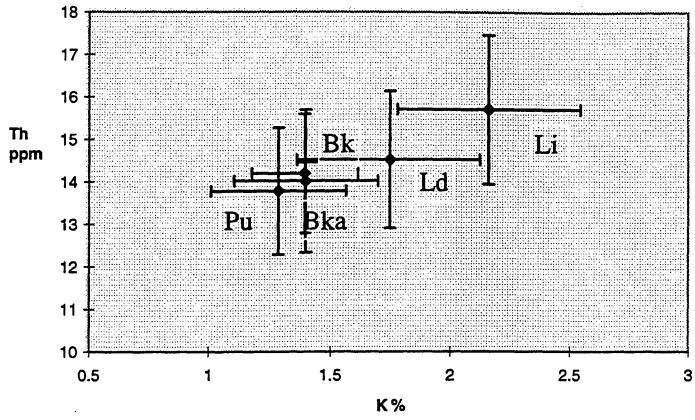

Figure 27 100m spaced airborne survey K and Th means for soil-landscape units assigned to hilly areas of metasediments in the Ladysmith area.

Similarly, alluvial and sloping plain units on different parts of the sheet may have similar signatures but can be successfully interpreted locally using the airborne data. In these cases, statistical analysis of regional unit signatures is not particularly useful.

3.4 Investigation of uranium anomalies associated with groundwater discharge sites

This section deals specifically with the regional interpretation of 'uranium' data. An initial observation was that particular U anomalies were associated with known areas of high water tables and salinisation. It was decided to investigate these anomalies, given the possibility that airborne U may detect salinization due to high water tables. As mentioned previously, regional uranium concentrations are interpreted from airborne measurements of gamma-rays emitting from the isotope ^{214}Bi (see Table 1). Resulting U images are therefore measure decay-products of this isotope which may or may not be in equilibrium. Due to low counts in this channel, 'uranium' images are often very noisy. Figure 4 shows uranium data for the airborne survey area (flown in May, 1992) and the data are difficult to interpret due to significant noise. Two image processing methods were employed in this case to improve the data.

3.4.1 Image noise correction

Two methods, Principal Components Analysis (PCA) and a method developed by the author (Bierwirth, 1994) were used to clean up the data:

1) PCA. This procedure rigidly rotates the coordinate axes to the directions of major variance within the data (Richards,1986) and represents them as images. The first principal component (PC1) images materials whose surface variation dominates the data. The second and subsequent PC axes show less dominant variations and the last PC commonly shows and isolates the noise. PC axes can be manipulated so that the noise isolation can be refined. Figure 28(a) shows PC4 from the analysis of the Wagga data set. Noise can then be removed from the data by rotating the first three PC axes back to the original channels.

2) Attenuation modelling. This technique finds the logarithmic average (weighted by gamma attenuation coefficients) of the four channel data and then removes this from the total count

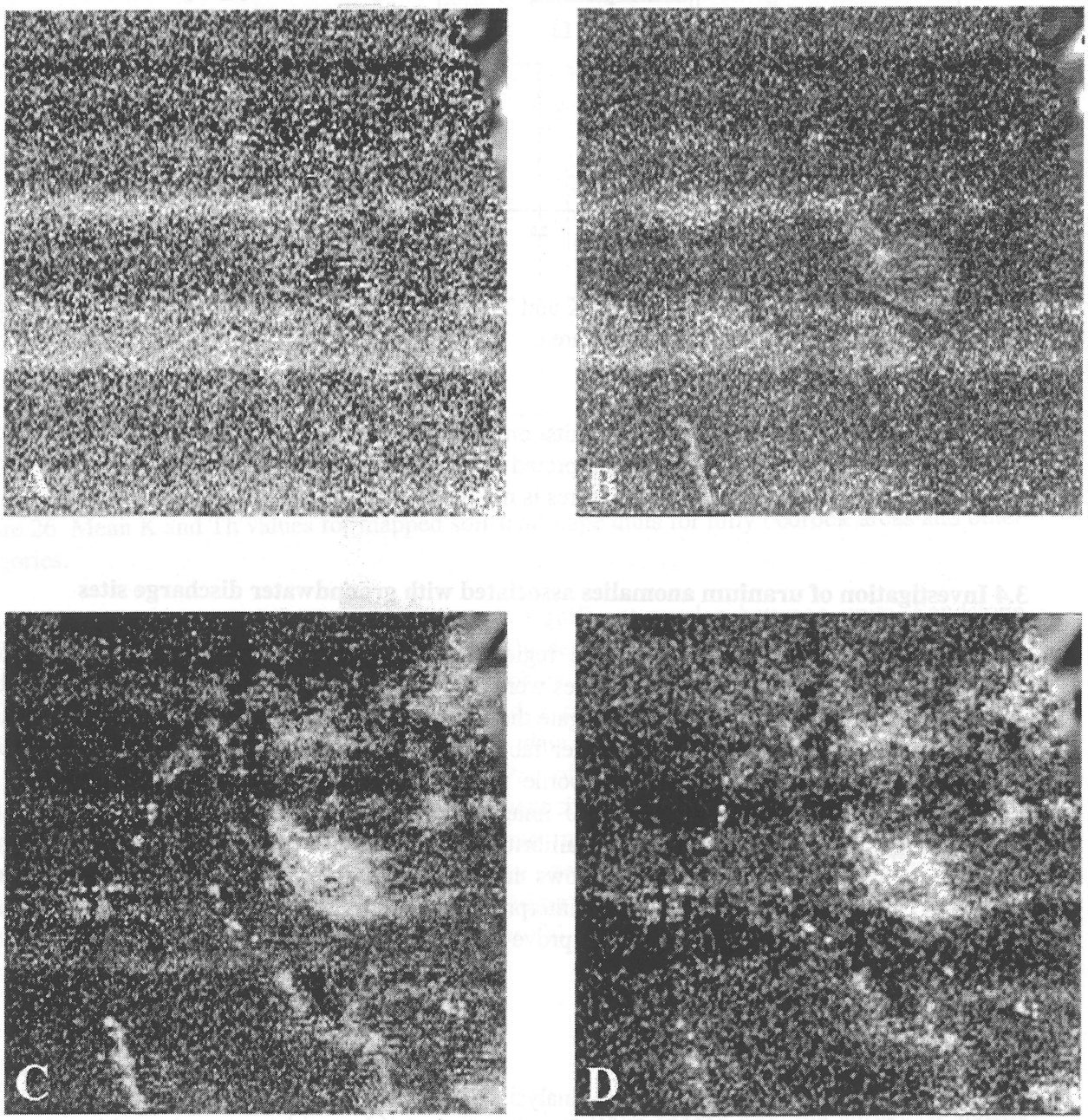

Figure 28. (a) Image noise derived from Principal Components Analysis. (b) noise derived from the 'attenuation modelling' algorithm (Bierwirth, 1994). (c) cleaned U image by the attenuation modelling method and (d) results of a 7x7 averaging filter.

(Bierwirth,1994). This isolates the noise largely contained in the uranium channel data (Figure 28b). The correlation between this noise image and the raw uranium image is then found and removed using PCA. Although the method is not conceptually well understood (being arrived at by experimentation), the results validate the method and show promise of further refinement by continued research.

The resulting cleaned-up version is shown in Figure 28(c). The two methods produced very similar results although the second method was deemed marginally better. Another approach is to attempt to lower the statistical noise by applying an averaging filter (Figure 28d). This reduces the spatial detail but is ultimately the most reliable method.

3.4.2. First Airborne Survey (May 1992) - Regional Uranium Anomalies

Figure 29 shows the noise-corrected uranium data in colour draped on the satellite acquired SPOT digital elevation model (DEM). Areas of exposed granite bedrock mapped by Raymond (1993) have been masked in white to eliminate areas where high U is bedrock controlled (granites commonly have high U contents). This study aimed to investigate the origin of the remaining area of high concentrations of uranium series isotopes, shown as red and yellow, which are not obviously controlled by bedrock geology. The four localities A-D are sites of ground investigations. After initial measurements with a ground spectrometer at sites B and C failed to find ground anomalies, a second small airborne survey was flown (see boxed area).

3.4.3. Second Airborne Survey (November 1993) - Verification

A small second airborne survey over the Kyeamba creek area (Figure 29), was acquired in early November 1993. The survey was flown at 100 metres line spacing, and gridded to a 50 metre pixel. Figure 30 compares the results from the two airborne surveys: May 1992 (Figure 30a) and November 1993 (Figure 30b). The uranium data have been draped over a digital terrain model derived from the positioning data acquired simultaneously by the aircraft.

Clearly, many of the U anomalies in the first survey were not reproduced in the second survey, with the exception of locality A (note that the color scale is not calibrated between the two images). Possible explanations for the difference include seasonal changes in radioactivity (for example, due to groundwater movement) and ephemeral accumulation of radon gas at the time of the first survey, which were not present during the second survey. Ground studies were carried out to investigate these possibilities.

3.4.4 Ground spectrometer surveys and soil analysis

Sites A and B are both within the Kyeamba Creek system and were covered by both airborne surveys: site A was the only area to display high U response in both. Site C is at the base of a sandstone escarpment at The Rock, west of Wagga. Site D is a diffuse zone of high U response within the Wagga Wagga township on the Murrumbidgee floodplain.

Ground gamma-ray measurements were taken along lines corresponding to aircraft flight line U anomalies at sites A (second survey), B and C (first survey) using a portable gamma-ray spectrometer. At site D, a number of point measurements were taken. The sampling strategy for ground measurements employed a grid of 3 x 3 (+1 random) points spaced 10 metres apart around

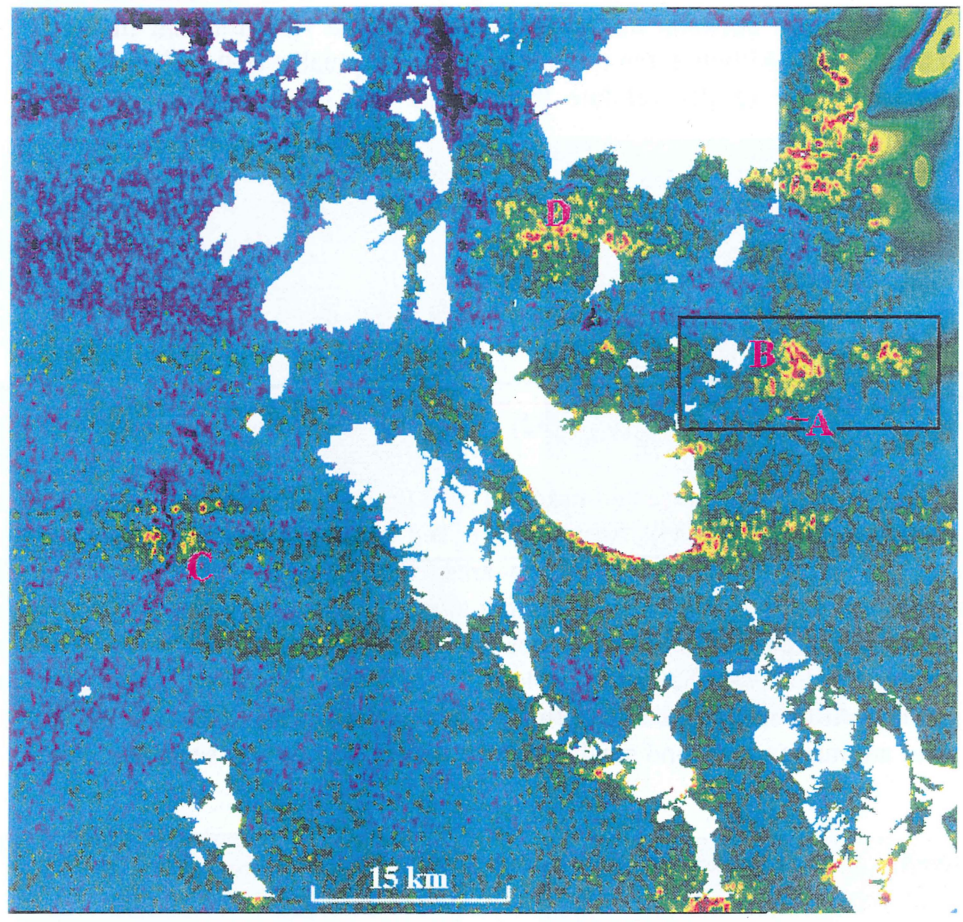

Figure 29. Uranium concentration for the Wagga 1:100000 sheet interpreted from AGS data. Red = high U, Blue = low. Areas mapped as granite are masked in white.

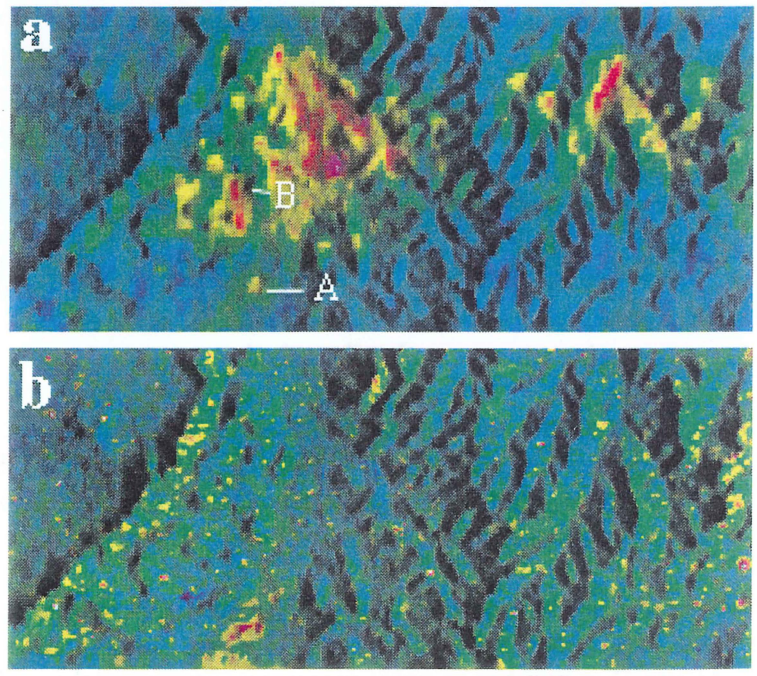

Figure 30 Ladysmith U data - two airborne surveys (a) 400m line-spaced - May, 1992. (b) 100m line-spaced - Nov, 1993. Colour coded U counts are draped on shaded elevation derived from the 100m survey.

the central aircraft sample point (fiducial), in an attempt to simulate the broad sampling of the aircraft spectrometer. The fiducial was located by using the on-board video system which provides visual identification of the sample point. The ten 30 second readings with the 0.35 litre crystal were then averaged. At sites A and B, measurements were taken at intervals over a 15 month period to investigate the possibility of seasonal variation in levels of radioactivity in soils due to groundwater fluctuations.

Generally all ground surveys at sites A and B (Figures 31 and 32) in the multidate survey area conform with the results of the second survey (see Figure 30). Large differences occur between overall concentration values from aircraft and ground spectrometers. This is due to a difference in calibration sensitivity constants for the two instruments. The ground spectrometer generally gives values close to expected concentrations for rocks and soils in the region. Ground investigation at each site is described separately.

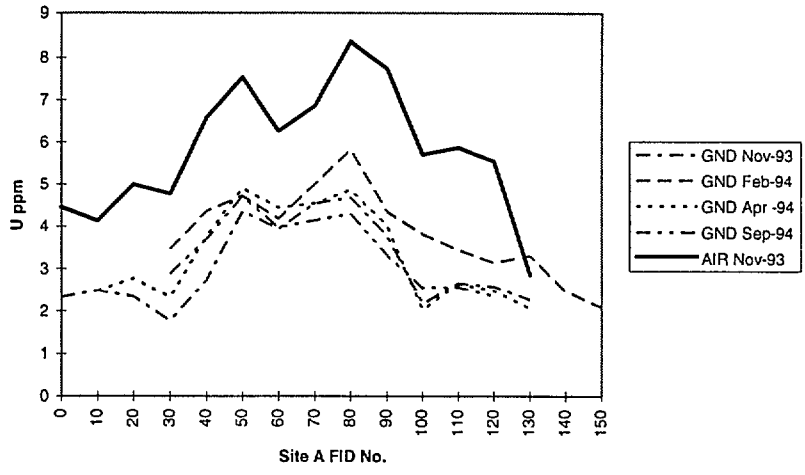

Figure 31. Aircraft versus ground profiles measuring Uranium concentration at Site A ("Springfield", Kyeamba Creek). Fids 80,90 etc correspond with aircraft sample points 70 metres apart.

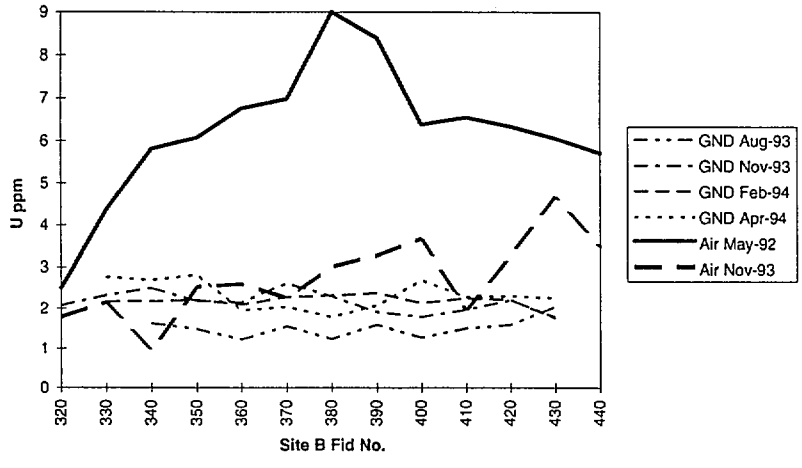

Figure 32. Aircraft versus ground profiles measuring Uranium concentration at Site B ("Mona Vale", Kyeamba Creek). Fids 320,330 etc correspond with aircraft sample points 70 metres apart.

3.4.4.1 Repeatable Anomalies

Site A: Results of ground spectrometer traverses at site A, relative to the airborne data, are shown in Figure 31. At site A, a small area detected in both the May 1992 and November 1993 airborne surveys, ground surveys showed elevated uranium concentrations correlating well with the aircraft profiles. The high ground readings coincide with unusually high soil concentrations of ^{238}U and ^{232}Th isotopes as shown by soil analyses (Table 9).

Table 9: Analyses of soil materials from areas of high and low U channel response on "Springfield" (A).

Sample	Fid 80 (average of 5 samples)	Fid 100 (average of 5 samples)
pH (1+5 H_20)	5.7	5.3
EC (uS/cm)	62	40
C (%)	1.51	0.87
Ex Ca (cmol/kg)	4.0	0.7
Ex Mg "	2.2	0.3
Ex Na "	0.44	0.01
Ex K "	0.27	0.14
CEC "	10.68	3
Coarse sand (%)	1.8	17.2
Fine sand (%)	23.4	60.8
Silt (%)	41.2	14.4
Clay (%)	29	6.2
Cs-137*	3.2	2.5
K-40*	652	706
^{238}U decay isotopes		
U-238*	134	35
Th-234*	141	34
Th-230+	133	40.5
Ra-226*	127	37
Pb-210*	92	40
^{232}Th decay isotopes		
Ra-228*	71	42
Th-228*	71	42

* Bq kg^{-1} Analysed using gamma spectrometry CSIRO Division of Water Resources, Canberra.
\+ Bq kg^{-1} Analysed using alpha spectrometry.

Having located an anomaly at site A which could be verified on the ground, soil samples were collected from the zones of high (Fid 80) and low (Fid 100) uranium channel response. Five samples were taken from each site, over an area of 20 x 20 metres, bulking the top 20 cm of soil. The samples were analysed for U and Th series nuclides using gamma spectrometry by the CSIRO Division of Water Resources; and for standard soil chemical and physical properties by the CSIRO Division of Soils. The average analyses for the 5 bulk samples from each site are given in Table 3. The two sites display very clear differences in soil texture and chemistry. The high U site (Fid 80) has much higher clay content (almost 30%), with correspondingly higher levels of exchangeable

cations and CEC. The analyses confirm the difference in U concentration: U levels at Fid 80 are over three times higher than at Fid 100, in approximate proportion to the difference in CEC. Neither site shows significant disequilibrium of ^{226}Ra, although ^{210}Pb is depleted in the high U zone.

The lack of disequilibrium suggests that the elevated ^{238}U soil concentrations are not deposited by groundwater since deposition of ^{238}U and ^{226}Ra would not be expected in equal concentrations. Also ^{230}Th, which is also in equilibrium, is not known to be soluble except in extremely acid conditions, so that it's concentration would be expected to be much lower if groundwater processes were involved. The results indicate that the anomaly at site A can be validated from ground and laboratory measurement and appears to be related to adsorption onto clays and mechanical transport of sediments.

3.4.4.2 Non-repeatable anomalies.

The anomalies detected by the May 1992 airborne survey at sites B, C, and D (Figure 29) , however were never detected in any other measurements and are seen to be truly ephemeral effects. At Site B (see Figure 32), part of the larger U anomaly that occurs only in the first airborne survey (see Figure 30), neither the second airborne survey nor any of the ground measurements detected elevated U levels. Similarly, at Site C the anomaly found in the first airborne survey could not be identified on the ground.

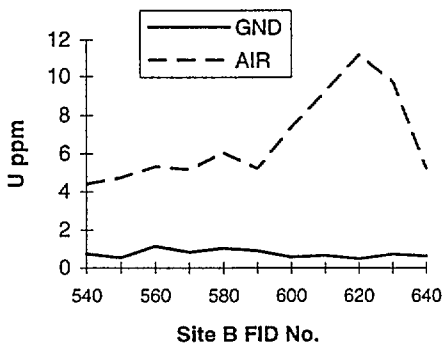

Figure 33. Aircraft versus ground profiles measuring Uranium concentration at Site C (near "The Rock").

Within the Wagga township (Site D) ground spectrometer readings were taken at five sites around the town. Figure 34 shows a scatter plot of aircraft versus ground measurements for site D compared to site A. While there is a good correlation at site A, the ground readings in the town were all low. Aircraft readings are generally higher due to calibration problems between the two instruments.

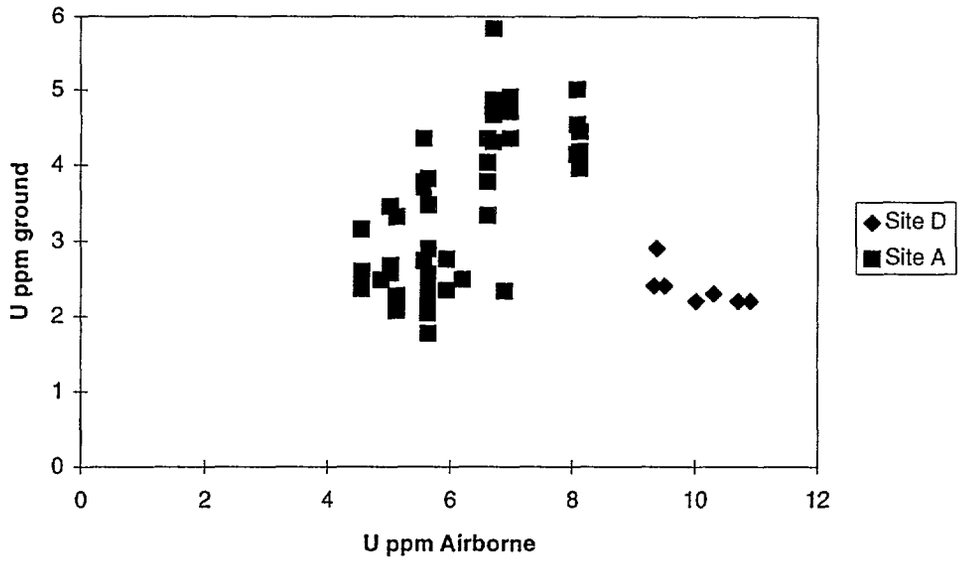

Figure 34. Scatterplot of aircraft versus ground spectrometer Uranium measurements for both sites A and D

3.4.5 Discussion - possible reasons for ephemeral anomalies

The initial airborne survey identified U anomalies, in the Kyeamba Land Care Area and in Wagga Wagga itself, which are significant in both areal extent (> 9 sq. km) and intensity (two to three times background levels), but which are not related to bedrock geology and could not be verified by later measurements. This raises the probability that the aircraft detected relatively discrete pockets of air with elevated radon levels.

Radon-222 is an element in the ^{238}U decay chain (see Table 2) and, based on the half lives of it's daughter products, can generate detectable Bismuth-214 in minutes. It has been recognised for some time that U channel AGS is subject to interference from atmospheric ^{222}Rn and various methods have been developed to correct for these effects. For example, Minty (1992) estimates atmospheric radon using full spectrum or multichannel observations from the shape and relative intensity of peaks, since attenuation in air is different to attenuation by cover. The correction factor is calculated every 100 seconds (about every 7 km) along the flight lines. The correction thus generates a map of airborne Rn on a 7 km grid - see Figure 35. The banding is due to variations in atmospheric radon levels for individual flights on different days. It can be seen that background radon levels were generally higher in the vicinity of the U anomalies under discussion (A - D). This image was used in earlier processing to correct for atmospheric radon. The underlying assumption is that radon in air is relatively well mixed, and is unlikely to vary significantly over distances less than a few kilometres. Thus the correction will not account for discrete pockets of radon of the size postulated here.

High radon concentrations in groundwater are common (Brutsaert et al, 1981) and significantly, both anomalies are in locations where groundwater levels are near the surface and soil salinity problems are being experienced. The Ladysmith area was one of the first in the region to develop salinity problems due to rising groundwater levels. Figure 36 shows areas of salinity outbreak in the Wagga Wagga township relative to 'uranium' anomalies. Also, the uranium anomalies shown

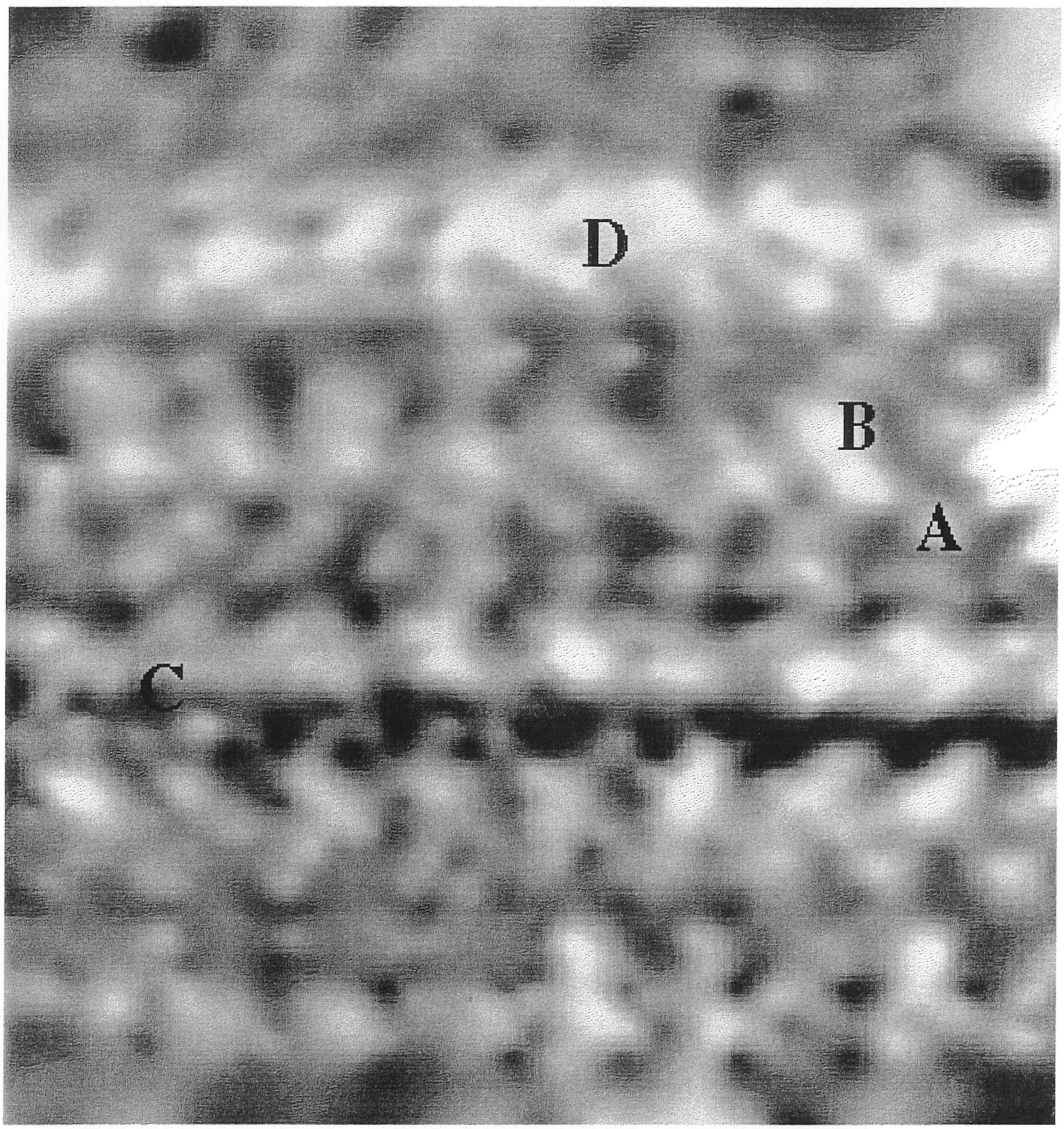

Figure 35. Atmospheric radon measurements derived by full spectrum analysis using data collected every 100 seconds (7 km) on each 400m spaced flightline.. Locations A-D relate to U anomalies (see Figure 29).

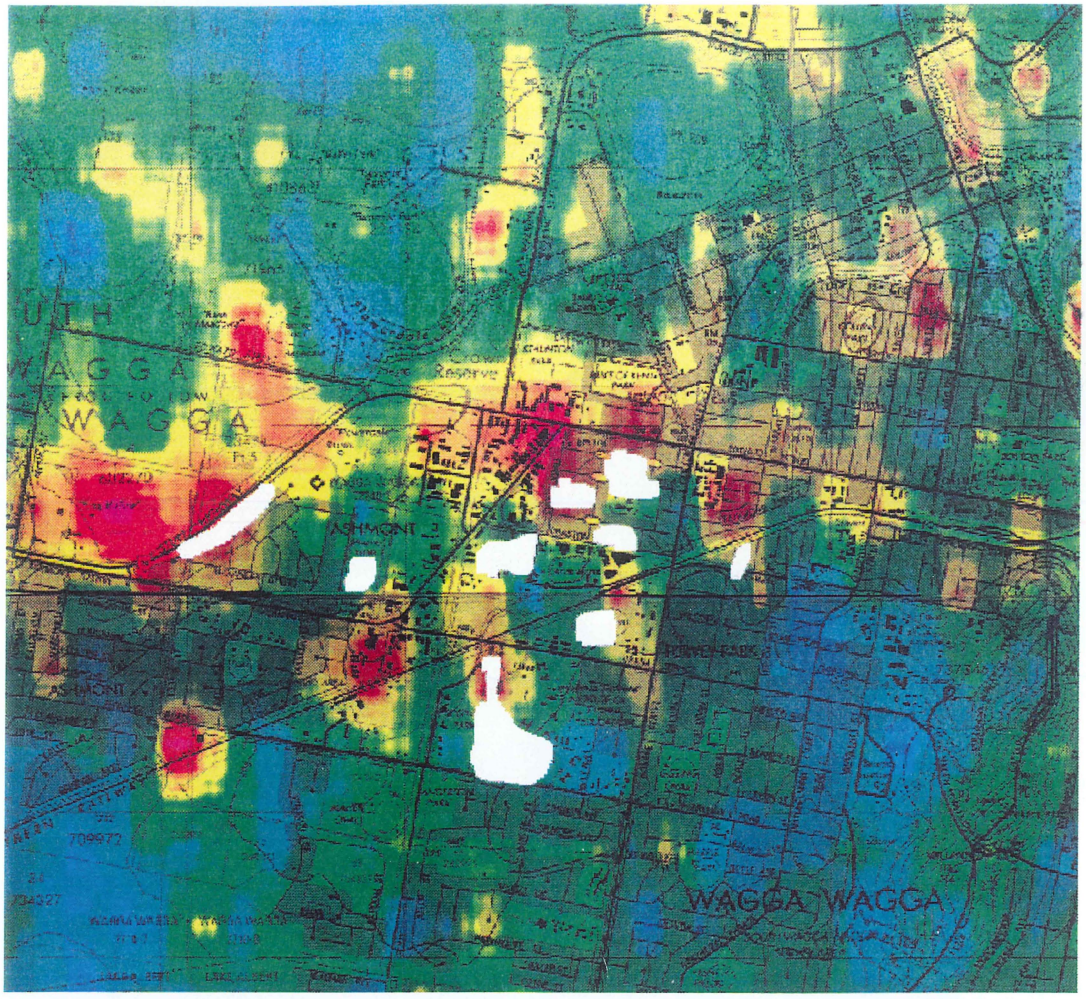

Figure 36. Uranium anomalies (red = high) attributed to radon in Wagga Wagga.. White areas are known sites of surface salinisation.

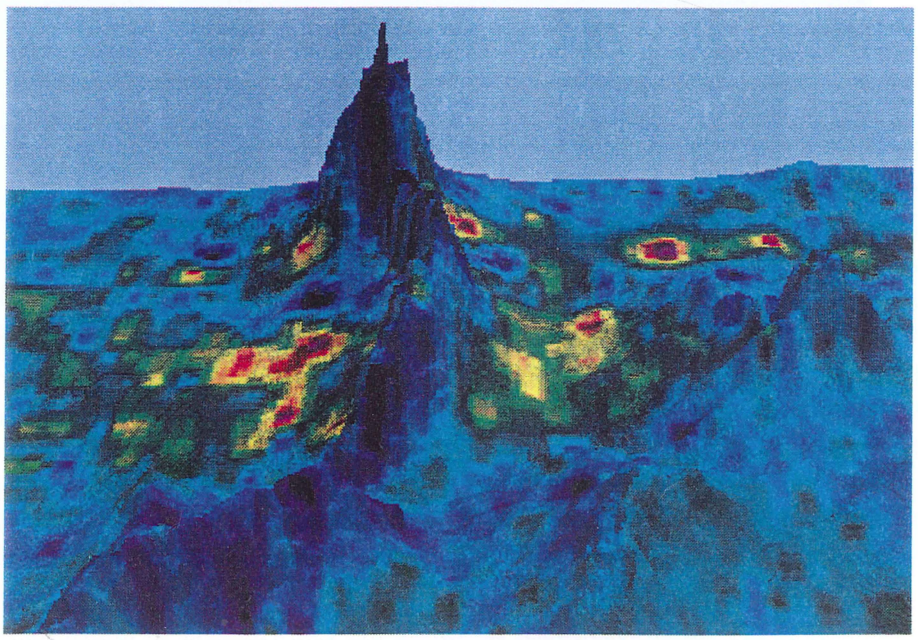

Figure 37. Uranium concentrations at 'The Rock' interpreted to be radon 'clouds' associated with groundwater discharge.

at the base of the Devonian sandstone units at 'The Rock' in Figure 37 are associated with observed waterlogging and groundwater discharge. At all three sites, discharging or near surface groundwater conditions correlate with ephemeral airborne anomalies.

Analysis of groundwater samples collected from two bores in the Kyeamba Land care area show high concentrations of radon gas (^{222}Rn). The water from the bores contained radon concentrations of 71.3 and 219.5 Bq/L respectively. For comparison, a Western Australian statewide survey of 69 Water Authority schemes found only 2 had radon levels exceeding safe levels (100Bq/L) for drinking water (Thorpe,1994).

Radon, released by the groundwater into the atmosphere is the likely source of the airborne readings. The fact that a second airborne survey and subsequent ground measurements failed to detect radon indicates a difference in conditions at the time of the first survey. Figure 38 shows wind speeds from a nearby weather station at the times of all gamma-ray measurements. At the time of the first survey, wind speeds were negligible allowing the gas to accumulate just above the surface creating 'uranium' anomalies.

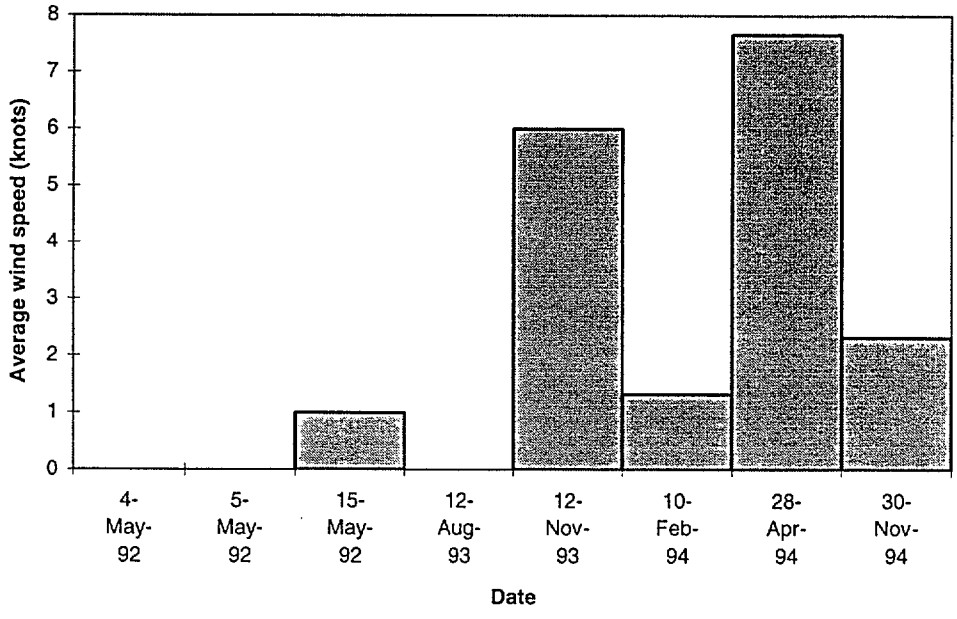

Figure 38. Average wind speed at the time of airborne (4-5 May 92/ 12 Nov 93) and ground gamma-ray measurements.

3.4.6 Conclusions and Recommendations

A number of airborne 'uranium' anomalies discovered on the Wagga Wagga map sheet are most probably due to the low lying radioactive accumulations of radon gas. Extensive ground spectrometer measurements and soil sampling failed to find evidence of ground accumulations of Uranium series elements except at one location where high U was related to deposition of radionuclides adsorbed onto clays. A second airborne survey failed to detect the phenomenon, indicating an ephemeral nature. Broad scale atmospheric measurements of radon during the initial survey show increased radon on the days the anomalies were flown. The correlation of anomalies with high groundwater levels in a number of locations and the lack of wind speed also indicate

radon as a possible source. Measurements of radon in groundwaters in the anomalous area reveal high levels of ^{222}Rn. All this evidence suggest that the observed phenomena are radon anomalies associated with high groundwater levels. This work and that of others (Ogden et al,1987) suggest that this finding could be highly significant if radon concentrations at the land-air interface could be used to determine groundwater levels and perhaps soil permeability without sinking expensive bores. The detection of radon at the surface may be useful in delineating areas of high groundwater levels and thus areas at risk from surface salinisation.

Regardless of their origin, the presence of ephemeral anomalies in the uranium channel which cannot be detected in repeat surveys means that great caution must be used in interpreting U data from AGS at detailed scales.

As a result of the findings of this work, it is recommended that:
1) a number of sites be selected for ground based studies of radon concentrations over time related to health risks in both urban areas and drinking water.
2) site research be conducted into the relationship of radon with groundwater levels, soil permeability and salinity.

3.5 Resolution of airborne data

3.5.1 Averaging effects of flying height

The spatial resolution of the image data for the Wagga Wagga sheet is clearly limited compared with other remote sensing tools. Data collected at 70 metre spacing along lines is severely averaged to compromise with the 400m distance between lines. Also there is a significant area between lines that contributes little to the signal. Pixel sizes may be in the order of 200 metres and the question is: how reasonable are airborne gamma-ray images in representing the actual in-ground variabilty of radioelements?

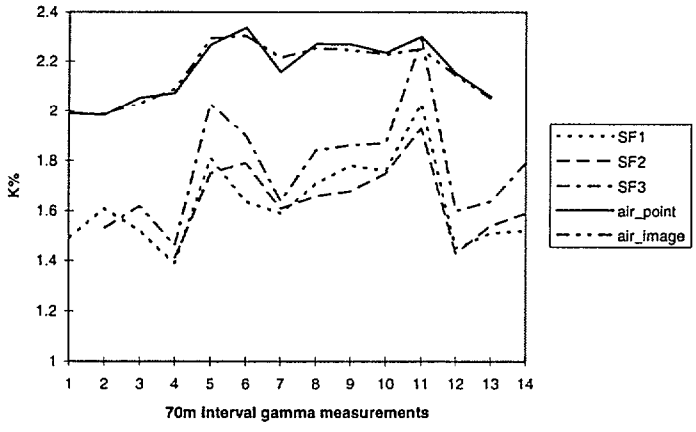

Figure 39. Comparison of ground and airborne spectrometer measurements of K along profile. SF1,2 and 3 are ground spectrometer profiles. Airborne data has been upwardly offset by 0.5% K for comparison.

Figure 39 shows the difference between ground versus airborne spectrometer measurements of K for a profile within Kyeamba Ck floodplain sediments (site A - section 3.4.4). The increased level of potassium is related to increased clay content in a small section of the floodplain. Ground readings were averaged over 25m squares in an attempt to simulate airborne readings. Nevertheless

there is considerably more detail in the ground readings. This is because aircraft measurements are averaging the ground signal due to the large effective field of view. Image data obtained for the line shows further averaging due to the gridding process. Ground readings also show good repeatability.

3.5.2. Effects of line spacing

The 100 metre line spaced survey at Ladysmith provided the opportunity to compare the effects of line spacing on spatial detail of images. Figure 40 shows images produced from the Ladysmith data at different line spacing. In producing 200 and 400 m spacing grids, lines were selectively removed from the data before the data was imaged. The cell size was left the same at 50m. Between the 400m and 200m grids there is significant improvement in spatial detail. Given the improvement in resolution from 400m to 200 m spacing, and only marginal improvement from 200m to 100m, it is justifiable that 200m is the most acceptable line spacing both in terms of spatial resolution and cost.

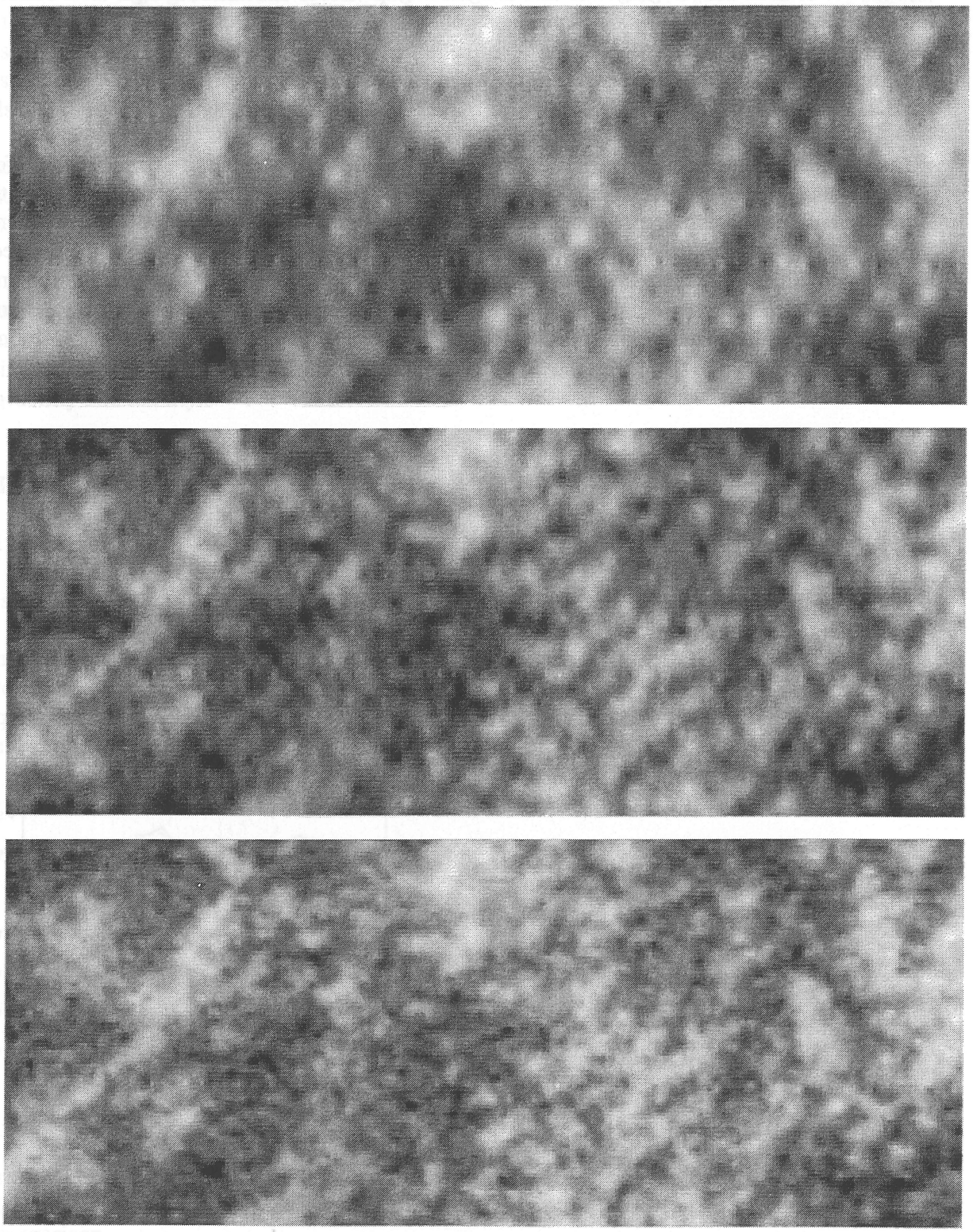

Figure 40. Comparison of three different line spacings derived from the Ladysmith 100m airborne survey - 400m (top), 200m (middle) and 100m (bottom). All images are K data interpolated to a 50m pixel.

4. DISCUSSION

4.1 Interpretation of results

Results of this study generally indicate that the three elements mapped by airborne gamma spectrometry have both unique and similar modes of distribution around the landscape. These modes can provide information about soil properties, soil mineralogy and geomorphic history. Radioelement distribution patterns are often a complex mixture of effects that require sensible interpretation. The approach taken in analysing the elements separately was seen to be important in understanding these effects.

As discussed in section 3.1.1 for areas with shallow soils on bedrock, gamma-ray signatures are variable and often high (with the exception of sandstones) and relate primarily to rock composition. These are generally areas of active erosion where fresh material is continually being exposed. As weathering proceeds, minerals break down and soils develop, there is often a loss of radioelements which are transported away attached to finer particles. In these geomorphically active areas gamma responses are a function of bedrock composition, the degree of weathering and soil thickness.

Away from actively eroding areas, there are large areas of colluvium and alluvium in the Wagga Wagga region. K, U and Th redistribute by adsorption onto and transport with clays and some K may be present within the clays. The level of adsorption depends on the type of clay. In relatively geomorphically inactive areas such as gentle slopes, geochemical weathering and fluid mobility of elements becomes important in understanding radiometric patterns. Importantly, after deposition, K leaches over time and Th does not under normal ranges of acidity. This means that in residual areas, K can be used to assess acidity/leaching over time and Th can be used to assess clay content or clay type.

4.2 Derived models for gamma-radiometrics interpretation

Sensible interpretation of gamma-radiometric data requires the integration of other data sets, the most important being digital elevation models. After subdividing into geomorphic and geological landscapes, the radiometrics can provide specific information about soil nutrients, texture and chemistry. In general at Wagga Wagga, K and Th images provide information on soils. The U signal is generally too low for soils but shows important groundwater discharge effects.

4.2.1 Mapping continuous soil variables

As discussed, the gamma-radiometric data are best interpreted on a local scale and within geomorphic and geological units. Some of the soil properties that can be mapped are outlined below including the appropriate geomorphic and geologic categories.

4.2.1.1 Soil Chemistry

4.2.1.1.1 Acidity/ Leaching.

(Geomorphically inactive soils, ie piedmont terraces and sloping plains, also colluvial slopes of metasediments and inactive alluvial areas)

Figure 41 shows regional sample results for K and pH. This is similar to Figure 9 which shows only areas classified as piedmont terraces and sloping plains. Figure 41 also includes lower footslopes of metasediments (pu) and granites (fh) as well as inactive alluvial areas (ob). The observed relationship between K and pH is significant in that, for these stable landscapes, K images may directly indicate pH. This relationship was used to create an acidity map (Figure 42). The (pu) category areas were not included because of the scatter in Figure 41

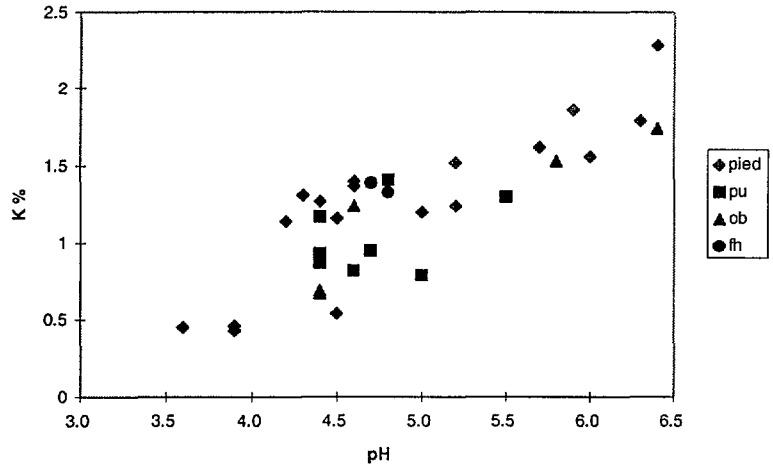

Figure 41. Acidity versus K in soil samples for residual landscape categories.

In Figure 42, only areas indicating pH < 6.5 were included to correspond with the range in Figure 41. Even so, most of the blue areas appear to be more related to high K, associated with active clay and silt deposition in alluvial environments, than high pH. Considering that low pH areas are associated with sandstone colluvium, it is unclear whether parent material or leaching is the dominant influence on acidity. Also, pH may be lowered by the use of fertilisers (Chartres et al,1990), although the effect of this is difficult to assess with respect to these data. Figure 41 may be a combination of several linear effects depending on the parent materials, leaching and fertiliser use. Nevertheless, it is apparent that K images are an important tool for indicating acidity in specific environments. These findings are, however, preliminary and the accuracy of pH mapping using K should be investigated further.

Results for the detailed study area at Ladysmith also show that K content defines, by association, the amount of leaching and the strength of development of the bleached A2 horizon. However, in a localised area such as this, the range of pH measurements was too low and measurement errors were perhaps too high for a direct pH/K relationship.

4.2.1.1.2 Aluminium toxicity

(Geomorphically inactive soils, ie piedmont terraces and sloping plains, also colluvial slopes of metasediments and inactive alluvial areas)

Soil sampling in the Wagga Wagga region showed that acid soils have high values of exchangeable Al. This means that K images can be used to indicate areas of Aluminium toxicity. A negative correlation between exchangeable Al and pH was observed in all categories, but logically Al toxicity can only be modelled in the above landscapes. Results from this study indicate that soils containing less than 1% K may be acid enough to produce near toxic levels of available Aluminium.

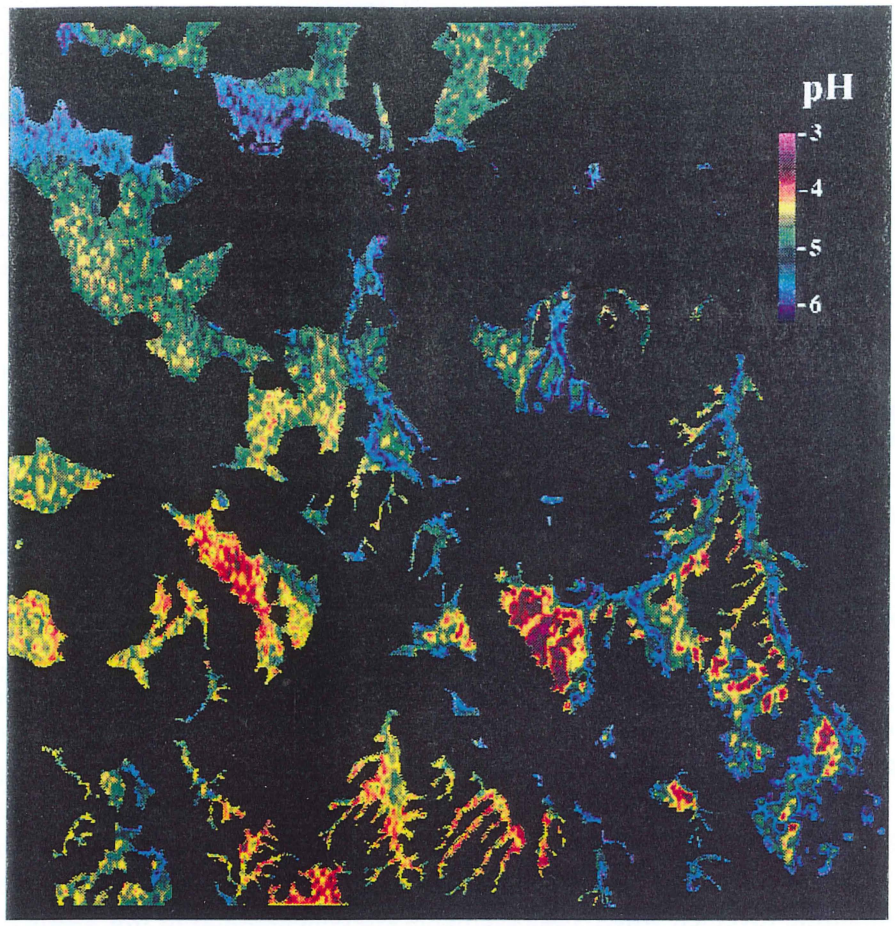

Figure 42. Surface soil acidity map for the Wagga Wagga 1:100000 sheet area - based on K values for residual soil-landscape categories.

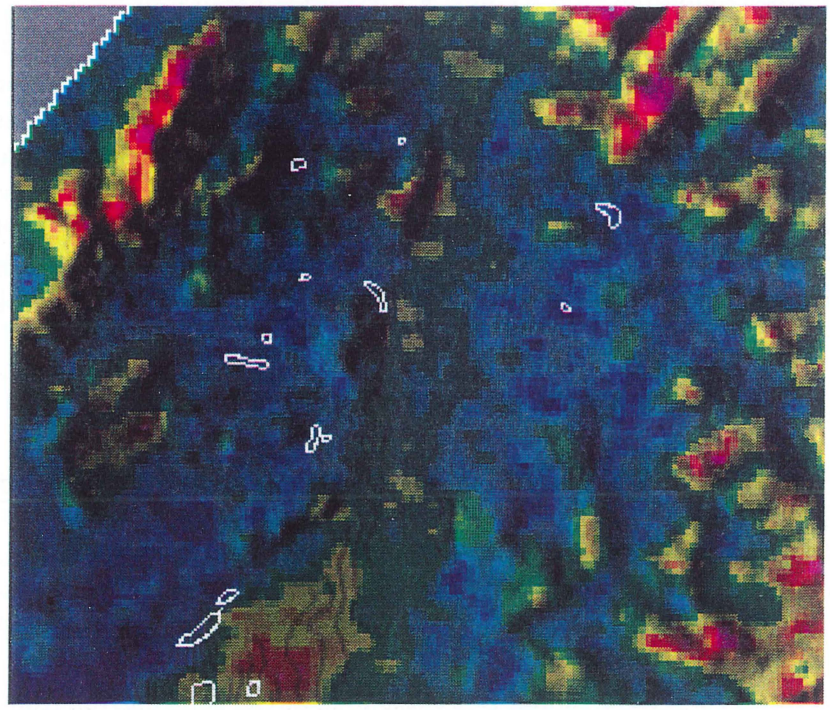

Figure 43. K concentrations (red = high, blue = low) combined with the DEM in the Kyeamba valley (100m airborne survey). White outlines are salt scalds.

4.2.1.2 Soil composition / nutrients

Soil mineralogy and available cations are important factors for land-use considerations. Different concentrations of radioelements are commonly related to mineralogy or nutrients. The following are examples of radioelement associations with nutrients encountered in the Wagga Wagga region:

- K images relate to total K content (all areas)
- extent of sandy colluvium shown by low K (sandstone areas)
- clay types, montmorillonite (low Th) versus illite, kaolinite (higher Th), on the Bullenbong Plain (inactive alluvial)
- feldspar content in granite areas, illite content in metasediment areas (both high K) (shallow bedrock areas)

4.2.1.3 Texture

Certain textures may be interpreted from the gamma images in particular areas:

- both K and Th positively correlate with silt and clay content in alluvial sediments around the Wagga sheet indicating that K and Th abundances may relate directly to texture in these areas.
- some low signals relate to sandy soils in alluvial areas and sandstone colluvium.
- gravel content can be mapped in shallow soils on bedrock. Generally signatures are high although this is sometime reversed where radioelements are concentrated in fine grained accessory minerals (Dickson and Scott, 1992) or in advanced granite weathering where only quartz and low signals remain (Wilford, 1992).

4.2.1.4 Salinity

In all of the soil analyses conducted for this study, there were no associations found between EC and radioelement concentrations. However, saline discharge sites were not studied in detail and it is possible that the airborne surveys were not spatially resolved enough to detect saline areas. Figure 43 shows known salinity scald areas overlain on K from the 100m Ladysmith airborne survey. It appears that scalding is not directly visible on the imagery but it is important to note that most of the scalds are within low K areas in low-lying areas. This may indicate that leached areas, having permeable soils, are prone to capilliary action and groundwater discharge.

4.2.2 Multichannel classification

This study has found that radiometric signatures require different interpretations for different areas. For example:
- sedimentary clays in shallow soils over bedrock in metasediment areas have an identical signature to alluvial clays on parts of the Murrumbidgee floodplain;
- aeolian clay deposits and old alluvial deposits on the Bullenbong Plain are inseparable radiometrically;
- alluvial cracking clays have similar responses to colluvial soils derived from sandstone;
- high uranium responses in some areas due to groundwater effects cause similar soils to have completely different responses.

For this reason, classification of the multichannel data can produce a large number of assumed soil similarities that do not exist. In some areas, K and Th patterns are not correlated since they show different properties. For example, on the Bullenbong Plain, Th shows clay types and K is showing the extent of leaching. Automated classification would produce a confused mixture of the two effects.

4.2.3 Automated soil-landscape units

It is possible to use the gamma-radiometric data for defining discrete soil units. Any classifications, however, must be tailored to the particular geomorphic or geological terrain. This should incorporate DEM modelling and might only involve a particular gamma element image. If one element best defines soil properties that define discrete soil types, then inclusion of other elements, in a mapping model, may degrade the model. An example is shown in Figure 44. At Ladysmith, K, slope and elevation were combined in a simple unsupervised classification (9 classes) in only those areas underlain by Ordovician metasediment geology (but including valley alluvium). White lines are the boundaries previously mapped using conventional air-photo interpretation and sampling (Chen and McKane, 1996). Detailed sampling in this terrain (see section 3.2.1.3) showed that K defined leaching properties and soil thickness. Th and U were less useful and quite noisy so were not used. Slope and elevation were included to enhance the topographic influences on soil development. This is a crude model but it serves as a useful demonstration since the classes have general correspondence with the mapped units. The radiometrics have provided an extra dimension. The floodplain has been separated into two soil-types based on K content; one related to recent clay deposition at least in the topsoil. The lower landscape unit (pu) shows variations of K relating to leaching conditions and colluvium thickness (not derivable from the DEM).

In flat country such as the Bullenbong Plain, the effectiveness of DEM analysis is limited. In this area, K and Th would be used in a tiered approach - K and Th both defining silty recent alluvial soils and only Th, which separates clay types, would be used in the bulk of the area.

5. CONCLUSIONS AND RECOMMENDATIONS.

Airborne gamma-spectrometric data (AGS) is a valuable tool for mapping soil types, soil properties and aspects of degradation. While not the complete answer, this data in combination with DEM's and traditional methods can improve both the speed and accuracy of soil surveying. In some cases, gamma chemical images can rapidly detect landscape properties - such as leaching/pH, windblown materials, basin-fill colluvium, radon discharge and sediment provenance - that are not achievable by other remote sensing methods.

This study has found that interpretations of gamma relationships with soil properties depends strongly on geology and geomorphic history. In erosional areas, K, Th and U images are influenced largely by bedrock mineral composition and weathering. In residual soils where pedogenesis occurs, K shows leaching patterns and may relate directly to soil pH whereas Th is immobile and may indicate clay content and type. In alluvial areas, all three elements may be associated with clay or silt particles, thereby indicating texture and associated properties.

A repeat 100m line-spaced survey revealed that AGS element maps are repeatable with the exception of the uranium image. The U image is often very noisy and sometimes shows radon effects that vary according to atmospheric conditions. Improvement of spatial detail at 100m

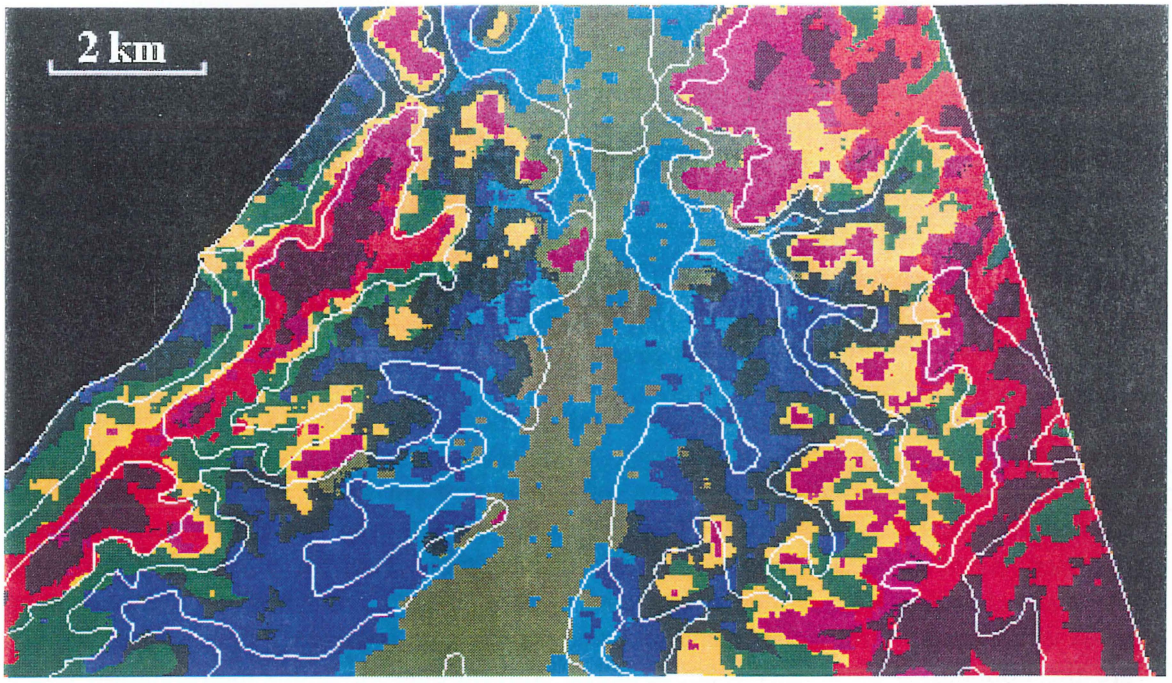

Figure 44(a). Classification (9 classes) of airborne K (100m line-spaced survey), slope and elevation for hilly areas of metasediments and alluvium. White lines are soil-landscape units.

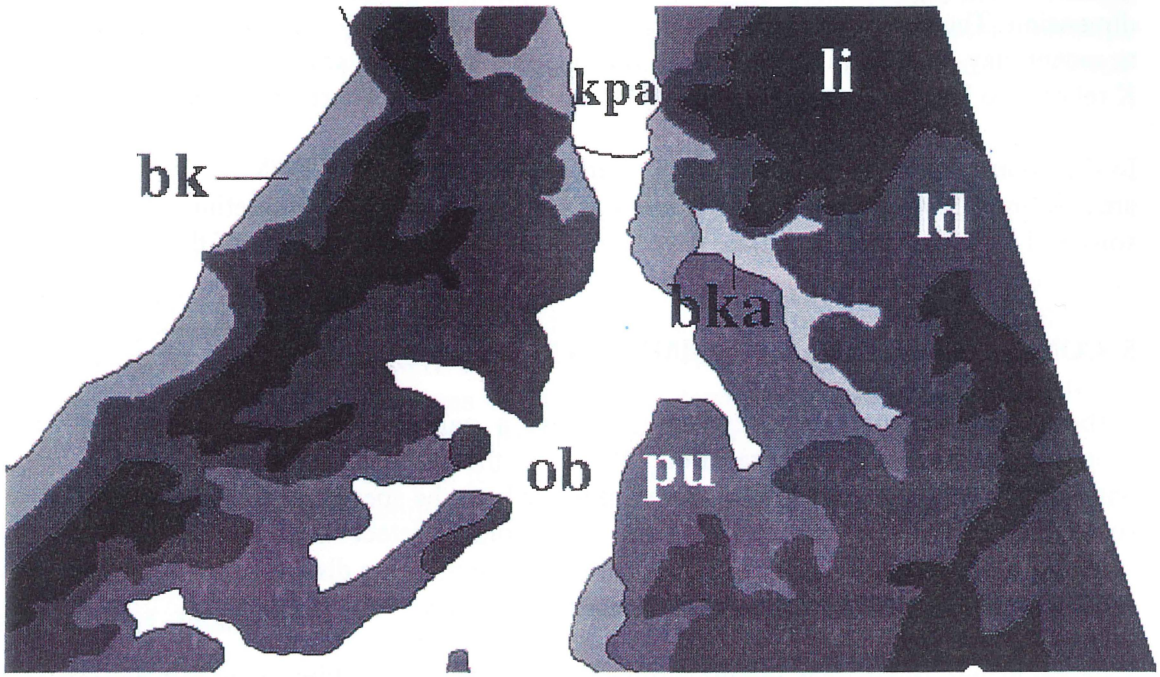

Figure 44(b). Soil-landscape units for the Ladysmith study area (after Chen and McKane, 1996).

Li - rolling to steep hills, shallow lithosols on Ordovician metasediments.
Ld - rolling to undulating hills, shallow chromosols.
Pu - undulating rises, moderately deep red chromosols and sodosols.
Bk,Bka - gentle footslopes, soils as for Pu.
Ob - alluvial soils, gently undulating plain, red brown chromosols and kandosols.
kpa - Murrumbidgee alluvium, dermosols and kandosols.

spaced aircraft lines is significant, but 200m spacing may be optimum at present due to flying costs.

Automated or GIS interpretation 'maps' can be generated by combining AGS data with geology and digital terrain data. Gamma element distribution patterns, however, are dependant on the specific geological and geomorphic history of an area and these relationships need to be understood.

Recommendations are that:

- further studies are required on potassium/acidity relationships.
- more research is needed on clay-type associations with thorium and uranium.
- general research is required to understand the mobilities of K,Th,U isotopes in relation to geology, geomorphology and pedogenesis in a variety of landscapes.
- field gamma measurements should involve vehicle-mounted large-crystal systems since hand-held spectrometers are inadequate for obtaining high resolution data.
- further studies be conducted on human induced radioactivity in areas of shallow water tables and associated with towns.

6. ACKNOWLEDGEMENTS

I thank the joint participants in the Wagga Wagga joint project, particularly Paul Gessler at CSIRO Soils and Dermot McKane from DLWR (NSW) who collected many of the soil samples and generally contributed their soil expertise.

From AGSO, I wish to thank Jim Kellet and Robyn Johnston for reviewing the manuscript. Robyn contributed significantly to the work on the groundwater-related uranium anomalies.

A number of soil samples relating to the uranium study were analysed at CSIRO Water Resources (Canberra) and the input from Andrew Murray and John Ollie is greatly appreciated.

7. REFERENCES

Beck, P.J., and Brown, D.R. (1987). Hydrogeological controls on the occurrence of radionuclides in groundwater of Southern Ontario. In: Radon, Radium, and other Radioactivity in Groundwater. Ed. Barbara Graves, Lewis Publishers.

Bierwirth, P.N. (1994). Image processing of airborne gamma-ray data for soils information: Wagga Wagga, N.S.W. Proceedings of the Seventh Australasian Remote Sensing Conference. Melbourne, March, 1994 , 2, pp927-934.

Brutsaert, W.F., Norton, S.A, Hess, C.T and Williams, J.S. (1981). Geologic and Hydrologic factors controlling Radon-222 in ground water in Maine. Ground Water, Vol 19, No.4 pp407-417.

Buckman, H.O., and Brady, N.C. (1960). The nature and properties of soils. Macmillan.

Chartres, C.J., Cumming, R.W., Beattie, J.A., Bowman, G.M. and Wood, J.T.,1990. Acidification of soils on a transect from plains to slopes, South-western NSW. Aust. J. Soil Research, 28, pp539-538.

Chen, X.Y., and McKane, D.J. (1996). Soil Landscapes of the Wagga Wagga 1:100,000 sheet and the Kyeamba Valley. Department of Land and Water Conservation Report. (In Press).

Charbonneau, B.W., and Darnley, A.G. (1970). Radioactive precipitation and it's significance to high sensitivity gamma-ray spectrometer surveys. Geological Survey of Canada, Paper 70-1, part B, 32-36.

Dickson, B.L., Giblin, A.M. and Snelling, A.A. (1987). The source of radium accumulations near sandstone escarpments, Australia. Applied Geochemistry, 2, pp 385-398.

Dickson, B.L., & Herczeg, A.L. (1992). Deposition of trace elements and radionuclides in the spring zone, Lake Tyrrell, Victoria, Australia. Chemical Geology, 96, pp151-166.

Dickson, B.L., and Scott, K.M. (1992). Interpretation of aerial gamma-ray surveys. CSIRO report 301R. 144p

Durrance, E.M. (1986). Radioactivity in Geology: principles and applications. John Wiley & sons. New York.

Dyck, W. (1978). The mobility and concentration of uranium and its decay products in temperate surficial environments. In: Uranium deposits. Their mineralogy and origin. M Kimberly (ed) Min. Assoc. Canada, Vol 3, p 57-100.

Galbraith, J.H., and Saunders, D.F. (1983). Rock classification by characteristics of aerial gamma-ray measurements. Journal of Geochemical Exploration. 18. pp49-73.

Gessler, P.E., Moore, I.D., McKenzie, N.J. and Ryan, P.J. (1995) Soil-landscape modelling and the spatial prediction of soil attributes. *Int. J. GIS*. Vol. 9, 4:421-432.

Gessler, P.E. and Ashton, L.J. (1996). Wagga Wagga Geographical Information System database: development, structure and user access. CSIRO Soils division working report.

Giblin, A.M., and Dickson, B.L. (1984). Hydrogeochemical interpretations of apparent anomalies in base metals and radium in groundwater near Lake Maurice in the Great Victoria Desert. Journal of Geochemical Exploration. 22. (1-3). pp 361 - 362.

Gillespie, A. R., Kahle, A.B. and Walker, R.E. (1986). Color enhancement of highly correlated images. 1. Decorrelation and HSI contrast stretches. Remote Sensing of Environment, 20, pp209-235.

Grasty, R.L. (1976). Applications of gamma radiation in remote sensing, in E. Schanda (ed), Remote Sensing for Environmental Sciences. Springer Verlag, Berlin. pp 257-276.

Grasty, R.L. (1994). Summer outdoor radon variations in Canada and their relation to soil moisture. Health Physics, Vol 66, No 2, pp185 - 193.

Graves, B. (ed) (1987). Radon, Radium, and other Radioactivity in Groundwater. Proceedings of the NWWA Conference, Somerset, New Jersey, Lewis Publishers.

Hudson, B. (1995). Reassessment of Polynov's ion mobility series. Soil Science Soc. America J. Vol 59, 1101-1103.

Killeen, P. G. (1977). Gamma ray spectrometric methods in uranium exploration - application and interpretation. In: Geophysics and Geochemistry in the Search for Metallic Ores. P.J.Hood (ed). Geological Survey of Canada Economic Geology Report 31 pp163-229.

Langmuir, D. (1978). Uranium solution-mineral equilibria at low temperatures with applications to sedimentary ore deposits. Geochim. Cosmochim Acta. Vol 42, pp547-569.

Langmuir, D. and Herman, J.S. (1980). The mobility of thorium in natural waters at low temperatures. Geochim. Cosmochim. Acta. Vol 44, pp1753-1766.

Mares, S. (1984). Introduction to applied geophysics. Riedel, Dordrecht. 581p

Martz, L.W. and de Jong, E. (1990). Natural radionuclides in the soil of a small agricultural basin in the Canadian prairies and their association with topography, soil properties and erosion. Catena, 17, pp85-96.

Minty, B. R. S. (1992). Airborne gamma-ray spectrometric background estimation using full spectrum analysis. Geophysics. Vol 57, no. 2 pp 279 - 287.

Mortvedt, J.J. (1994). Plant and soil relationships of uranium and thorium radionuclides. Journal of Environmental Quality. Vol 23, pp 643-650.

Ogden,A.E, Welling, W.B, Funderburg, R.D and Boschult, L.C. (1987). A preliminary assessment of factors affecting radon levels in Idaho. In: Radon, Radium, and other Radioactivity in Groundwater. Ed. Barbara Graves, Lewis Publishers.

Raymond, O.L. (1992). The Geology of Wagga Wagga and the Kyeamba Valley. 1:100,000 scale preliminary edition. Australian Geological Survey organisation.

Richards, J.A. (1987). Remote Sensing Digital Image Analysis. An introduction. Springer-Verlag, Berlin.

Scheepers, R. and Rozendaal, A. (1993). Redistribution and fractionation of U, Th and rare-earth elements during weathering of subalkaline granites in SW Cape Province, South Africa. Journal of African Earth Sciences, Vol 17, No. 1, pp. 41-50.

Thorpe, P. M. (1994). Radon -222 content of groundwater in Western Australia. Hydrology Report No. 1994/14. W.A. Geological Survey.

Velde, B. (ed), (1995). Origin and mineralogy of clays, clays and the environment. Springer, Berlin.

Wedepohl, K.H. (ed), (1969). Handbook of geochemistry, vol II-5. Springer Verlag, Berlin.

Wilford, J.R. (1992). Regolith mapping using integrated Landsat TM imagery and high resolution gamma-ray spectrometric imagery - Cape York Peninsula. Record 1992/78. Australian Geological Survey Organisation.

Wollast, R. (1967). Kinetics of the alteration of K-feldspar in buffered solutions at low temperature. Geochim. Cosmochim Acta. Vol 31, pp635-648.

APPENDIX

SOIL RADIOELEMENT SAMPLING RESULTS

1. Introduction
2. Ladysmith samples
3. Wagga Wagga 1:100,000 sheet regional samples
4. Bullenbong Plain samples

1. Introduction

Soil sample analyses used in this study were performed by CSIRO Soils, AGSO and NSW Department of Land and Water Conervation (DLWC) (formerly CALM). For certain samples, a series of elements, including the gamma-emitting K, Th and U, were analysed at AGSO. Only these samples are represented here and soil property information is shown with the permission of CSIRO and DLWC. Table 10 lists parameter descriptions and units for all tables.

Table 10. Description of listed parameters and their measurement units.

Parameter	Description	Units
Site	site number and horizon	n/a
Depth	depth of sample	cm
U	all isotopes of uranium	ppm
Th	" " thorium	ppm
Pb	" " lead	ppm
Rb	" " rubidium	ppm
Y	" " yttrium	ppm
K	" " pottasium	%
pH	pH, 1+5 H_20	
EC	electrical conductivity	uS/cm
Total C	total carbon	%
Exc. Ca	exchangeable Calcium	cmol/kg
Exc. Mg	exchangeable Magnesium	cmol/kg
Exc. Na	exchangeable Sodium	cmol/kg
Exc. K	exchangeable Potassium	cmol/kg
CEC	cation exchange capacity	cmol/kg
East	AMG grid easting	metres
North	AMG grid northing	metres
K (gamma)	potassium measured by ground spectrometer	%
U (gamma)	uranium " " " "	ppm
Th (gamma)	thorium " " " "	ppm
C	clay	%
S	silt	%
FS	fine sand	%
CS	coarse sand	%
G	gravel	%

FC	field capacity	%
PWP	permanent wilting point	%
OC	organic carbon	%
Psorp	phosphorus sorptivity	%
DP	clay dispersion in water	%
Vol	rock volume	%
Txt	field texture	?

2. Ladysmith samples

Table 11. XRF/AA analyses of soil samples

Site	Depth	U	Th	Pb	Rb	Y	K
3.1	3.5	3.5	15	15	86	30	1.21
3.2	19	3.5	16.5	22	118	32	1.52
8.1	2	4.5	18.5	16	130	37	2.3
8.2	15	5	19	14	131	37	2.29
9.1	3	5	19	21	102	35	1.51
12.1	3	4.5	17	23	153	37	2.14
16.1	3	4	19	22	167	37	2.77
16.2	35	6.5	24.5	23	207	43	3.3
17.1	2	4.5	17.5	27	138	39	2
21.1	6	3.5	19.5	18	87	28	1.45
21.2	36	6.5	37	36	157	38	2.47
27.1	3	3	17	18	137	34	1.55
27.2	16	3.5	20.5	23	205	36	2.59
29.1	8	4.5	16	11	81	31	1.24
29.2	29	4	20.5	13	88	28	1.4
33.1	5	5.5	18	21	160	33	2.14
33.2	17	4.5	22	23	161	35	2.6
33.3	37	8.5	36.5	33	189	35	2.53
39.1	5	4.5	17.5	22	117	44	1.79
39.2	28	4	19	27	170	44	1.96
39.3	62	5.5	20	30	193	37	2.1
45.1	7	4	18	18	93	36	1.42
45.2	22	5	19.5	17	95	38	1.74
52.1	4	5	16	22	140	29	2.88
52.2	21	5.5	22	30	153	35	2.94
55.1	4.5	4.5	16.5	18	82	41	1.36
55.2	20	4	18	20	89	47	1.53
55.3	47	4.5	18.5	22	124	33	1.59
55.4	89	4	18	21	101	35	1.44
55.5	146	5	16.5	32	118	45	1.53
58.1	6	4.5	14	15	63	29	0.91
58.2	27	4.5	15.5	16	70	36	1.01
61.1	4	3	13.5	15	74	31	1
61.2	14	4	16	17	81	32	1.11
67.1	2	3.5	15.5	16	82	41	1.14
67.2	25	3.5	16	17	87	43	1.44
69.1	12.5	3	17.5	17	88	40	1.52
69.2	33	3.5	19.5	23	98	42	1.75

72.1	4	4.5	16	18	82	41	1.49
72.2	22	4.5	19.5	35	93	51	1.67
78.1	6	4.5	15	18	69	34	1.15
78.2	21	4	15.5	20	67	34	1.15
78.3	40	5	18	22	102	36	1.43
79.1	6	4	17.5	18	101	40	1.74
79.2	24	4	20	25	136	51	2.23
79.3	56	5.5	22	30	119	47	2.17
79.4	77	4	20	27	156	45	2.21
79.5	112	3.5	20	22	139	50	2.05
79.6	171	3.5	19	24	146	41	2.09
81.1	4	3	14.5	16	67	37	1.21
81.2	18	4	18	16	82	43	1.48
81.3	41	3.5	16	17	70	35	1.36
81.4	82	5	20	22	101	50	1.38
81.5	132	4.5	18.5	30	86	38	1.23
81.6	177	3	17.5	19	109	42	1.5
83.1	8	3.5	17.5	22	121	42	1.94
83.2	34	5	18.5	33	165	43	2.68

Table 12. Soil properties for samples analysed with XRF/AA (see table 11)

Site	pH	EC	Total C	Exc. Ca	Exc. Mg	Exc Na	Exc.K
3.1	5.49	94	2.66	1.7	0.76	0	0.53
3.2	5.59	34	0.36	1	0.89	0.07	0.12
8.1	5.43	104	3.94	5.1	1.5	0.3	0.79
8.2	5.58	55	0.3	1.2	0.83	0.03	0.17
9.1	4.92	149	6.81	5.2	1.8	0.08	1.3
12.1	5.51	180	3.45	4.5	0.85	0.06	0.71
16.1	5.54	95	2.44	2.9	0.71	0.05	1.3
16.2	6.14	30	0.47	2.4	0.65	0.01	0.4
17.1	5.36	113	3.1	2.3	1.1	0.12	0.94
21.1	5.67	70	1.53	1.3	0.74	0.01	0.85
21.2	5.76	29	0.29	2.8	5	0.08	0.53
27.1	4.96	124	2.2	1.1	0.53	0	1.3
27.2	4.83	100	0.58	0.59	0.39	0	0.64
29.1	5.03	65	0.87	0.86	0.31	0	0.38
29.2	5.77	35	0.28	1.4	0.5	0	0.17
33.1	5.46	78	1.96	1.9	0.96	0.06	0.87
33.2	4.87	30	0.68	0.49	0.66	0.05	0.2
33.3	4.79	42	0.32	0.54	4.3	0.09	0.34
39.1	6.05	83	1.69	2.1	1.2	0.06	0.87
39.2	6.48	32	0.62	4.6	3.8	0.08	0.94
39.3	6.89	30	0.32	4.9	6.7	0.07	0.88
45.1	5.21	63	1.31	0.95	0.71	0.1	0.22
45.2	6.37	16	0.28	0.66	0.85	0.07	0.08
52.1	5.48	40	2.59	1.9	0.99	0.13	0.84
52.2	5.11	25	0.49	0.32	1	0.04	0.15
55.1	5.54	49	1.92	1.8	0.52	0.04	0.98
55.2	5.74	42	0.46	1.3	0.36	0.02	0.48
55.3	7.1	20	0.13	4.1	1.8	0.04	0.74

55.4	6.84	33	0.12	3.3	2.9	0.07	0.22
55.5	7.1	32	0.05	7.2	9.2	0.26	0.6
58.1	6.03	46	1.41	3.5	0.22	0.06	0.09
58.2	5.07	26	0.35	0.36	0.06	0.03	0.07
61.1	6.17	119	2.51	5.1	1.7	0.16	1.4
61.2	6.52	127	0.41	1.1	0.58	0.05	1.4
67.1	5.52	51	1.76	1.3	0.31	0.06	0.57
67.2	5.57	21	0.27	1	0.21	0	0.21
69.1	5.27	67	0.93	2.2	0.42	0	0.67
69.2	6.56	21	0.19	2	0.38	0.01	0.29
72.1	4.92	102	1.68	1	0.31	0	0.55
72.2	5.26	44	0.43	1.3	0.52	0.03	0.29
78.1	4.86	54	1.23	0.76	0.29	0.01	0.31
78.2	4.63	81	0.13	0.36	0.14	0	0.14
78.3	5.6	35	0.28	2.1	1.2	0.02	0.33
79.1	5.53	132	2.66	4.9	1.4	0.04	0.81
79.2	6.24	57	1.07	7.4	1.7	0.04	0.51
79.3	7.11	19	0.13	3.8	1.7	0.03	0.18
79.4	7.1	25	0.26	9.6	5.2	0.1	0.52
79.5	7.48	27	0.16	6.6	5.2	0.21	0.42
79.6	8.16	34	0.09	8.1	6.6	0.6	0.34
81.1	5.02	77	1.9	1.1	0.24	0.02	0.55
81.2	5.43	35	0.49	1.5	0.3	0.04	0.28
81.3	6.71	11	0.07	0.98	0.33	0.02	0.09
81.4	7.93	34	0.08	4.5	3.5	0.26	0.18
81.5	7.92	55	0.13	2.2	2.9	0.41	0.12
81.6	8.5	56	0.06	6.5	10.1	1.6	0.34
83.1	5.64	136	2.4	2.6	1.1	0.02	0.61
83.2	6.48	39	0.28	2.7	1.6	0.05	0.38

Table 13. Location and ground spectrometer measurements at Ladysmith sites

site	East	North	k(gamma)	U(gamma)	Th(gamma)
1	545070	6102850	2	3.1	14.1
3	548750	6106510	1.4	3.5	15.6
4	548170	6105370	2.3	3.7	15.8
5	549850	6104710	2.4	3.6	17.5
6	548510	6108470	2.1	3.4	18.6
7	545490	6104110	1.9	3.2	12.9
8	549350	6101930	2	2.5	15.1
9	541070	6102330	2	3.9	16.7
10	540070	6101870	3	4.1	19.3
11	545650	6105490	1.9	2.7	14.9
12	543130	6104170	3.3	3	17.5
14	547930	6100770	2.9	2.9	13.6
15	550870	6101990	1.6	3.1	13.3
16	544710	6107070	2.1	4	16.9
17	540870	6102110	2.8	3.2	15.9
18	545530	6106310	2.6	4.3	14.7
19	547390	6101890	1.1	2.8	12.1
20	549950	6102810	3.4	4.3	19.7
21	548490	6105790	1.4	3.1	15.5

22	548870	6106990	1.7	4.3	25.8
23	542190	6100970	1.1	3.1	12.3
25	547510	6107510	2.1	3.3	16.1
26	544430	6108570	1.8	5.6	14.9
27	548630	6102430	1.9	2.5	13
29	549830	6106090			
30	549250	6104410	2	2.6	13.5
33	550710	6101930	2.5	3.2	17.1
35	547570	6102730	1.3	3.2	13.6
36	543350	6101770	0.8	2.5	12.9
37	542150	6100930	1.2	3.2	12.6
38	548370	6104730	1	2.6	11.5
39	545390	6106910	1.8	3.4	15.5
40	545310	6108170	1.3	3.7	14.1
41	547370	6104470	0.8	2.7	11.2
43	550410	6101010	1	2.7	12.7
44	547770	6108830	1.8	2.9	18.9
45	550090	6105570	1.3	3	12.3
48	544610	6103990	1	3.2	11.6
49	549750	6104230	1.5	2.7	13.8
51	546870	6101070	0.9	2.9	10.8
52	551170	6101590	3	3.7	16.4
53	542850	6104310	1.4	3.1	12
54	548210	6104850	0.9	2.8	12
55	547910	6103890	1.2	3.5	14.5
56	547170	6107950	1.4	2.9	13.6
57	544130	6106250	1.6	3.4	12.6
58	545530	6104930	1	2.7	12.3
59	547590	6100950	1.2	2.7	13.3
61	545090	6103110	1	2.1	12.5
62	546970	6106270	1	3	12.4
63	544050	6108310	1.2	3.6	12.9
65	544890	6101230	1.1	2.3	13.3
67	545270	6106030	1.4	3.6	11.8
68	544930	6107610	1.1	3.4	11.6
69	548810	6104670	1.4	2.3	14.1
71	547850	6102370	1.1	2.6	13.5
72	545370	6105930	1.3	3.7	12.4
76	548910	6100850	1	2.9	12.7
77	546950	6105810	1.3	2.4	12.4
78	544450	6102530	1	3.1	11.5
79	545670	6107050	1.6	3	16.4
81	548250	6103650	1.2	3.4	14
82	547470	6101230	0.7	2.8	11.1
83	544830	6104970	1.8	2.8	15.4
85	546870	6108610	1.4	3.7	16.5

3. Wagga Wagga 1:100,000 sheet regional samples.

Table 14. Location and some soil property results for regional samples where XRF/AA radioelement data was obtained (see Table 15). The 'soil' column represents soil landscape units from Chen and McKane (1996). Symbols and units are given in Table 10.

site	lay.	soil	East	North	UPP Depth	Low depth	Hor.	C	S	FS	CS	G	FC	PWP	NEA	EC
3	1	gr1	531930	6103850	0	0.2	A1	8	18	56	17	1	24.8	3.0	29	0.05
4	1	eb1	537800	6123200	0	0.15		26	17	43	10	4	26.9	7.3	42	0.04
5	1	gl1	538050	6124900	0	0.2	A	8	11	46	33	2	14.7	3.0	59	0.05
11	1	eb1	538600	6119425	0	0.2	A	17	7	36	39	1	17.0	6.1	40	0.06
12	1	eb1	538700	6119425	0	0.2	A	12	10	50	27	1	19.5	4.4	32	0.03
15	1	bk1	526850	6122875	0	0.15	A	13	14	64	9	0	33.7	5.3	20	0.05
21	1	ya1	519275	6114100	0	0.15	A1	9	12	49	30	0	25.2	4.5	43	0.07
21	2	ya2	519275	6114100	0.15	0.35	A2	9	10	45	35	1	15.9	2.5	38	0.03
22	1	ya5	519450	6114075	0	0.1	A	16	28	46	6	4	40.8	10.5	69	0.86
23	1	mu1	518850	6114125	0	0.1		6	17	35	39	3	20.6	3.3	62	0.03
43	1	vi1	508450	6095025	0	0.25	A1	7	10	61	22	0	30.0	3.8	27	0.07
56	1	ob1	538075	6090800	0	0.3	A	13	17	61	9	0	34.6	8.2	53	0.09
57	1	bs1	537100	6091000	0	0.1	A1	4	15	48	31	2	23.1	3.8	72	0.10
57	2	bs2	537100	6091000	0.1	0.35	A2	7	10	37	45	1	13.5	2.5		0.03
62	2	ob2	542800	6090275	0.12	0.25	A2	17	26	44	12	1	20.8	4.3	74	0.09
67	1	mf1	538050	6093800	0	0.1	A	6	6	34	35	19	21.6	4.2	67	0.15
85	1	mf1	536750	6094475	0	0.12	A	10	15	34	31	10	21.8	4.9	51	0.07
87	1	gb1	501225	6072250	0	0.15	A1	14	15	56	11	4	35.1	7.6	65	0.18
87	2	gb2	501225	6072250	0.15	0.26	A2	12	18	52	13	5	21.4	3.3	69	0.16
93	1	bl1	533850	6088275	0	0.14	A	25	7	57	11	0	25.8	9.6	76	0.05
101	1	bl1	533650	6089075	0	0.13	A1	5	14	77	4	0	29.7	4.2	34	0.06
101	2	bl2	533650	6089075	0.13	0.35	A2	4	23	67	5	1	20.6	1.3	21	0.05
103	1	ga1	504505	6126550	0	0.12	A	2	2	41	55	0	7.0	1.5	0	0.03
105	1	ya1	518275	6113450	0	0.1	A1	7	13	46	33	1	21.8	3.5	64	0.08
105	2	ya2	518275	6113450	0.1	0.28	A2	3	11	42	41	3	13.4	0.9	45	0.03
107	1	be1	509175	6115825	0	0.14	A	16	17	55	10	2	29.2	6.4	83	0.03
107	2	be3	509175	6115825	0.14	0.6	B2	40	9	38	9	4	29.7	10.5	62	0.03
107	3	be4	509175	6115825	0.6	0.8	B3	57	8	26	4	5	32.4	15.8	71	0.04
110	1	bu1	501600	6115350	0	0.08	A	64	12	21	1	2	41.1	22.2	85	0.09
110	2	bu2	501600	6115350	0.08	0.5	B2	59	19	20	1	1	41.9	17.7	83	0.09
111	1	be1	506850	6110450	0	0.08	A	17	14	58	9	2	32.0	7.1	57	0.12
111	2	be3	506850	6110450	0.08	0.4	B1	20	15	56	7	2	25.5	7.0	67	0.05
114	1	li1	541475	6085150	0	0.15	A1	11	19	48	17	5	34.8	6.8	51	0.06
115	1	ld1	541525	6083125	0	0.08	A1	11	22	38	18	11	35.9	7.7	69	0.08
117	1	ob1	542950	6078725	0	0.08	A1	11	30	57	2	0	42.6	7.7	60	7.00
117	2	ob2	542950	6078725	0.08	0.22	A2	7	45	46	2	0	24.7	3.0	31	0.35
118	1	wa1	542375	6078550	0	0.12	A1	10	22	62	6	0	40.5	6.4	33	0.12
123	1	li1	536275	6082675	0	0.2	A1	9	14	53	16	8	30.3	5.1	46	0.09
128	1	rb1	534175	6105425	0	0.12	A1	12	18	61	8	1	31.3	4.4	62	0.06
135	1	eb1	540600	6119100	0	0.15	A	17	19	53	9	2	31.3	8.8	86	0.10
141	1	kp1	540175	6116650	0	0.28	A	22	39	27	9	3	36.4	11.2	97	0.07
148	1	ld1	527575	6107225	0	0.3	A1	16	22	53	9	0	30.1	7.3	82	0.06
151	1	ld1	523250	6123950	0	0.1	A	12	13	46	14	15	29.7	6.3	71	0.19
153	1	bk1	526125	6125750	0	0.25	A1	20	28	42	6	4	30.5	8.6	76	0.03
156	1	kp1	522325	6118575	0	0.32	A	21	39	32	8	0	32.8	9.2	95	0.05

161	1	be1	518375	6120475	0	0.1	A1	7	7	55	31	0	20.9	7.9	53	0.09
161	2	be2	518375	6120475	0.1	0.3	A2	13	16	40	31	0	19.0	4.5	91	0.04
168	1	rp1	506875	6115750	0	0.08	A	48	21	28	3	0	40.3	14.6	91	0.08
168	2	rp2	506875	6115750	0.08	0.45	B2	81	11	8	0	0	61.0	24.1		0.02
168	3	rp3	506875	6115750	0.45	0.8	B3	79	11	10	0	0	55.7	24.1	79	0.99
176	1	fh1	538925	6107400	0	0.08	A1	12	15	48	21	4	26.0	6.7	84	0.09
176	2	fh2	538925	6107400	0.08	0.2	A2	15	13	44	23	5	18.1	5.1	91	0.05
184	1	ob1	530000	6106975	0	0.1	A1	11	18	57	14	0	26.5	4.8	69	0.04
184	2	ob2	530000	6106975	0.1	0.35	A2	16	26	49	9	0	19.7	5.2	86	0.68
189	1	pe1	520825	6106525	0	0.15	A1	11	10	61	18	0	25.4	4.7	52	0.06
189	2	pe2	520825	6106525	0.15	0.3	A2	12	13	50	23	2	14.7	4.0	68	0.01
196	1	kp1	535675	6110750	0	0.1	A1	23	26	45	6	0	29.8	8.0		0.05
202	1	li1	532675	6083500	0	0.22	A1	13	32	49	5	1	42.6	9.2	57	0.07
202	2	li4	532675	6083500	0.22	0.42	C1	22	34	38	6	0	38.6	9.1	53	0.04
203	2	gl2	533075	6081225	0.1	0.2	A2	14	15	33	24	14	19.5	6.8	65	0.06
215	1	pu1	534525	6076825	0	0.1	A1	8	14	54	16	8	27.8	5.0	59	0.06
215	2	pu2	534525	6076825	0.1	0.25	A2	4	18	58	14	6	19.1	2.6	64	0.02
222	1	pe1	518175	6106675	0	0.18	A	17	8	54	19	2	22.7	9.0	59	0.10
224	1	pu1	525700	6079900	0	0.12	B2	9	16	65	6	4	29.7	4.1	45	0.04
224	2	pu2	525700	6079900	0.12	0.25	B3	11	19	62	8	0	19.9	2.8	75	0.02
239	1	ma1	521125	6091375	0	0.1	A1	13	22	49	14	2	26.3	6.7	74	0.30
239	2	ma2	521125	6091375	0.1	0.3	A2	11	37	48	4	0	20.9	3.1	85	0.08
245	1	ri1	513700	6091100	0	0.18	A	10	8	62	12	8	37.0	7.8	51	0.05
246	1	pu1	519950	6087825	0	0.15	A	12	17	65	6	0	33.8	6.5	72	0.04
246	2	pu3	519950	6087825	0.15	0.35	B2	48	14	33	5	0	32.8	12.8	86	0.02
257	1	pu1	511625	6078525	0	0.1	A1	9	19	60	10	2	36.8	4.7	65	0.05
257	2	pu2	511625	6078525	0.1	0.22	A2	9	20	50	18	3	22.3	3.1	70	0.03
262	1	re1	506550	6094300	0	0.15		5	8	73	11	3	17.4	3.6	27	0.03
262	2	re2	506550	6094300	0.15	0.5		4	5	40	8	43	11.7	1.9	46	0.02
277	1	ma1	508000	6098800	0	0.2	A1	5	8	82	5	0	9.0	5.5	33	0.19
284	1	wo1	534125	6096150	0	0.08	A1	10	13	33	37	7	19.8	5.2	77	0.04
284	2	wo2	534125	6096150	0.08	0.2	A2	20	14	34	28	4	19.4	6.7	88	0.03
287	1	bu1	504100	6109100	0	0.1	A	27	19	50	4	0	32.0	9.4		0.12
287	2	bu2	504100	6109100	0.1	0.7	B2	57	11	31	1	0	43.5	18.3	93	0.34
287	3	bu3	504100	6109100	0.7	0.85	B3	47	16	35	2	0	42.3	17.2	89	1.02
295	1	vi1	504125	6091250	0	0.15	A1	9	15	74	2	0	30.6	5.1	54	0.10
295	2	vi2	504125	6091250	0.15	0.22	A2	10	9	71	9	1	13.1	2.1	60	0.03
301	1	bk1	505000	6082700	0	0.15	A1	12	15	64	9	0	33.7	6.7	57	0.12
301	2	bk2	505000	6082700	0.15	0.35	A2	13	17	56	9	5	26.5	5.4	76	0.05
302	1	gb1	500650	6080425	0	0.15	A1	12	19	64	5	0	33.2	8.7	75	0.14
302	2	gb2	500650	6080425	0.15	0.25	A2	14	20	61	5	0	25.5	4.8	90	0.07
304	1	fa2	503825	6122700	0	0.1	A	40	42	18	0	0	58.4	20.2	86	0.11
311	1	kd1	545300	6080925	0	0.1	A1	16	32	25	22	5	23.1	6.2	73	0.05
311	2	kd2	545300	6080925	0.1	0.35	A2	11	11	31	19	28	18.3	4.6	78	0.02
320	1	ld1	526950	6115475	0	0.1	A	9	16	19	27	29	20.9	5.1	69	0.07
320	2	ld2	526950	6115475	0.1	0.3	B	8	25	22	27	18	22.0	5.3	67	0.05
322	1	ri1	504450	6088400	0	0.12	A1	7	7	70	10	6	36.7	5.4	42	0.05
323	1	ro1	504350	6089075	0	0.06	A1	7	5	56	17	15	28.9	5.4	40	0.04
325	1	rb1	534400	6104450	0	0.1	A	16	18	49	16	1	28.7	6.8	80	0.07
325	2	rb2	534400	6104450	0.1	0.28	A2	10	20	51	17	2	21.9	3.2		0.04

Table 15. XRF/AA and soil property results for regional samples.

site	lay.	pH	CEC	EXC. Ca	EXC. Mg	EXC. Na	EXC. K	EXC. Al	OC	P Sorp	U	Th	Pb	Rb	Y	K
3	1	4.4	5.2	1.1	0.6	0.4	0.5	0.0	0.68	149	4	11.5	23	164	27	2.56
4	1	5.0	4.9	3.1	1.5	0.6	0.8	0.0	0.76	236	4.5	18	31	86	41	1.54
5	1	5.4	5.7	2.5	1.0	0.3	0.6	0.0	1.35	25	3.5	17	38	101	34	2.38
11	1	5.6	6.7	3.6	1.0	0.4	1.0	0.2	1.11	140	3.5	16.5	27	111	38	2.4
12	1	3.8	6.0	1.8	0.6	0.6	0.8	0.1	0.98	101	3.5	19	25	94	38	2.36
15	1	5.1	6.7	3.1	1.0	0.6	0.8	0.0	1.46	150	3.5	13	15	55	31	1.05
21	1	5.0	5.6	2.5	0.8	0.4	1.2	0.0	1.64	136	3	12	21	129	31	2.54
21	2	4.9	4.7	1.1	0.4	0.3	0.6	0.0	0.28	119	3	14	21	128	35	2.62
22	1	6.0	16.5	10.2	5.9	0.9	0.9	0.0	2.87	264	8	15.5	19	94	37	1.75
23	1	4.8	2.3	1.0	0.6	0.3	0.3	0.0	1.80	166	5.5	14.5	26	170	45	3.31
43	1	6.0	11.1	6.2	2.5	0.3	0.9	0.0	1.27	116	2.5	10	11	47	20	0.72
56	1	5.1	6.9	4.5	1.4	0.4	1.0	0.0	1.61	240	3.5	13	24	154	28	2.16
57	1	4.5	5.2	1.4	0.7	0.2	0.5	0.0	1.14	135	3.5	11.5	34	237	25	3.45
57	2	5.2	5.3	0.7	0.5	0.2	0.5	0.0	0.08	93	3.5	11	32	240	29	3.55
62	2	4.6	2.8	1.5	0.6	0.5	0.3	0.0	0.24	173	4.5	17	16	67	38	1.24
67	1	5.1	8.7	4.9	1.0	0.6	0.6	0.0	2.69	60	6.5	9	101	460	22	6.13
85	1	5.4	7.7	3.8	0.8	0.4	0.7	0.0	1.14	148	9	13	43	335	36	3.85
87	1	5.3	8.8	6.9	2.7	0.3	1.1	0.0	2.71	250	3	14	18	74	29	1.18
87	2	4.4	4.1	0.9	1.3	0.5	0.4	0.0	0.37	189	3	16	17	61	32	1.12
93	1	4.5	7.3	3.0	2.9	0.2	0.8	0.6	2.12	374	3	12	15	40	22	0.54
101	1	3.6	4.5	2.1	0.6	0.5	0.5	1.1	1.83	194	3	10	8	29	21	0.45
101	2	3.9	2.8	0.9	0.5	0.4	0.2	0.4	0.21	134	3	11	9	23	25	0.46
103	1	5.9	3.0	1.4	0.3	0.2	0.5	0.0	0.43	65	1.5	6.5	11	72	15	1.86
105	1	5.2	7.1	3.5	0.8	0.4	0.8	0.0	1.28	175	3.5	13	22	141	31	2.98
105	2	5.9	5.6	1.1	0.5	0.3	0.3	0.0	0.09	68	2.5	11.5	22	133	28	2.37
107	1	4.6	8.1	3.2	1.2	0.4	0.6	0.0	1.30	225	3	13.5	20	77	33	1.4
107	2	5.2	10.2	4.3	3.0	0.4	0.4	0.0	0.24	328	3	16.5	19	95	34	1.52
107	3	5.7	13.7	7.1	6.0	0.5	0.7	0.0	0.14	533	3.5	18	23	117	31	1.62
110	1	5.2	27.6	17.5	10.7	0.7	1.7	0.0	4.23	442	3	14.5	25	106	37	1.65
110	2	6.3	21.4	11.1	9.9	2.7	0.8	0.0	0.50	322	3	20.5	32	115	48	1.7
111	1	4.6	8.8	3.0	1.7	0.6	2.1	0.5	2.36	303	2.5	14.5	19	79	31	1.37
111	2	4.4	5.1	2.2	2.6	0.7	0.9	0.0	0.62	250	3.5	14	19	73	32	1.27
114	1	4.8	5.1	1.0	1.4	0.5	0.9	0.0	1.44	193	5.5	21	36	167	51	2.54
115	1	4.3	6.1	2.1	1.8	0.4	0.9	0.5	2.58	241	4.5	17.5	24	121	35	1.7
117	1	4.4	4.2	0.9	2.6	0.8	0.4	0.3	2.42	282	3.5	13	14	46	31	0.67
117	2	4.4	1.9	0.2	1.9	0.9	0.2	0.0	0.14	165	5	14	20	37	33	0.69
118	1	3.9	7.5	1.9	0.6	0.5	0.3	2.6	3.18	347	4	12.5	15	38	30	0.43
123	1	5.3	8.9	3.1	0.9	0.4	1.0	0.0	1.70	169	3.5	12.5	15	100	23	1.31
128	1	4.2	5.1	3.7	0.7	0.2	0.5	0.2	1.65	230	3.5	13.5	17	108	32	1.14
135	1	6.1	10.6	7.5	1.9	0.5	1.4	0.0	1.79	147	5	18	28	111	42	1.77
141	1	5.8	14.7	12.6	2.9	0.3	2.0	0.0	1.81	169	5	17	27	152	41	2.77
148	1	4.7	9.9	4.1	1.3	0.3	0.4	0.0	1.13	217	6.5	16	23	143	38	1.8
151	1	4.8	5.9	3.4	1.2	0.3	1.6	0.0	1.98	193	2	13.5	21	75	31	1.18
153	1	5.8	10.2	5.1	1.9	0.6	0.6	0.0	0.61	235	4	17.5	20	85	38	1.45
156	1	5.3	11.9	10.2	2.5	0.3	1.2	0.0	1.25	179	4	19	26	153	42	2.78
161	1	6.3	13.2	11.4	2.6	0.3	0.4	0.0	3.35	94	3	8	14	78	19	1.79
161	2	6.4	9.4	3.8	1.7	0.3	0.8	0.0	0.46	91	2	13	18	99	29	2.28
168	1	4.4	8.3	2.8	4.1	1.7	1.1	0.1	1.46	558	3	18	30	92	41	1.69
168	2	6.4	24.0	6.5	12.5	7.1	1.6	0.0	0.53	477	3.5	18.5	32	138	44	2.28

168	3	7.6	25.3	4.4	11.9	11.8	2.0	0.1	0.12	332	3.5	18	26	134	45	2.49
176	1	4.8	8.8	3.8	0.8	0.3	0.8	0.0	1.95	169	3	15.5	22	89	43	1.33
176	2	4.7	5.2	2.1	0.6	0.3	0.8	0.1	0.88	157	4.5	16.5	24	94	46	1.39
184	1	5.8	3.2	0.8	1.0	0.6	0.5	0.1	0.76	169	4	15	21	95	34	1.53
184	2	6.4	1.9	1.5	1.7	0.5	0.5	0.1	0.10	89	4.5	15.5	21	111	32	1.74
189	1	5.0	9.5	3.7	1.5	0.2	0.6	0.0	1.66	188	3.5	13	14	71	28	1.2
189	2	4.3	0.1	0.6	0.9	0.2	0.3	0.0	0.16	126	3	13.5	13	67	30	1.31
196	1	5.2	10.7	7.0	2.6	0.2	0.7	0.0	1.05	226	7	15	29	176	40	2.1
202	1	4.1	5.5	1.1	1.4	0.6	0.6	1.2	3.96	581	4.5	13.5	20	73	29	1.12
202	2	4.3	7.1	0.2	2.5	0.8	0.3	0.6	1.83	605	5.5	12	32	274	27	2.54
203	2	3.8	4.2	0.4	0.8	0.3	0.4	1.6	1.25	374	6	13.5	42	286	28	2.67
215	1	4.7	4.0	1.3	0.5	0.4	1.0	0.0	1.36	200	4	13	17	66	27	0.95
215	2	4.4	4.8	0.2	0.2	0.2	0.3	0.0	0.09	115	3.5	13.5	14	57	27	0.87
222	1	6.0	12.0	9.1	2.9	0.2	1.1	0.0	2.22	177	3	11.5	16	93	27	1.56
224	1	4.6	3.0	2.0	0.7	0.3	0.4	0.0	1.04	161	3.5	15.5	15	57	31	0.82
224	2	5.0	3.0	2.0	0.5	0.4	0.4	0.1	0.21	114	3.5	15	12	54	37	0.79
239	1	4.7	11.2	8.0	2.2	0.4	2.3	0.0	2.34	167	4	13.5	26	117	30	1.43
239	2	3.9	3.2	1.8	0.8	0.3	0.3	0.1	0.17	152	4.5	18.5	20	114	36	1.63
245	1	4.7	8.0	3.8	1.8	0.3	1.0	0.0	2.85	229	3.5	12.5	18	60	21	0.93
246	1	4.4	4.9	2.5	0.8	0.2	0.8	0.0	1.31	251	4	15.5	16	67	33	0.93
246	2	5.5	11.4	5.7	2.8	0.3	0.9	0.0	0.28	468	4.5	19	22	113	32	1.3
257	1	4.4	5.7	1.4	0.7	0.2	0.6	0.3	1.76	257	3.5	12	19	114	29	1.17
257	2	4.8	4.7	1.1	0.6	0.2	0.4	0.0	0.36	98	3.5	12.5	18	124	32	1.41
262	1	4.4	2.5	0.9	0.4	0.2	0.5	0.2	1.67	137	2.5	7	7	43	16	0.69
262	2	4.3	2.0	0.5	0.5	0.2	0.3	0.5	0.25	172	2.5	8	10	47	22	0.65
277	1	5.1	10.6	9.4	1.8	0.2	1.2	0.0	1.90	93	4	13.5	16	99	29	1.25
284	1	4.5	4.3	1.3	0.7	0.6	0.6	0.2	2.00	162	5.5	8	34	371	26	3.17
284	2	4.0	5.4	0.8	0.7	0.3	0.3	0.5	0.89	290	6.5	11	38	397	26	3.64
287	1	5.0	8.8	4.4	3.7	1.2	1.0	0.0	1.49	377	4.5	18	21	84	37	1.34
287	2	7.6	19.7	8.9	10.6	5.4	0.9	0.0	0.29	394	4.5	17.5	22	112	42	1.48
287	3	8.3	28.0	21.6	11.2	7.7	0.9	0.0	0.06	249	4	16	20	102	36	1.58
295	1	4.5	4.0	3.0	1.0	0.4	0.8	0.5	1.79	276	3.5	10	12	52	23	0.89
295	2	5.2	6.4	1.5	1.0	0.4	0.3	0.0	0.20	109	2.5	10	12	40	19	0.7
301	1	4.9	9.3	3.9	1.6	0.4	1.0	0.0	1.44	199	4	14.5	20	77	28	1.23
301	2	4.8	8.2	1.9	1.1	0.5	0.8	0.0	0.48	127	4	15	20	70	31	1.24
302	1	5.8	15.7	14.5	2.9	0.3	1.3	0.0	2.87	241	3.5	14.5	16	59	31	1
302	2	5.9	7.7	5.2	2.5	0.3	1.0	0.0	0.86	175	4	17	18	62	34	1.09
304	1	4.8	21.0	9.8	7.4	0.6	1.1	0.0	4.51	577	8.5	23	34	186	51	2.79
311	1	4.2	2.4	1.8	0.8	0.6	0.5	0.3	2.27	322	4	14	18	66	26	0.79
311	2	4.2	1.9	1.2	0.5	0.5	0.2	0.1	0.70	278	3.5	14.5	15	57	23	0.74
320	1	4.7	6.5	1.8	0.6	0.2	0.8	0.0	1.94	205	3	14.5	27	124	28	2.7
320	2	4.4	4.5	0.8	0.4	0.3	0.4	0.1	0.58	219	3	14.5	25	135	29	2.94
322	1	4.4	12.0	2.6	0.8	0.4	0.7	0.0	2.85	195	3	8	12	52	21	0.93
323	1	4.1	6.8	1.4	0.5	0.3	0.5	0.4	2.71	273	2.5	7.5	14	56	14	0.78
325	1	4.5	8.7	3.5	1.4	0.3	1.0	0.5	2.10	326	4.5	12	18	125	30	1.16
325	2	5.2	5.5	2.8	1.3	0.3	0.5	0.0	0.38	141	4.5	11	16	121	29	1.24

4. Bullenbong Plain samples

Table 16. Location and some soil properties for Bullenbong Plain samples.

site	lay.	EAST	NORTH	upp depth	low depth	VOL	TXT	C	S	FS	CS	G	DP	FC	PWP	NEA
1	1	501705	6110723	0	0.3	0	13	62	17	19	2	0	55	47	18.3	96
2	1	501900	6110722	0	0.3	0	13	43	19	35	3	0	55	40.9	14.9	78
5	1	505196	6107985	0	0.3	0	8	33	16	43	8	0	22	38	12.4	74
6	1	504971	6107983	0	0.3	6	13	30	17	45	8	0	34	27.3	9.3	89
7	1	506027	6104639	0	0.3	0	13	38	16	40	6	0	27	35	11.6	97
8	1	506333	6104678	0	0.3	6	13	14	17	58	11	0	30	26.9	4.9	60
9	1	507176	6104664	0	0.3	0	7	37	16	38	7	2	48	31.7	11.6	78
10	1	501241	6107929	0	0.3	0	13	41	33	23	3	0	33	38.4	13.6	80
11	1	501028	6107977	0	0.3	0	13	51	27	20	2	0	46	42.2	16.4	93
12	1	500572	6107975	0	0.3	0	13	29	45	24	2	0	37	40.2	12.5	70
13	1			0	0.3	0	13	40	13	40	7	0	24	40.1	14.8	79
14	1			0	0.3	0	8	27	16	50	7	0	42	27.2	8.5	60
15	1	500507	6107974	0	0.3	0	13	29	46	22	3	0	27	40.3	12.3	77

Table 17. Soil properties and ground spectrometer measurements for Bullenbong Plain samples.

site	EC	pH H2O	pH CaCl2	CEC	Ca	Mg	Na	K	Al	OC	P	SORP	K gamma	U gamma	TH gamma
1	0.2	8.1	6.1	28	8.6	9	8	0.9	0	0.59	1	417	1.07	2.58	12.05
2	0.19	7.4	6.2	23.4	5.7	7.4	8.8	0.7	0	0.94	1	346	1.21	2.52	14.54
5	0.18	6.7	6	17.1	4.7	5.2	3.4	1.6	0	2.1	12	221	1.1	1.9	10.6
6	0.11	5.9	5	10.8	1.9	2.6	2.2	0.8	0.1	0.83	4	318	1.1	1.8	11.4
7	0.09	6.5	5.4	16.9	5.1	5.3	1.4	1.3	0	1.31	2	299	1.3	2.2	12.4
8	0.04	5.7	4.7	6.7	3.4	0.8	0.6	0.8	0	0.98	3	264	1.2	1.9	11
9	0.09	6.3	4.9	12.5	3.5	4.2	3.5	0.6	0.1	0.77	2	363	1	2.2	13.4
10	0.07	6.2	4.7	16.4	6.2	4.9	3.3	0.6	0.2	0.91	1	418	1.3	2.3	14.6
11	0.07	6.3	4.9	22.5	8.3	6.8	4.2	0.7	0	1.09	2	422	1.4	2.9	15.1
12	0.1	5.4	4.7	14.5	7.4	3.5	0.5	1.3	0.1	1.69	4	316	1.6	2.9	16.4
13	0.18	7.5	6	23.1	7.4	7.4	6.1	1.4	0	1.16	3	326	1.1	1.5	11.4
14	0.05	6.1	4.7	9.1	3	2.7	2.1	0.7	0.2	0.84	6	264	1	2.1	12.6
15	0.08	5.6	4.7	14.9	7.8	3.7	0.7	1.1	0	1.44	2	311	1.8	2.7	16.4